# The Physical State of Water in Dormant Bacteria

Michael DeLay

Submitted in partial fulfillment of the
requirements for the degree of
Doctor of Philosophy
in the Graduate School of Arts and Sciences

COLUMBIA UNIVERSITY
2018

# Abstract

## The Physical State of Water in Dormant Bacteria

Michael DeLay

Anomalous behaviour of water confined in nanoscale gaps influences many biological and technological processes. However, due to the small size of confining structures, it is historically difficult to manipulate and study water's dimension-dependent transport character. Experimental studies of nanoconfined water are generally limited to artificial test structures, and/or single-file channels, and so transport behavior of biologically nanoconfined water remains elusive. We utilize poroelastic bacterial spores coated onto a nanomechanical sensor to probe photo-thermal evaporative relaxation in a biological setting and report viscous water, 7 orders of magnitude larger than that of bulk liquid, and via thermodynamic investigations reveal an activation energy close to ice. Overall, these experiments characterize transport behaviour of nanoconfined water *in vivo*, and highlight the dramatic effects of nanoscale confinement on water that could impact myriad natural and synthetic processes.

Following from this work, a hypothesis is pursued in which the bacterial lifecycle is intimately connected with transitions in the physical structure of the internal water. We expand an initial idea proposed in *Science,* 1960 by J.C. Lewis, N.S. Snell and H.K. Burr that the low water content of the spore core is accomplished through compressive contraction during development[2]. During sporulation, the genetic material is packaged with chelating chemicals within a special water-responsive, layered coating that electrostatically pulls the water out of the core. Together, these agents produce the extremely dehydrated, hydraulically tensioned, and stable spore-phase organism. During

germinative re-awakening, an event lacking a complete mechanistic theory of sensation, the core is rehydrated and the organism subsequently reanimated. This work's findings regarding the spore's physically restrained but exchangeable water support the idea that the physical state of the water contributes significantly to tensioning the organisms into a 'charged' but dormant configuration. This dormant but spring-loaded phase of the bacterial lifecycle is subject to awakening by agents (nutrient or otherwise) which disrupt surface tension including amino acids, salts, surfactants, and hydrostatic pressures. In the least, it must be acknowledged that the slowed water observed herein enforces slowed biochemistry and thus dormancy.

Taken together we present a picture where internal spore water, even that which is exchanged with the external environment, is nanoconfined and slowed under tremendous tension (negative pressure). The mechanism governing this slow water appears to be unlike that any previously described, the majority of which are typically based upon crystalline surfaces, the likes of which are not found in the spore. We consider that the spore water structure itself participates, in certain environments, in the signaling chain of the organism through stabilizing a delicately balanced and highly tensioned architecture. Presently we are working toward testing the hypothesis and expanding our understanding with new methods, including additional structural mutants and expanded biophysical techniques.

# Table of Contents

# List of Figures, Tables, and Illustrations

# Acknowledgements

First and foremost, I wish to thank my mentor, Ozgur Sahin. In addition to exemplifying thoughtful and wide-ranging work in physical and biological sciences, Dr. Sahin is a uniquely kind and considerate colleague whom always brings a unique insight to any scientific matter. I will be eternally grateful for our time spent in conversation, attempting to disentangle the physical contributions to the world's seemingly endless complexities, biological and otherwise. From Professor Sahin I have learned how to live, not simply perform, as a scientist.

The consideration of spore biology from a physical stance has a long history and among many I wish to thank all the pioneers of spore water state concepts, especially Lewis, Snell, & Burr, C. Rice, and D. Popham, A. Driks, and again, O. Sahin. Along those lines, much work has been done previously regarding spore mechanics and I wish to thank the individuals who first characterized spore water-responsiveness, including K. Wheeler and in particular, my friend and former colleague, Xi Chen. Xi was instrumental in helping me to acclimate to physical sciences and develop the new methodologies we utilize throughout this work, in addition to being an inspiring young investigator in his own right. I wish to specifically thank another friend and collaborator, Ahmet-Hamdi Cavusoglu, whom has been invaluable in bringing me up to speed on water chemical theory, coding, and all things analytic. Together we have all spent countless hours pondering the spore and the spore has in return taught us all so much, and not just about its own nature, but about the nature of the physical universe in general.

I wish to thank my lab in general for making the laboratory a comfortable and productive workplace through endless roads of discussion and bottomless respites of laughter. I would also like to thank each of my committee members, specifically Lars Dietrich, Jonathan Dworkin, and Mike Sheetz for their constructive questions and concerns regarding my work from the very first proposal

onward. I have learned something from each of you at each engagement and my appreciation for challenge cannot be overstated.

Finally, I wish to thank my family. In particular, thanks to my mom, Pamela DeLay, for being one of the most interested and caring parents I've ever known. Mom, you make my friends jealous in this respect: case-in-point, you probably know everything about spores before even opening this document. Thanks for nurturing me into a (highly?) functional person. Thanks to my dad, Charles DeLay, for demonstrating dedication to one's work, always slaving away in the studio after work when I was growing up. Thanks to Mom and Dad for delivering me into the wonders of the creative arts and discovery in general. Thanks Grandpa, Clarence 'Pete' Peterson, for pushing and pulling me and all of his children and grandchildren through each of life's briar patches with your wisdom and strength. Additional thanks to all of my extended family, particularly the Saba family, for your love and kindness. Together my family have all conspired to make my life relatively painless compared to the most. This has freed to less mortal concerns, like spores and harmony. Speaking of music, I couldn't have made it this far without music itself, as well as all of my friends and collaborators in music. I wish to thank my friend and roommate Dave Polk for specifically inspiring me to look beyond the surface of sound, science, art, and society. I am always learning from each of you. Last, and far from least, I owe unquantifiable thanks to my friend, and partner through this academic marathon, Anastasia Bendebury. Sitting at the last lines of this immense document, I can't imagine having written the first word of this work without you. In addition to your unique critical attention in science, your friendship has been the lifeblood of my experience in New York. Thank you!

# Dedication

This work is dedicated to Grandpa Clarence 'Pete' Peterson for establishing a tradition in the pursuit of greatness through love embodied in the following advice:

*Make what you love into your work, and so find it is no longer work.*

# Preface

*"The [spore dormancy] hypothesis that the bare essentials of a vegetative cell-DNA and indispensable enzymes- are rendered hydrophobic or otherwise stabilized on a molecular level lacks simplicity and elegance [and so mechanics cannot be ignored]" – J.C. Lewis et al. Science, 1960*

The authors of the above statement go on to suggest that "the speed and trigger-like action of physiological and mechanical germination seem inconsistent with a stripping of covalently bonded hydrophobic groups". The purpose of this work is to detail the physical state of internal spore water and thereby expand upon one hypothesis concerned the mechanical cause of spore germinant surveillance and the maintenance of dormancy. Chapters 1 and 2 provide some background on spores and anomalous water behavior, respectively. Chapters 3 and 4 contain findings that have been submitted for peer review as of October 5$^{th}$, 2017, and detail the presence and character of ultraslow intraspore water, which is highly viscous, and of high intermolecular bond energy, in a geometry-dependent fashion as the spore swells in response to ambient humidity. Chapter 5 presents new methods and investigates this water structure as it appears in liquid, where germination is most often examined in the laboratory. Notably, we find water transport remains slow in liquid, and is disturbed by chemical germinants, and so this method suggests an effective means to detail the contribution of the physical state of water to liquid germination in future work, which is suggested in Chapter 6.

This work should prove of interest not only to spore biologists, but also to physicists and physical chemists interested in experimental means of assessing water transport in conduits below the nanometer size scale. Water is known to behave anomalously at these confinement lengths, however relevant experimental methods have not been achieved to date. With the spore as an experimental

platform, one can directly tune the confinement length that water will experience by adjusting relative humidity. Finally, we have tangentially worked for many years in the Sahin Lab on clean energy alternatives involving evaporative harvesting using spores, and thus, understanding transport kinetics will also be of use in refining our engineering endeavors.

This research was conducted at Columbia University and supported by awards from the NIH, Department of Energy, and Packard Foundation.

# Chapter 1: The Spore as a Phase in a Lifecycle

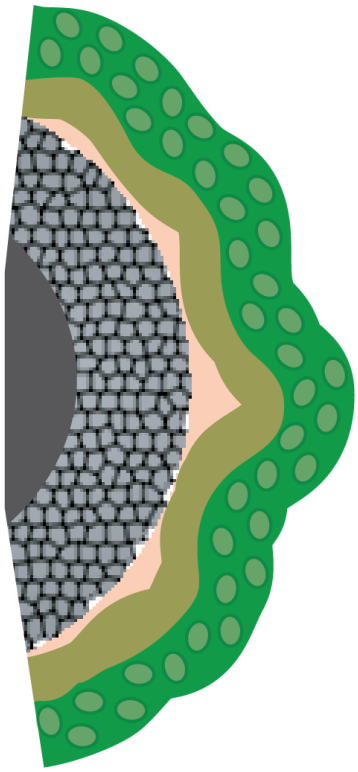

**Figure 1.1| The spore is a variably dehydrated, multilayered bacterium.** cartoon represents the core (dark), cortex (grey), and coat (green) layers. The spore is assembled from inside outward, beginning with compressive dehydration of the genetic material, where upon metabolism and transcription of the spore is paused.

To endure scarcity of sustenance, specialized bacteria of the Firmicutes phylum enter a metabolically dormant phase known as the endospore or simply, the spore [3]. The bacterial spore is the longest-lived cellular structure known to exist[4]. Spores of diverse species can persist for hundreds of millions of years[5]. This life-cycle of spore-producing bacteria is biphasic, with the bacterium undergoing a distinct physical transformation to dormancy as the organism is deactivated through a process known as sporulation, and then later re-activated through a process known as germination. There are a range of metabolically dormant bacterial cell types, and this thesis will focus on that of the model organism, *Bacillus subtilis* (Fig 1.1). Note that the cycle of *B. subtilis* is not reproductive, as it does not provide population growth but only stabilization (the spore is produced with a 1:1 correspondence to the mother bacterium, which is lysed during sporulation). This life-cycle begins with a vegetative bacterium, processes through sporulation mechanisms, resulting in the spore formation, and terminates through germination, by which the vegetative form is restored. The spore is formed and matured within a single bacterium known as the mother cell[6]. The spores that emerge are resistant to a wide diversity of environmental assaults, including ultraviolet radiation, harsh chemicals (peroxide, bleach), desiccation, and other common

disinfectants. Their ability to persist appears virtually unlimited temporally, with groups claiming germination of spores that had been dormant for millions of years[7]. The sporulation process is initiated by simple differential cell division. The sporulating bacterium copies its genetic material and relocates each copy to alternate poles of the cell. One pole of the cell, known as the forespore, is

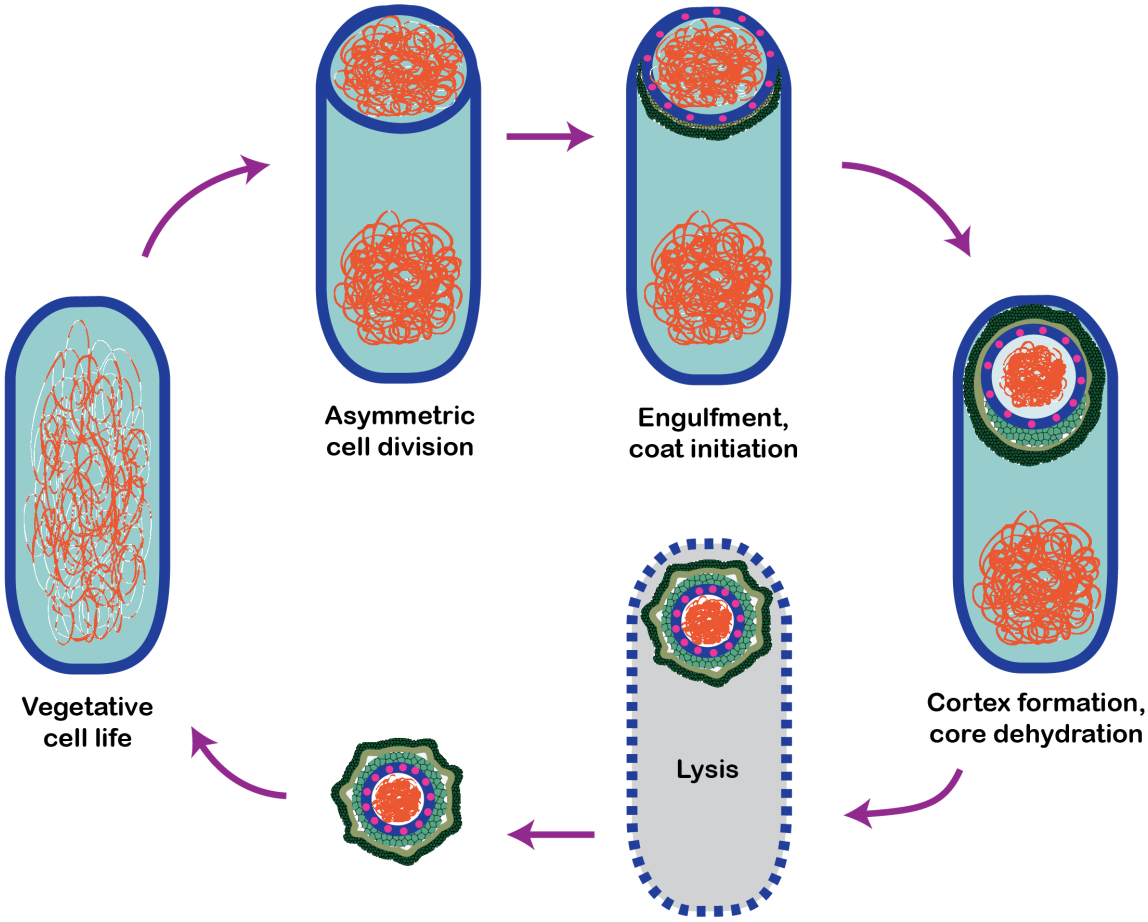


**Figure 1.2| The variably hydrated lifecycle of the Bacillus bacterium.** Following from the McKenney *et al,* 2013 Coat review, this panel illustrates that the production of the coat and cortex are accompanied by a dehydration of the genetic material. By reducing the size of the compartment during development, the core is pressurized and dehydrated.

destined to develop into a mature spore, while the mother cell constituting the other pole is eventually lysed. For other bacteria, such as Metabacterium polyspora, more than three separate spores can be formed inside of a single mother cell[8].

In *B. subtilis* sporulation is a biochemical process that begins with the triggering of sensor kinases in response to nutrient depletion.[9] These kinases phosphorylate the transcription factor known as Spo0A. Spo0A transcribes a wide range of target genes, including the spore-developing sigma factors, as well as those involved in the asymmetrically polarizing morphogenic program[6]. The initiator of this cascade, KinA, is sufficient to initiate the entire process in the laboratory[9]. This polarized cell, now comprised of the smaller forespore and the larger mother cell then proceeds through a process known as engulfment, whereby the former is formally taken up by the latter (Fig 1.2). At this point the forespore is contained within a double membrane inside of the mother cell. As soon as this septum is formed, the sigma G family of transcription factors is activated, and this event is accompanied by the dehydration of the core[10]. This procedure is accompanied by the creation of

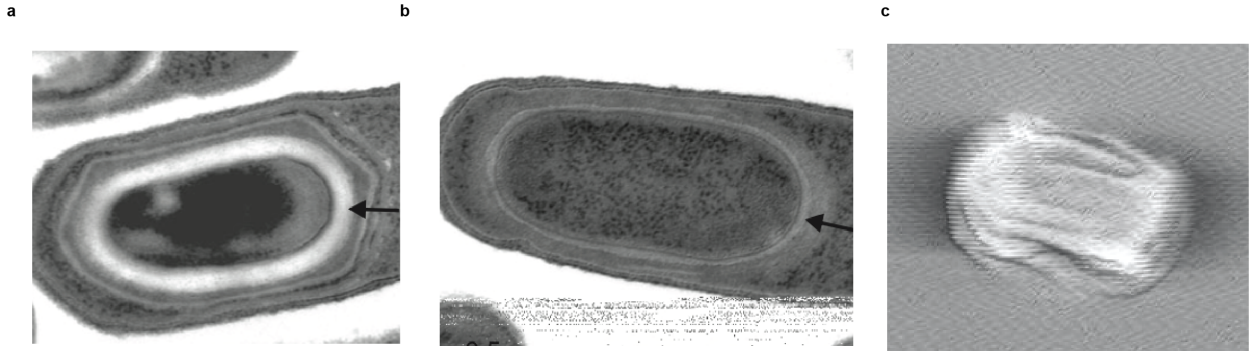


**Figure 1.3| Cortex-deficient mutant spores a**, **b**, reprinted SEM from Bukowska-Faniband & Hederstedt 2013, showing the depletion of the cortex layer in spores of *B. subtilis* inside of mother cells (WT in **a**) after genetic deletion of the transpeptidase, SpoVD in **b. c**, shows AFM image of one cortex-deficient mutant we examined (sample thanks to Dworkin group) displaying the characteristic 'shriveled' appearance.

the protective structures known as the outer coat and cortex, which are deposited by the mother cell, after being activated by the daughter cell's sigma G. Once activated, the mother cell begins her sigma K program of cortex and coat production[10]. The cortex is assembled between the inner and outer of the aforementioned double membrane, largely under the direction of the transpeptidase SpoVD[11,12].

Mutants which lack this structure fail to develop appreciable cortex (see Fig 1.3). We will consider cortex and coat function in depth throughout this work. To summarize the cortex structure, we will

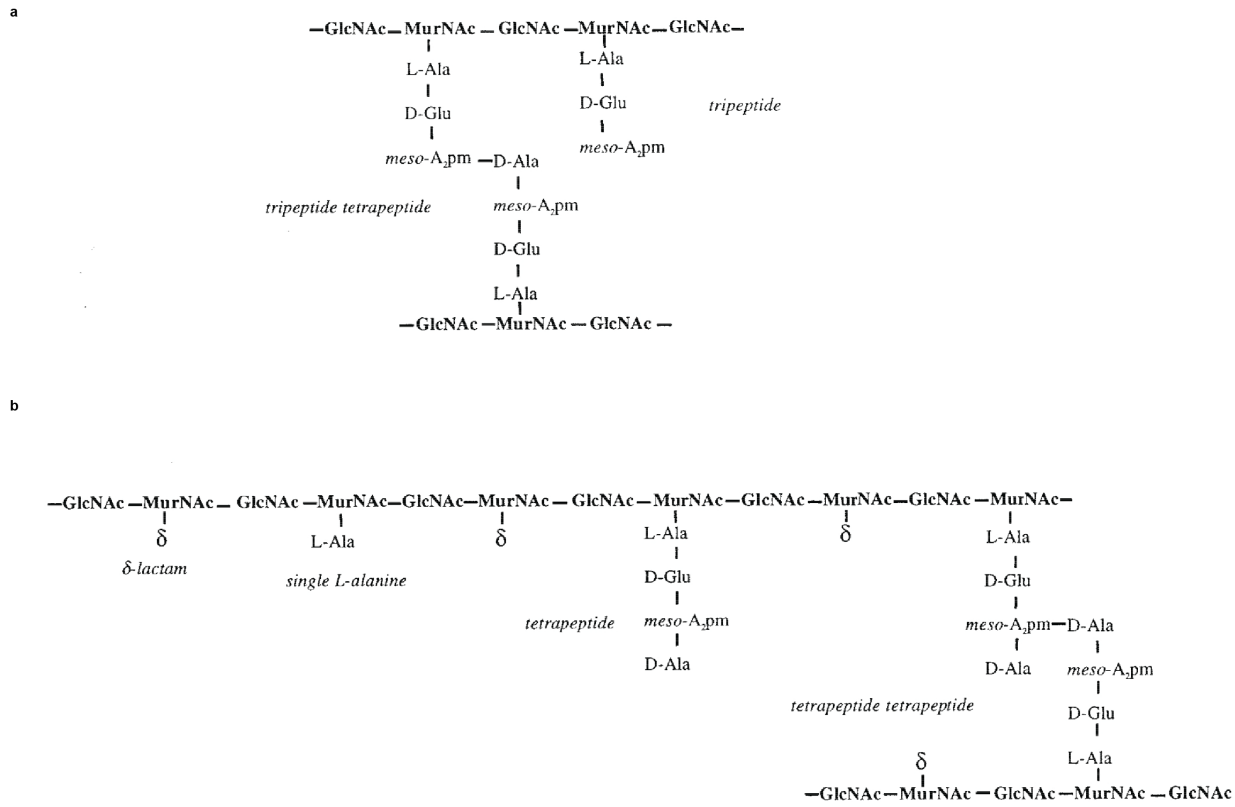


**Figure 1.4| Structure of spore peptidoglycan compared to that of vegetative phase cell. a,** Vegetative cell wall peptidoglycan reprinted from Atrih *et al* 1999. This structure diagram of the cortex pepditoglycan from spores in **b** reveals that ~50% of the MurNAc residues have lost peptide chains to simple muramic-*∂*-lactam. All other residues are cleaved to single-Alanines or 3-4 peptide strands that then undergo cross-linking between glycan strands. This means only 3% of the total spore muramic acids end up cross-linking[1]. It is plausible the abundance of externally exposed Alanine could participate in hydrogen bonding.

begin by assuming it is comprised of layers of porous peptidoglycan, much more loosely cross-linked than that of the vegetative cell wall (Fig 1.4). Atop the cortex is the coat, which is composed of more than 70 proteins. Coat layers are placed onto the outside of the forespore in a coordinated fashion by the mother cell[13].

Emergence of the vegetative bacterium from dormancy in nature appears to result from environmental cues, which indirectly influence specific proteins at the spore's core [14,15]. This activation during favorable (nutritious and moist) conditions triggers an irreversible cascade beginning with partial rehydration of the core and the release of dipicolinic acid, followed by activated hydrolysis of the cortex, complete core rehydration and eventual outgrowth. Germination has in fact been recently described precisely in these terms by Peter Setlow in the latest of his annual reviews on the subject as "events beginning at the time of addition of agents that trigger germination (germinants) and ending when spore core water content (25–45% of wet weight during dormancy) rises to 80% of wet weight."[16] Hydration is then essential to defining the reactivating transition of the bacterium.

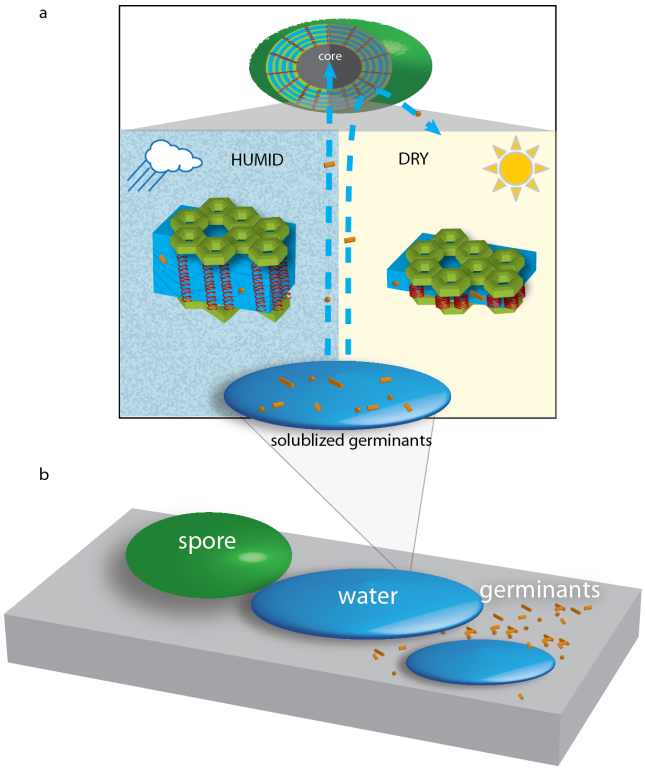


**Figure 1.5| Hydration sensitive sieving of the spore coat & cortex.** **a**, The spore responds to humidity by extending its cortex/coat by 4-12%. **b**, this mechanism narrows the pore size of the cortex/coat material, and thereby closes off the spore to germinant sensing in the absence of sufficient hydration.

In addition to typical nutrient germinants, which we will discuss at length, spores respond to non-physiological triggers, which include CaDPA, cationic surfactants, electric pulses[17], and very high pressures[16]. Vegetative cell-wall fragments also can induce germination in an alternative pathway through activation of a Ser/Thr kinase[18]. Many of these triggers could also be considered hydrostatic in that they are expected to affect the structure of water (CaDPA binds and sequesters free water). Interestingly, the non-physiologic germination cues are highly conserved across all spore forming species. Lysozyme will also serve to

germinate the spore if the outer coat is rendered permeable. The coat/cortex are very diverse in their exact amino acid compositions and also differ significantly from the vegetative cell in composition (see Figure 1.4). Importantly, the structure appears to serve some variable and complex sieving abilities, as small molecules face a high resistance to diffusion (into the spore) whilst in its most dried state where internal dimensions narrow to single water-molecule lengths (see Fig 1.4, 1.5, and also Chapters 2, 3). The cortex and coat together appear to serve as a molecular sieve, with the coat sieving large molecules, including lysozyme[19] and the cortex sieving smaller molecules. Chapters 3, 4, and 5 of this work show that this sieving is tuned by structural changes to the spore as it responds to the variable hydration of its environment. It generally appears that when the coat/cortex structure is actively destabilized after development, germination will proceed to some stage.

Regarding physiological nutrient-sensation as a trigger of germination, much progress has been made to date, however a unified canonical signaling pathway, from ligand-binding to signal transduction has yet to be clearly established. First, it is known that there exists a class of spore-proteins that are in some way generally responsible for nutrient sensing during germination. The field has termed this class Germinant Receptors (GRs). It is worth noting that these are termed receptors though no direct interaction between the germinants and these proteins has been directly measured(*)[18,20]. Setlow says, "Germinants are sensed by interactions with germination proteins, *presumably by direct protein binding. However this has generally not been shown but rather inferred* from changes in germinant specificity or affinity due to mutations in suspected germinant-binding proteins"[16](author emphasis). These GRs are all generally found within the inner membrane of the spore, directly below, and tangential to, the cortex. These GRs are expressed in very low quantities, only hundreds per

[*] Binding possibilities to a GR have been suggested in theory for glucose and demonstrated for separate GR-independent Ser/Thr kinase for vegetative cell wall fragments, but not spore peptidoglycan. We note that cell wall fragments may disrupt interfacial tension prior to any receptor binding events, and that kinase signaling requires mobile water within the core.

spore. One bacterium, *C. difficile* and family, have no GRs whatsoever but happen to be activated directly exclusively by bile salts[21]. The totality of the inner membrane GRs is termed the germinasome.

The germanisome is organized through clusters of GRs[22]. GRs seem to group together during dormancy and are required to be completely intact with all subunits present. GerD presence is necessary for the GRs to form clusters. In addition to GR subunits and DPA channel subunit, SpoVAD, GerD does not appear to be exposed to external solution chemistry (biotinylation), however[23]. Following some lag phase after germination addition (>30 minutes) the GR foci dissipate diffusely. Of the *B. subtilis* GRs, GerD is degraded or lost immediately at the start of germination, prior to the raft dispersal of all germinasome foci[24]. The variability in the lag time from germinant addition is so large that certain populations can be isolated which require days to germinate after addition of triggers. These super-dormant spores may have less GR quantity in general[25].

L-Alanine, a ubiquitous *B. subtilis* structural element is unique as a germinant in *B. subtilis* and other species, and is also a ubiquitous *B. subtilis* cortex structural element. This is the same alanine found among the 20 amino acids encoded within the human genome, not the D-alanine that is a dominant component of bacterial cell walls. It is, however, a highly common protein found in other eukaryotes, accounting for a large percentage of amino acids found in eukaryotic biological structures, second only to leucine in abundance[26]. L-alanine is also found on as a single residue side chain on 20-

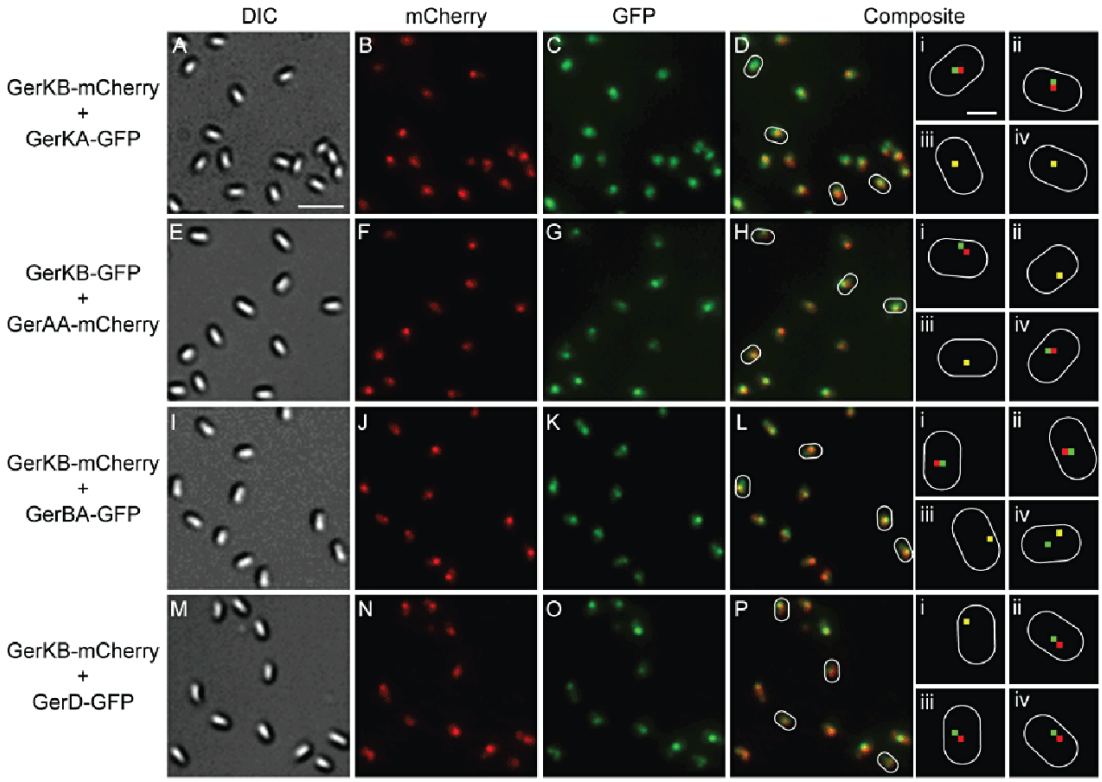


**Figure 1.6| Co-localization of GRs in dormant spores.** Reprinted from Griffiths *et al* 2011, we see the overlapping spatial localization of GerK, GerA, GerB, and GerD. Different proteins cluster independently of each other and require GerD for this, yet GerD clusters in the absence of other proteins. These rafts diffuse immediately upon germination.

40% of the muramic acid residues within the cortex peptidoglycan[27]. This contributes to the fact that only 3% of the side-chains in the cortex are able to form covalent peptide cross-links. It raises the

possibility that the excess alanine side-chains could participate in hydrogen bonding, and/or electrostatic tensioning. Interestingly, it was known early on that the spore peptidoglycan contained both D- and L-alanine of more or less equal proportions, and in great abundance[28]. Interestingly, these alanines are usually found as sidechains (linkers) in the peptidoglycan, and so when they are isolated and purified they predominantly exist as exposed side chains. There is some evidence that the germinating bacterium uses this as a template for the construction of its nascent cell wall[29] (vegetative peptidoglycan, see Fig 1.4). D-alanine is known to competitively inhibit L-alanine. This principle is often used by biologists to halt L-Ala induced germination[30]. There is evidence that racemase enzymes in the coat of many species convert small amino acids, including Ala, from L- to D-[31,32]. Racemases can help the bacterium quorum sense local density and adjust self- L-Ala levels to prevent colony overgrowth or, alternatively, to amplify low density germination levels. Radiation also induces a stable free radical in alanine, so it is reasonable to assume that this could account for some part of the spore's resistance to radiation[33]. Alanine also has surfactant-like properties[34] and therefore disrupts hydrogen-bonds and other transient electrostatic configurations.

The only known molecular stimuli which singularly affects all spores of all species is a well-known cationic surfactant, dodecylamine[16,35]. Warmer temperatures also facilitate faster dodecylamine germination in WT spores[36]. Surfactants by definition disrupt surface tension or interfacial tension. It is suggested that this particular surfactant mediates initiation of germination via the release of CaDPA, and that the SpoVA channel plays a role in this[15]. To this end it was shown that dodecylamine germination was enhanced by increased channel density in the inner membrane. It has also been shown that the conserved SpoVAC subunit of the SpoVA proteins, which outnumber other GRs by a factor of 6-fold, can act as a mechanosensative channel, in which activity is controlled by membrane tension[37]. We expect the membrane to be under significant negative pressures due to finely balanced water chemistry[38]. If the inner membrane has regained some fluidity (perhaps due to surfactants

disturbing the immobilizing hydrogen bonded water network), any SpoVAD channels already intact and present, should be expected to yield hydraulic flow. There is some indication that the SpoVA channel is associated and possibly activated through interactions with GRs[16]. Note that dodecylamine alone does not result in complete hydration of the core[35]. Beyond these data, it is not clear whether there is any additional role of dodecylamine in the spore biochemistry.

Alanine, a common germinant, can also act as a surfactant in both single molecule and polymeric form[34]. It is interesting that alanine is often embedded into the cortex with its hydrophobic group exposed (see Fig 1.7)[39]. This arrangement serves to pattern the predominantly hydrophilic

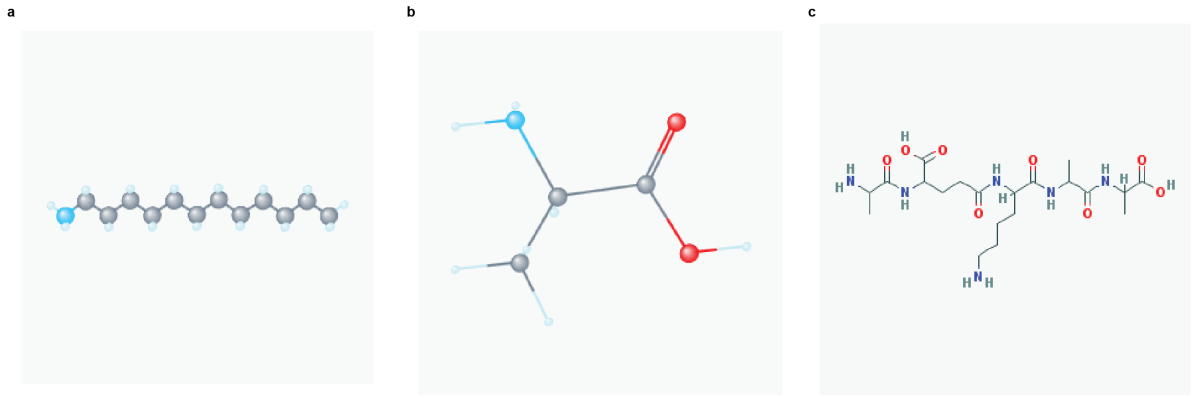


**Figure 1.7| Dodecylamine (surfactant), Alanine, and Peptidoglycan Structural Relationship.** **a**, Universal spore germinant, Dodecylamine (PubChem ID:13583) **b**, Spore germinant & cortex structural component, L-alanine (PCID:5950) **c**, one configuration of peptidoglycan's pentapeptide group with regular hydrophobic Alanine-based side groups (PCID:4294676). All images courtesy of the PubChem database.

cortex with small, semi-regular hydrophobic contacts. In general, the spore's outer layers appear to alternate heterogeneously between hydrophilic and hydrophobic domains, though a hydrophilic D-Ala subunit must be included into most GRs in order for full activity to be observed[16]. Generally, the spore cortex appears to supplement highly hydrophilic –OH and carbonyl groups with randomly patterned hydrophobic groups. Compared to the vegetative cell, it has only 1/10$^{th}$ of the covalent cross links.

While the spore undergoes development during sporulation, the lipid mobility of the germanisomic inner membrane abruptly decreases[40]. This is fascinating, because during germination the viscosity of this inner membrane is lowered to that of a vegetative cell[40]. In the vegetative cell, there is recent evidence for lipid raft domains using neutron-scattering techniques[41], thus supporting the idea that altered fluidity of the inner membrane likely leads to novel arrangements of GR components.

Beyond physiological germination conditions, it is known that spores will germinate in response to moderately high pressures of 150 MPa and high pressures of >500MPa[14]. For the higher-pressure paradigm, this is thought to be in part due to the forcing of a mechanosensative dipicolinic acid receptor/channel (DPA), SpoVAC, which forms after the germination signals are received[15,37]. Lower pressure induced germination is shown to result from activation of the GR cascade[42]. It is not understood, however, how this receptor/channel comes to be forced chemically in the natural world, where such external pressures are not expected. Because SpoVAC is part of a larger SpoVA class of proteins, it is conceivable that the DPA channel is formed through transient assembly of physically separated subunits[43]. In fact, the structure of the SpoVAC protein has been likened to various synthases, and there has been speculation in the literature that's role during development may be able to package the DPA by acting as a receptor for the molecule. This is intriguing when you consider that synthase processes are highly active during development but if against a diffusion gradient could run backward and release a significant quantity of energy: the DPA-DNA complex is a very tight interaction, denser than either molecule alone [44] and may act as a compressed spring later during germination.

It is known that there exists some humidity-dependency with respect to germination in several species[45]. Also, spore killing by toxic compounds, which is thought to be indicative of permeability

to germinants and implies a humidity dependency of germination. This phenomenon has been considered in relation to swelling; however, these explanations are based on container size [46,47]. In other words, if the vessel is large, it will be able to take in more liquid and hence more germinants [46]. A closer inspection reveals this idea to be over-simplified: Reduced diffusivity to container size does

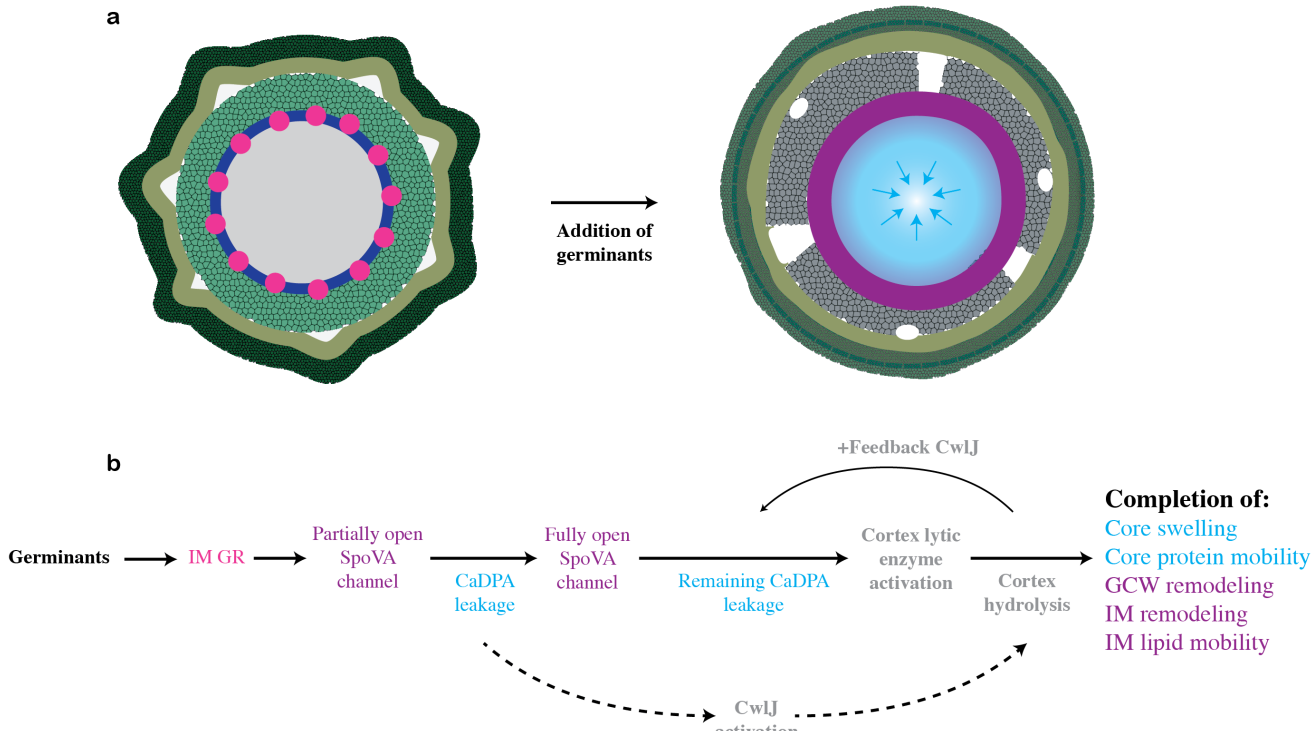


**Figure 1.8| The *Bacillus* germination flow diagram. a,** cross-sectional spore cartoon showing physical changes in the spore are coupled to the hydration of the inner structures. **b,** Adapted from Setlow *et al* 2017, we see that the activation of inner membrane germination "receptors" (GRs) results in GR diffusion/delocalization and possible opening of the mechanosensative SpoVA channel, resulting in partial hydration of the core, and release of DPA. This DPA activates lytic enzymes which degrade the coat/cortex and core protein mobility is re-established, whereby outgrowth proceeds. A feedback loop results in amplification of core hydration and DPA displacement.

not explain speedy resumption of biologic activity alone (frozen-like to fluid-like transition). Also, molecules from these studies, including formaldehyde and chlorine dioxide, are miniscule compared to known germinants such as amino acids, sugars and nucleic acids necessarily introduced from the

external environment during germination[45]. Water within the spore, it should be noted, obeys no such idealized gas conditions when confined at the nanoscale. Furthermore, as we shall see in the following Chapters 2 & 3, spore water is not treated to a simple 'bag of gas' experience within the spore where diffusion kinetics dominate.

Once commitment to germination has been established, the path forward is fairly straightforward regardless of stimuli, and yet is highly species specific. For *B. subtilis*, the initial signal-transducing raft produces channel activity of SpoVA, which then leads to cortex hydrolysis via cortex embedded enzymes (see Figure 1.8). DPA leakage feeds back, leads to further SpoVA activity, core swelling and all other phenotypes of fully realized germination. Interestingly, when the cross-linking density of the cortex is increased, there is an increase in speed of response to germinants like alanine and dodecylamine, however once initiated DPA release is slowed[48]. This might suggest that the core is untensioned by the reciprocal pulling of the more adhered coat. CaDPA diffusion is then limited as porosity decreases. The cortex is eventually hydrolyzed by embedded lytic proteases and pseudo-proteases, and outgrowth proceeds. It is thought that cortex hydrolysis may result from perturbations to the structure of the peptidoglycan itself, and can precede DPA release in some species[16](see Fig 1.8).

In summary, the spore is a dormant phase in the life-cycle of certain ancient lineage bacteria. The cell is de-activated and stable against environmental assaults through specialized and dynamic cell-wall structures that develop during sporulation, which can then be actively catalyzed during outgrowth. The re-activation of the bacterium in nature is signaled largely by chemical triggers through an inner membrane complex of GRs. Moderate hydrostatic pressures of ~150-200 MPa can accelerate GR germination rates. Large hydrostatic pressures in excess of 500MPa directly produce germination. All of these relays, chemical or physical, result in the hydration of the core's genetic material and overall

re-animation of the organism's biochemistry. Because water is confined at the nanoscale within the spore where anomalous behavior is expected, and because water is intimately connected with the lifecycle of the organism, we seek to understand its behavior in greater detail. Spore water state is controlled by environmental factors and appears to play a role in maintaining structural integrity and biochemistry, and hence, dormancy of the spore. The correspondence between the physical state of water and spore dormancy are follows from a hypothesis proposed by Lewis *et al, 1960*. The hypothesis is resolved by several historic lines of inquiry, including the known role of interfacial tension in germination, and that all known spore species are germinated by a particular surfactant.

# Chapter 2: Spore Hydromechanical Evolution

Water is the most anomalous liquid and it is essential to the lifecycle of all biological organisms, including bacteria and the spore[49]. This chapter will focus on the spore's water responsive materials and relate this to anomalous water behavior observed throughout nature and biology. Spores come from the Firmicutes phylum, which is historically marked by a thick peptidoglycan cell wall that causes them to be stained, in preponderance, Gram-positive. A small minority of these species to do not

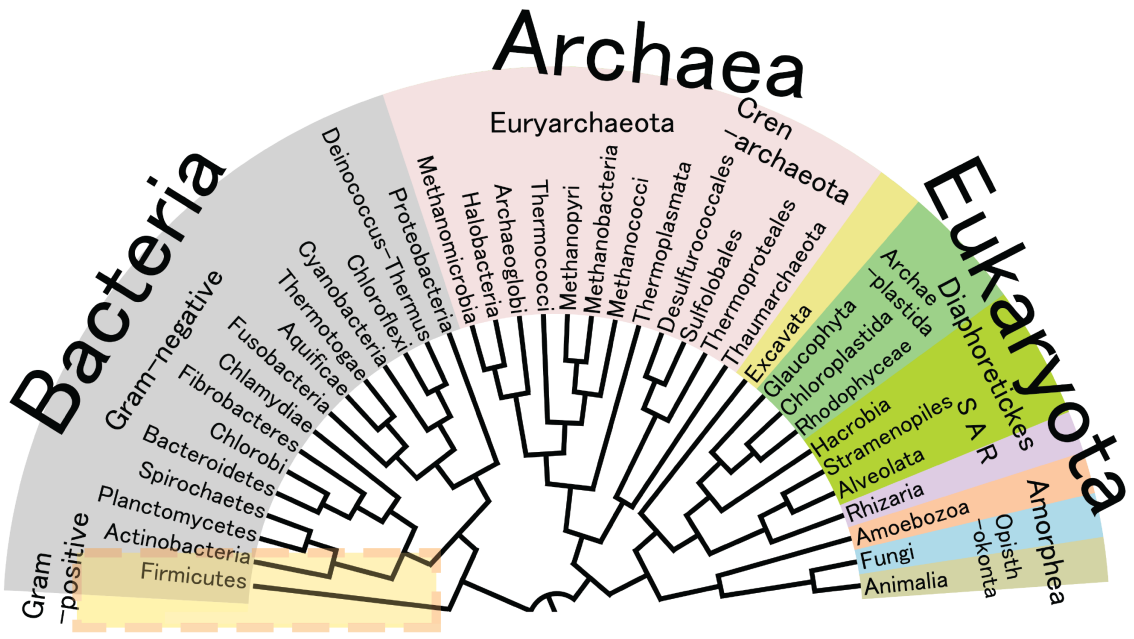


**Figure 2.1| Spores are a specialized form of bacterial from the Firmicutes phylum**, which is among the earliest branches of life on Earth. Adapted from *Wikimedia* creative commons "Phylogenetic Tree of Life" via data from Chiccarelli *et al* 2006.

stain as heavily due to the increased porosity of their wall structure. Spores retain a peptidoglycan mesh in a specialized wall that separates their genetic material from the outer surfaces[43]. Because this wall structure sits atop the genetic material at the core of the spore, it is referred to as the 'cortex'. It should be noted that the spore-forming Firmicutes are a particularly ancient class of bacteria, and so

behavior of this specialized structure must also be considered in this primordial context (see Fig 2.1)[50]. The Firmicutes' early branch in the evolution of life on Earth is also relevant when evaluating possible mechanisms available to the organism's unique two-phase life-cycle.

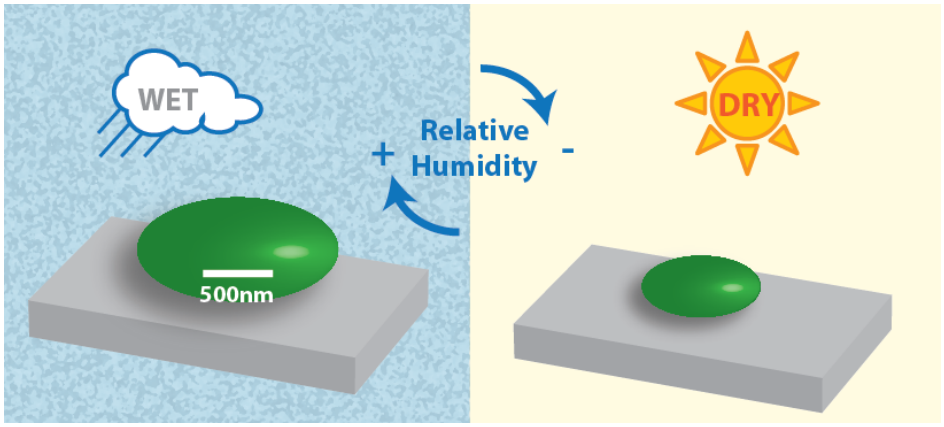


**Figure 2.2| Humidity-responsive spores.** Spores rearrange their shapes as ambient humidity shifts. This behavior is initialized during dehydration/coat production, where it produces the characteristic rucks and wrinkles seen on the spore surface as these materials adjust to the decreased internal dimensions. This can lead to size changes of up to 18% in certain species across a full range (0-100%) of relative humidity.

The spore is multilayered, with the cortex and outer coat atop a core containing dehydrated genetic material. The cortex and coat perform some environmental-sensation action in addition to their role as variable physical barrier for the genetic material: spores of several species have demonstrated a remarkable humidity-responsive capability, swelling up to 18% of their desiccated size through some as-of-yet poorly understood structural transformation (the volume of water taken up does not correspond directly to the swelling observed)[47,51,52]. The precise evolutionary advantages that lead to the swelling behavior remain unclear, although several subsequent questions have been raised in the literature to that end [2,43,52]. It has been suggested that during development the spore's water-responsive (swelling) materials aid in the wicking-like dehydration of the core while the genetic material is simultaneously chelated by DPA[16]. Other water-responsive biological actions, such as the ice plant's daily unfolding[53], show that the spore is not unique in its ability to harness water to change

shape and that this ability can be enlisted in functions including, but not limited to, environmental sensation[53]. Other examples of this effect can be seen in pine cone seed dispersal and sap ascent in trees[54,55]. The Argonaut nautilus is capable of manipulating water pressures to achieve variable buoyancy and navigate depth[56].

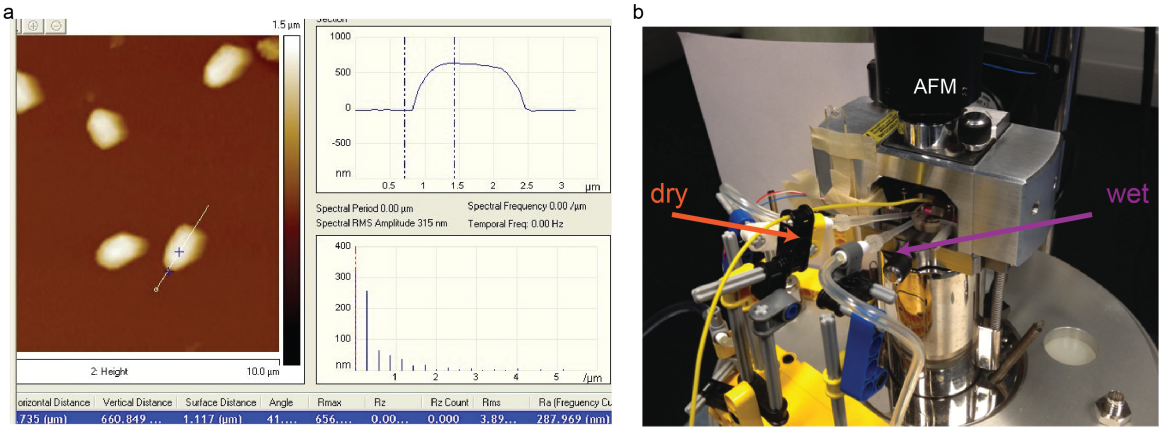


**Figure 2.3| Humidity-dependent strain measurement method. a**, Spores are examined by tapping mode AFM for height change in response to **b**, variable humidity directed precisely toward the scanning location.

The spore appears to develop its swelling behavior as a direct result of dehydration during development after the initiation of the Sigma G/K programs. Our group initially modeled that this dehydration produces the rucks or wrinkles in the coat as the coat (deposited in 100% hydration) responds to the decreasing volume of the inner spaces as they are tightened via crosslinking into place[38]. It is assumed that the cortex layer also undergoes buckling-like behavior, although its macro geometry remains smooth and spheroidal in contrast to the rucks of the coat. This may suggest that the tensile forces are distributed uniformly among the pores. The dehydration process appears to be essential in tensioning the spore materials and may explain their extreme physical properties including high elastic modulus[52] and viscous stabilization of the signal-sensitive inner membrane[40]. It appears to be important in germination as well. Recall from Chapter 1 that the appearance of membrane

tension-sensitive channels in this inner membrane is concurrent with the earliest phases during emergence from dormancy.

Initially, spore-swelling in air was observed through automated scanning microscopes and

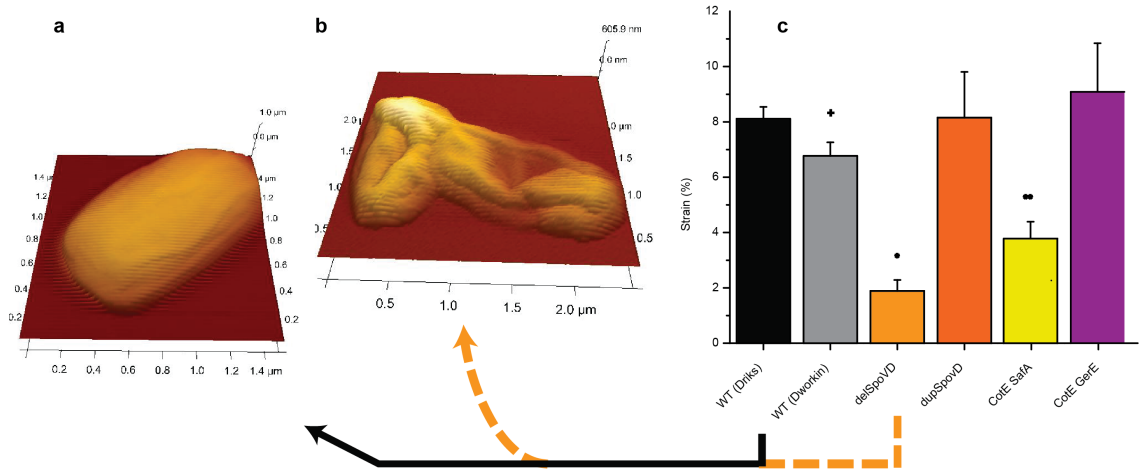


**Figure 2.4| Spore-layer-dependent strain. a**, tapping mode image of WT and **b**, pair of SpoVD cortexless mutants along with strain measurements for various mutant spores. Error bars equal standard error for at least 5 spores. Two-tailed T-test, *p<.01

ellipsoid-intensity models[47]. For the purposes of this work, we have adopted a more physical approach to measurement through atomic force microscopy (AFM)[38,52]. By directing a variably humid airflow at the scanning stage we can observe this swelling through a nanoscale force sensing cantilever (see Fig 2.3). Alternatively, and arguably less subject to air/thermal noise, the entire AFM can be enclosed inside of a humidity controlled chamber. The latter technique is used sparingly as it may risk damage to the scanner mechanism.

The spore's water-responsive behavior has, to date, been primarily ascribed to the cortex/coat[47,52,57]. Others have argued that the core itself may have a certain 'sponginess'[58]. However, if this gel-core is present it could not exchange water with the external world and is therefore not directly involved in spore-swelling. This understanding is based on core-water NMR studies where deuterium labeled, desiccated spores are left open to ambient exchange for weeks[57]. In support of this

theory, my initial examinations of substructural mutants have shown that genetic deletion of the cortex is sufficient to maximally reduce humidity-responsiveness (75% of mean WT strain) [see Fig 4b]. Deletion of *cotE* and *saf A* also seemed to diminish response. *Saf A* transcribes proteins which may be involved in articulating the cortex to the coat[59], while c*otE* encodes a bulky coat protein. This may imply that in the *saf A* mutants the coat has become uncoupled and no longer transduces mechanical impulses from the cortex.

The spore's cortex layer is entirely comprised of peptidoglycan (murein) arranged into an unspecific, heterogeneously patterned, geometric architecture (see Fig 2.5). Peptidoglycan is a regularly cross-linked sugar mesh found in the cell wall of vegetative bacteria and traditionally used to discern Gram-positive strains. This structure lends itself to elastic responsiveness to turgor and to maintenance of structural integrity[60]. Developing spores receive this substance in an externally applied fashion while entirely occluded within the confines of a 'mother' bacterium[6,61]. To date, due to the inaccessibility of the spore during development, nearly all structural coordination descriptions of its cortical peptidoglycan have relied upon the related vegetative isoform[62]. Spore peptidoglycan is comprised, heterogeneously, of a chain of glycans with regularly-spaced protein branches. Unlike the

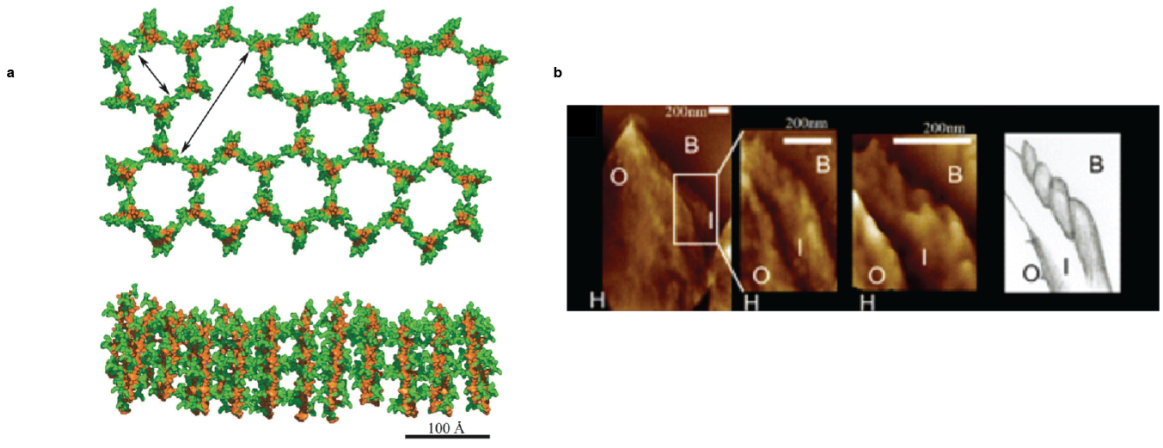


**Figure 2.5| Repeat polymeric organization in bacterial peptidoglycan. a**, NMR of synthetic peptidoglycan polymers yields this hypothetical lattice structure reprinted from Meroueh *et al* 2006 and supports the spring-like organization of rigid glycans (orange) and flexible protein cross-links (green) **b**, Hayhurst *et al* 2008 yield a coiled meso-structure via AFM imaging of cell wall peptidoglycan.

vegetative cell, the spore peptidoglycan is much more sparsely cross-linked; it contains about $1/10^{th}$ the crosslinks. This means only 3% of the total peptides are cross-linked. The remaining peptides can be accounted for as follows: ¼ of the peptides terminate in bare L-alanines, 1/4 are bulky unlinked acids (24 possible types), and half are hydrophilic delta lactams. Precise arrangement of these chains is stochastic, resulting in a somewhat cloudy nanoscale picture of spore cortex peptidoglycan.

Much of the sparse information available regarding the coordination of the cortex has come from AFM studies [63]. In one particular study (conducted in the usual hydrated conditions) we see a small 100nm window granted below the fractured outer sporecoat into what is possibly the outer crust of the cortex, which appears as a latticework of 10nm pores arranged into a hexagonal honeycomb pattern. This data can be aligned with a pre-existing peptidoglycan model on the related vegetative isoform (Figure 2.5a)[64]. This particular model is produced through examination of homogenous chains of synthetic 'peptidoglycan' with NMR and assigns geometry of sugars and peptides in a crystalline fashion, while native spore peptidoglycan is heterogeneous. The authors present a model structure to include sheets of the honeycomb-like peptides arranged in layers and connected in the z-dimension via the glycan spokes, although the spore is expected to be non-crystalline. Figure 2.4 simply serves to illustrate that the simplest arrangements of peptidoglycan produces a series of pores, on the order of a few nanometers. These pores are both flexible and rigid depending on the structural coordination of the matrix. The peculiarities among the arrangement of alternately hydrophobic and hydrophilic elements in peptidoglycan may also force water into certain behaviors.

Water has been shown to perform biological functions through structural rearrangement in the higher ordered cellular systems of many species, such as seed dispersal in pinecones [53,54,65]. In the case of sap ascent in trees, water itself can bear the force of tension to perform work — evaporation actually pulls water skyward against gravity, thus perfusing the tree through a porous network of

confining capillaries[55]. In this case, as in that of the spore's cortical paradigm, the water is said to be under negative pressure; that is, the water is tensioned [52].

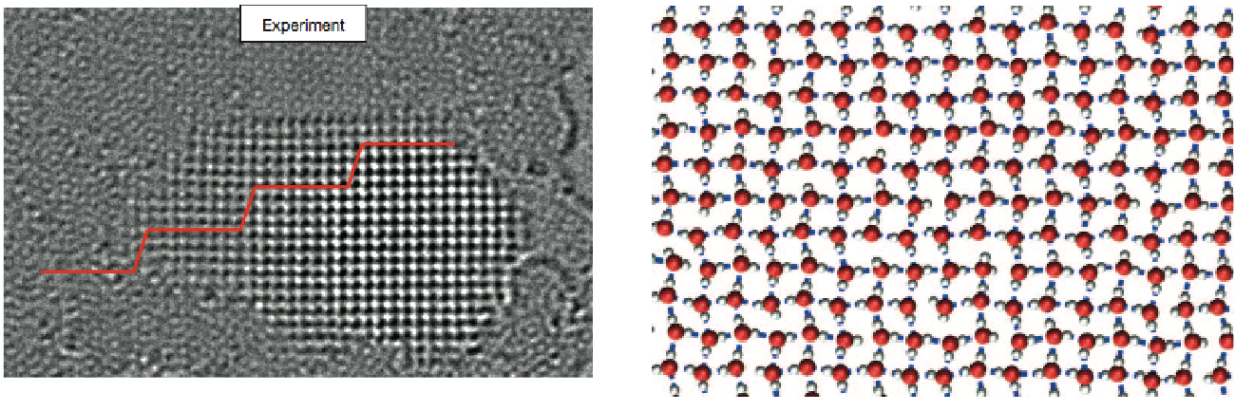


**Figure 2.6| Nanoconfinement induces dense square ice in graphene.** TEM and accompanying MD simulation of square ice appearance in graphene when between layers at ~1GPa. Adapted from Algara-Siller *et al*, 2015.

Actually, within the coat/cortex of the spore, we expect confinement on the order of 0-1.5nm (see chapter 3 for calculations and discussion of this estimated pore size, *d*). At these very small confinement lengths we expect the water to behave quite unlike the water we are accustomed to in its bulk form[54,55,65-67]. When water is restrained at the nanoscale, it can exhibit altered viscosity, and the molecules proceed toward a more immobile state[67-69]. This effect has been demonstrated experimentally in synthetic systems, such as water confined within porous clay, carbon nanotubes, and silica pores [68,69]. Nanoconfined phase shifts toward crystal ice have been modeled as between quartz surfaces when approaching two angstroms [70]. In effect, when water is trapped within a tight porous material, a dramatic slowing of its molecules' respective motion is observed. Note that ices have been observed in graphene when confined to single molecule layers (see Fig 2.6)[71].

With its unique phase-density relationship and myriad contradictions to ontological conventions, water defies physical-chemical expectations at each occasion. The hydrogen bond (HB) can be thought of as largely responsible for many of the anomalous properties of water. This interaction can be defined as a local bond whereby in the interaction X-H•••A, X-H participates as a proton donor to A. The bond energy can vary significantly over -0.2 to -40 kcal/mol[18]. Water is quite unique among H-Bonding molecules due to the two lone-pair electrons on oxygen. This geometry allows for up to four bonds formed at any given time as is found in traditional hexagonal ice. The H-bond strength and multiplicity is therein responsible for liquid water's relatively lofty boiling point and solid water's diminished density. A recent paper from by Ceriotti *et al.* suggests that the quantum state of hydrogen-bonding protons in water can necessitate many observed oddities in nanoscale character[72]. They imply that much of the reported ordering from the nano- to meso- scales may derive from perturbations in a vast quantum hydrogen-bonding network. In such a case, the strength of the molecule comes from the whole of the bulk. H-bond fluctuations are limited or enhanced in such a way that the network may assume a new order and the result could be seen macroscopically as a phase or density aberration.

Extreme conditions of confinement can lead to immobilized layers of crystalline water; essentially providing for a phase change in violation of traditional phase/temperature relationships for this magic molecule. Maheshwari and colleagues (2013) eloquently illustrate this phenomenon in a model system where water is nanoconfined between layers of clay, marking the first observation of a phase transition above the bulk freeing temperature of water[9]. This occurs in the temperate region, thermodynamically, between 280 and 290K. In addition to this novel finding they suggest the presence of an additional low temperature transition (~240K), symptomatic of partial freezing of the confined water. Perturbations of the HB network due to lack of exploratory freedom by individual molecules would lead to an inability to complete the crystal arrangement necessary for hexagonal ice.

In their experiment, the team uses NMR to retrieve chemical shifts and transverse relaxation times for the confined water protons relative to bulk phase. They correlate their findings to data obtained from identical parameters through positron annihilation spectroscopy (PAS), making the identification of these new phase transition points a very compelling statement. A separate evaluation of the pros and cons of various water modeling MDs is given by Mao *et al.* (2012)[11, 12]. Generally, these simulations produce parameters that are best accounted for by various models. This reinforces the idea that water will behave very differently depending on its external environment.

Hu *et al.* model thermal conductance properties of water layers in a similar nanoconfined environment and detail some intriguing effects[6]. The scientists again make use of MD simulations to find that thermal conductance between two quartz surfaces is maximized at a particular length of about 2A of insulation. This is an interesting finding, in that this is approximately the length of confined frozen water under the conditions in their simulation, while considering the alignment of vibration states between the water and the hydrophilic quartz surface hydroxyls. It is of particular importance that in the optimally confined conditions, the authors indicate that almost all of the water molecules HB with at least one of the silanol head groups on both surfaces. This interaction across the interfaced HB network creates glue that effectively forces the water into a more solid-like, less diffuse state.

These data are suggestive of the aberrant behavior of confined water are fascinating, in particular the ability of water to undergo a phase transition and appear frozen above the bulk freezing point. However, thus far we have not been able to empirically phrase the degree to which water molecules are immobilized as confinement is systematically imposed. That is to say that it is difficult to tune and adjust the confinement length experimentally, and so simulations often prevail as the dominant research. Chivazzo *et al.* provide this piece of puzzle by modeling the boundary conditions

of related nanoconfinement through a series of molecular dynamic simulations and produce a scaling factor to describe observed decreases in diffusion constant as the walls close in on the water molecules. For this modeling, they make use of nearly 60 separate cases with varied size and surface architecture of nanoparticles, nanopores, proteins, and nanotubes. Additionally, they are able to fit results from many studies in the literature including silica nanopores (Milischuk, 2011), carbon nanotubes (Liu, 2005) and myoglobin (Makarov, 1998). All together they are able to produce a single linear scaling element to describe the self-diffusion of water in confined geometries. Their scaling parameter is introduced as the ratio between the total water volume of influence and the total volume accessible to the water molecules. This parameter, $\theta$, therefore ranges from zero in bulk water to one in totally confined, icy molecules. As external validation, the scientists use their approach to accurately predict MRI relaxivity of iron oxide nanoparticles embedded in mesoporous silicon substrates. Each of these findings are particularly noteworthy when one considers the standard behavior of water under pressure in bulk. Taken together we obtain a very wide and complete view emerges of how water readily loses its liquid/vapor nature when backed into a corner. But confinement is not the only physical constraint that specifies anomalous water behavior.

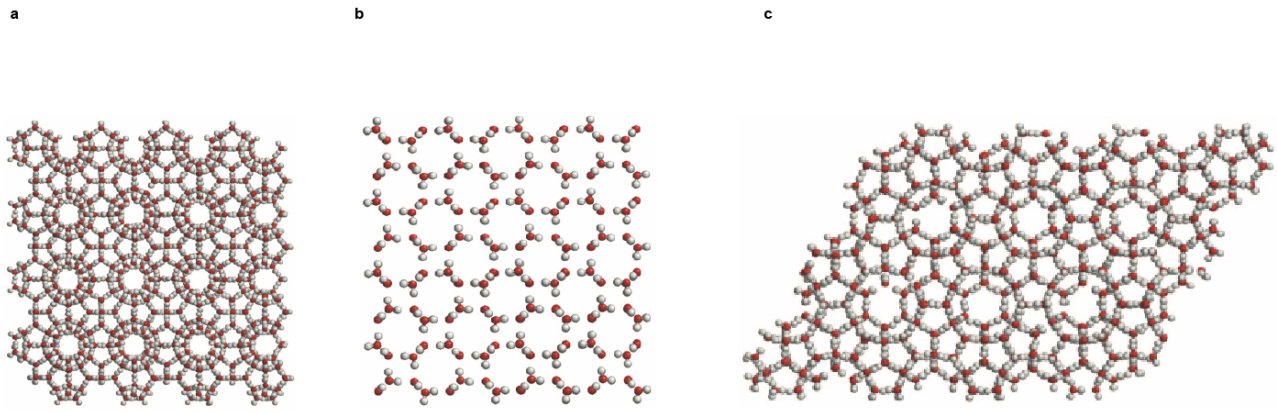


**Figure 2.7| Proposed structures of negative pressure ices** adapted from Conde *et al* 2009. **a**, empty-hydrate type sI with disordered proton **b**, type sII with disordered protons and **c**, type sH with disordered proton

It has been long understood that water under extremely high pressures can lead to decreased densities and these conditions predict "ice" to exhibit abnormal crystal structures (see Fig 2.7)[5]. Many of the models used to examine these configurations have recently been turned toward the examination of lattices available at negative pressures as well. The TIP5P series of models, based on five-site coordination has been found success in predicting thermal conductivity, sheer viscosity, and temperature trends but not specific heat[11]. Stanley *et al.* (2002) initially used this modeling algorithm to examine the effects of negative pressure on phase. The authors concluded that when water is stretched there was a minimum density available and that this corresponded to ice. In their model, further tugging across the molecules leads to H-bond destabilization and a reanimation of local self-diffusion[17]. In other words, there is a distinct threshold to the loss of the solid phase and this must be considered.

Later in 2009 a study was published with a synergistic algorithm, which combined favorable aspects of the TIP models (see Fig 2.7)[5]. These authors take the discussion one step farther by examining the configurations of various hypothetical ices in negative pressure regimes. Their new model allows them to imagine hypothetical ice lattices, such as hydrates with the seed (guest) element

removed. They are also able to provide several hypothetical phase diagrams. The key features of each negative pressure ice are (1) densities below that of traditional Ih ice [i.e. the most stable phase for that temperature in bulk] and (2) virtual negative pressure ices do not obey the traditional hexagonal lattice arrangement and are subject to intramolecular rearrangements [i.e. proton disorder, loss of tetrahedral architecture]. Interestingly, the author's novel modeling algorithm predicts the presence of standard ice during extremely pressures down to nearly -4000 bar before phase condition makes the shift into type sII, a lower density lattice based on an empty hydrate shell. This stands in contrast to the TIP5 model, for which they also provide a phase diagram comparison (see Fig 2.8 for comparison of various hypothetical ices). In the traditional TIP5 we see a more heterogeneous blend of phases, with ice i' dominating at most temperatures and moderate negative pressures. This is not remarkable, as i' was among the first predicted negative pressure ice, based on lattices inferred "accidentally" from crystallography data[5].

In 2012, Azouzi corroborated the plausibility of the TIP5 series via cavitation threshold via experiments on water inclusions in quartz[1]. They conclude the line of density maxima, prior to cavitation, peaks at 922.8 $kg/m^3$ for ambient temperatures. This finding implies a new constraint for the minimal density of negative pressure ices. For instance, many of the hypothetical empty hydrates from the models by Conde *et al.* would be violate this experimentally defined parameter. In other words, the H-bonds in water molecules are shown to tear apart, yielding vapor at the low molecular density required for many "virtual ices." This leaves us largely to the classically modeled dataset, and the ice i and i' arrangements. Interestingly, and perhaps satisfying previous discussions of H-bond proton shuttling, protons of these ices are predicted by the TIP5 simulations to be of regular order[2]. It could be extended that fluid proton nature of the H-bond network in liquid phase water is perturbed

| Phase | $N$ | $\rho$ (g cm$^{-3}$) | $\frac{A_{sol}}{Nk_BT}$ | Phase | $N$ | $\rho$ (g cm$^{-3}$) | $\frac{A_{sol}}{Nk_BT}$ |
|---|---|---|---|---|---|---|---|
| | TIP4P/2005 model | | | | TIP5P model | | |
| II | 432 | 1.175 | −25.563 | **II** | **432** | **1.254** | **−23.054** |
| XI | 360 | 0.928 | −25.898 | XI | 360 | 0.994 | −22.827 |
| **Ih** | **432** | **0.928** | **−26.252** | Ih | 432 | 0.992 | −22.968 |
| ice i | 1024 | 0.874 | −25.315 | ice i | 1024 | 0.934 | −22.827 |
| ice *i'* | 1024 | 0.874 | −25.327 | ice *i'* | 1024 | 0.934 | −22.829 |
| sI | 368 | 0.819 | −25.672 | sI | 368 | 0.871 | −22.317 |
| sII | 1088 | 0.807 | −25.720 | sII | 1088 | 0.862 | −22.420 |
| sH | 408 | 0.788 | −25.528 | sH | 408 | 0.840 | −22.156 |

**Table 2.8| Virtual ices and their predicted densities** from Conde *et al.* (2009). Comparison of new integral TIP4P/2005 model with the TIP5P model for various ices, possibly suggesting parameters for configuring solid phase occurrences in "stretched-water" negative pressure conditions.

by the opposing forces of negative pressures and crystallizes under favorable, though expanded and perhaps somewhat unexpected, thermal conditions. Together these data provide a view of water as a fluid H-bond mosaic, which can seize up into different arrangements depending on how it is uniformly pulled or compressed. Once more we can begin to see how these principals could appear in nature and perhaps our own bodies. Consider the negative pressure systems within trees that allow the transport "pulling" of water from the very depth of root systems, hundreds of meters into the sky. In Chapters, 3 and 4 we shall see that the spore, too utilizes negative pressure to its advantage.

Bulk water when cooled can order into hexagonal lattices largely due to the tetrahedral nature of its intramolecular geometry during hydrogen bonding. This crystal structure requires more space than the disordered liquid form and the resulting phase displays decreased density. Recently, it has been hypothesized that a similar ordering of molecules could occur in single molecule layers with tight proximity to a hydrated substrate. It is fascinating to imagine implications of this principle on the local density of water at these interfaces. Work by Kimura *et al.* demonstrates this effect through

frequency modulation analysis during AFM scanning[8]. The team used this technique to acquire convincing layer-by-layer virtual images of this effect on a silica substrate.

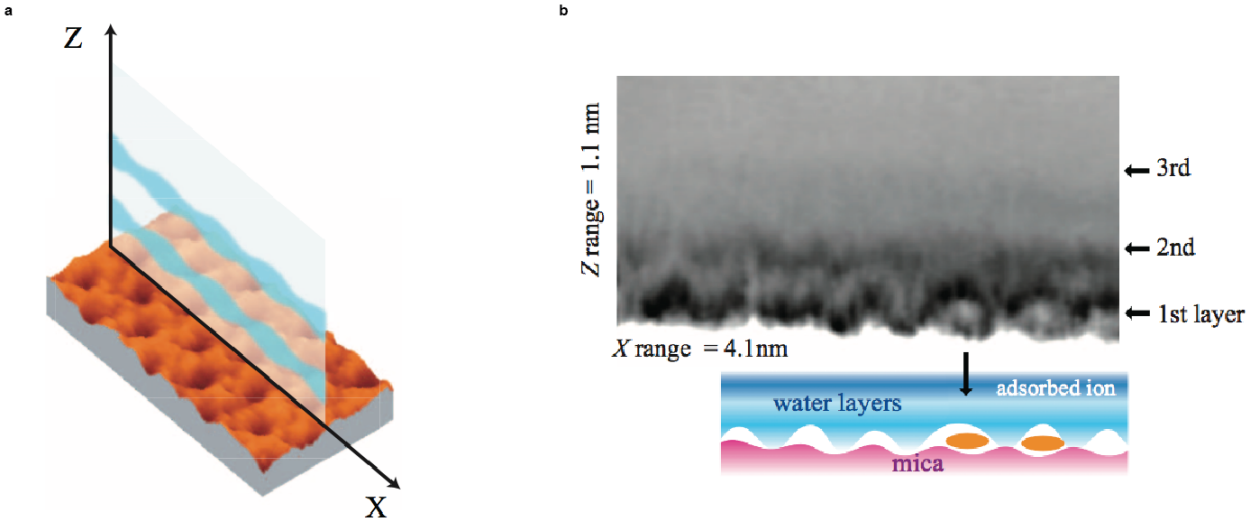


**Figure 2.9| Visualization of ordered water at a surface** adapted from Kimura *et al* 2010. **a**, basic setup illustrating the scanning orientation for **b**, where we visualize the presence of force layers and presence of ionic impurities.

The experiment was performed after Jarvis *et al.* 2000 discovered that while an AFM tip, oscillating in tapping mode, approached a solid surface in liquid water, there was a notable repulsive effect that seemed to be separated into regular steps of resistance[7]. These steps of force dissipation turned out to yield a theoretical solvation shell separation of 2.2A; a value within reasonable bounds for the size of single water molecules. Kimura expanded these findings twofold by manipulating the substrate and solution as well as creating a two-dimensional representation of the effect by scanning in the X-range for several nm in addition to the approach Z-range of approximately 1.1 nm. At the SiO2 surface, there is some charge where Al has replaced one in four of the Si atoms. As the water interacts with negative charges, a contrast is readily observed. Because this muscovite/mica substrate crystal surface is arranged in a hexagonal lattice, there is a heterogeneous density distribution of molecules in the respective hydration shells mirroring this arrangement. This is, of course, a result of

charge interactions between the water and substrate. At the first hydration layer, new forces arise, such as Coulomb interactions and van der Waals forces, which perturb the traditional thermal properties of the water molecules from those observed in bulk[4]. The effect is most visible at the first and second layer. In addition to these observations, the researchers introduced 1M potassium chloride into their aqueous solution. The potassium ions are adsorbed onto the substrate and induce a noticeable regular effect on the hydration shells. This may be thought of as a surfactant-like interaction. Finally, they conclude by repeating their imaging motif on a crystalline array of biomolecules, using the bacteriorhodopsin from the archaea bacterium *Halobacterium salinarum*. The lattice here is crystalline, unlike what would be found in a bacterial membrane.

Given that this hydration shell ordering can be observed with controlled crystalline biomolecules, how might anomalous water behavior manifest in biological systems? Martin Chaplin of the University of South Wales a long history of studying anomalous water behavior with respect to biology and publishes a regular review in *Nature* and an extensive website discussing biological implications of water in nature (see Fig 2.10)[73,74]. In one particular example, Sheikh and Jarvis examine bio-interfaces via membrane hydration in lipid rafts[16]. These studies were performed with artificial lipid membranes and underscore the important principal that differential arrangement of lipid head-groups in the membrane can dictate patterned ordering of water at those interfaces. In short, lipid rafts are regions of the cell membrane that exhibit increased solid phase behavior and are thought to contribute widely to surface molecule aggregation and myriad signaling applications. The authors hypothesize that the specific size and arrangement of these rafts is, in turn, specified in some part as a result of the hydration shell ordering. For instance, these two-layer hydration shells are observed only at the raft-water interface and within a 10nm annulus surrounding the raft, but not at the raft-

nonraft border region. An implication of this observation is that the ordering of water might limit the closest distance of adjoining rafts to 20nm as well as the actual size of the rafts themselves by preventing coalescence. Additionally, this effect might slow the lateral diffusion rates of raft components as well as providing a non-negligible energy barrier to certain extracellular protein domains. This is not to say that the hydration layers would prevent external protein interactions but

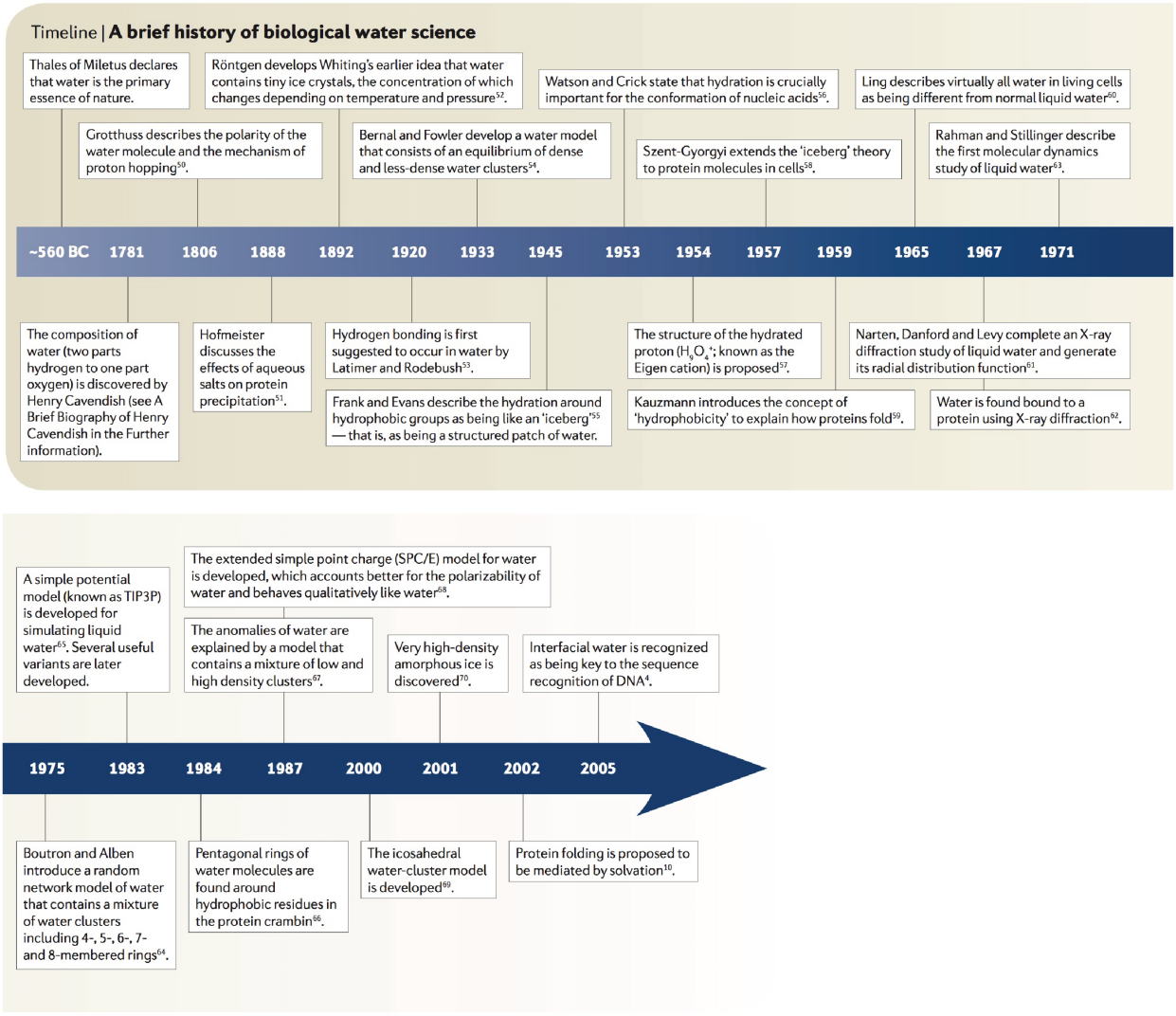


**Figure 2.10| Ordered water in biological sciences** from Chaplin, 2006. Life cannot exist without water, and it was soon discovered that hydrogen bonding produces a wide array of anomalous behaviors relevant to biology including 'iceberg'-like hydration structures around hydrophobic groups, pentagonal ice rings in protein folding, and is involved DNA-sequence recognition by transcription factors.

that they are certainly affected in terms of localization and kinetics. All told, the authors provide an intriguing example of how biology makes use of ordered water.

Based on the results of these studies one is compelled to imagine that anomalous behavior of water at surfaces and in relation to organic compounds may have vast implications in biology. Indeed, water transport itself is tightly regulated in the body and diseases have been known to arise from subsequent disregulation[19]. This has been extensively detailed through the understanding of aquaporins[75,76]. Aquaporins actually provide a single file squirt-gun like effect where water is transported much faster than diffusion and viscosity is lowered significantly. Furthermore, water diffusion is an integral aspect of diagnostic medicine, as evidenced by techniques such as diffusion magnetic resonance imaging (MRI). A 2004 study by Paran *et al.* describes how in a xenograft model of breast cancer, the response to anti-estrogenic drug, tamoxifen methiodide (TMI), can be monitored through changes in volume fraction of slowly diffusing water[13].

Water is in fact observed to be involved in biological communication and signalling[74,77]. Cells may indeed transmit information through water structures at great speeds through quantum delocalization, which makes for a much faster electronical communication when compared to long-range diffusion. An example of this is shown in electron transport where water structures mediate charge transfer[78]. Sequence recognition of DNA has been shown to be highly dependent on in the interfacial water structures which mediate the interaction[79]. In general, water organizes biology, which organizes water as into patterns and structures[80] to help perform more biology.

In fact, within the spore we see all of the criteria for anomalous water behavior: patterned hydrophobic/hydrophilic surfaces, nanoconfinement, and negative pressure. Water physics has recently been implicated in spore resistance to UV and peroxides[81]. Spore biology increasingly

demonstrates the need to look beyond simple diffusion in order to understand the mechanics of the spore lifecycle. Water's physical state may offer this explanation[43].

In summary, the spore is a dormant phase in the lifecycle of an ancient bacterial lineage, and this gives us a window into conserved biological mechanisms of the earliest evolutionary periods available to history. Spore-forming bacteria live in an intimate harmonic relationship with water throughout their dormat and waking life. Using water they are capable of dramatic cellular rearrangement in response to the ambient hydration conditions. These kinetics result from tension-relaxation dynamics between the spore surface (i.e. coat/cortex) and the water's diffusive potential in air (relative humidity). This spore-water, being nanoconfined and highly tensioned, is expected to behave divergently from an idealized gas/liquid. The divergent behavior or water under the conditions found within the spore can dramatically affect water transport and therefore the stability of biochemistry. Thus, physically extreme conditions within the spore can be expected to promote anomalous water states that may play a role in dormancy.

# Chapter 3: (S)poroelastic Water Transport

We have to this point seen how the spore evolved hydromechanical abilities. The cortex/coat structure acts through some yet undetermined mechanism in the developmental dehydration of the core during sporulation to ensure long-term dormancy. Deuterium NMR has shown that the remaining core water is inaccessible to external exchange with atmospheric water while the spore is dormant[57]. It is furthermore known that the first macroscale phenotypic observation in re-activation of the organism is the rapid increase in core-water content from less than 25% wet weight to greater than 80%[16]. Also, the spore retains the ability to change its size in response to humidity gradients[47], which can also affect its ability to germinate[45]. Overall, water itself and the hydromechanical action by spore's outer-most structures, primarily the cortex and coat, appear to play a significant role in the stabilization of dormancy and life-cycling of the spore-forming bacterium. This chapter outlines experiments and theory utilized to understand transport kinetics, and detail water's physical state.

In order to better understand the internal spore water itself, as well as how the outer spore-structures interact with this water, a high temporal-resolution microcantilever sensor system was developed. Microcantilever sensors have been studied previously for use in antibiotic resistance diagnostics[82] and even to study other aspects of spore-water transport[83]. The basic principle is illustrated in Fig 3.1, where spores are coated onto one side of a traditional AFM cantilever. The microscale deflection of the cantilever is amplified by an AFM laser-photodetector system and is produced by the nanoscale contractions of the spores as they experience humidity cycling. While the cantilever itself does respond also to the bilayer heating effect, these responses are extremely fast as the cantilever cools quickly[84] compared to the relaxation of the spores, so this effect is negligible and not limiting.

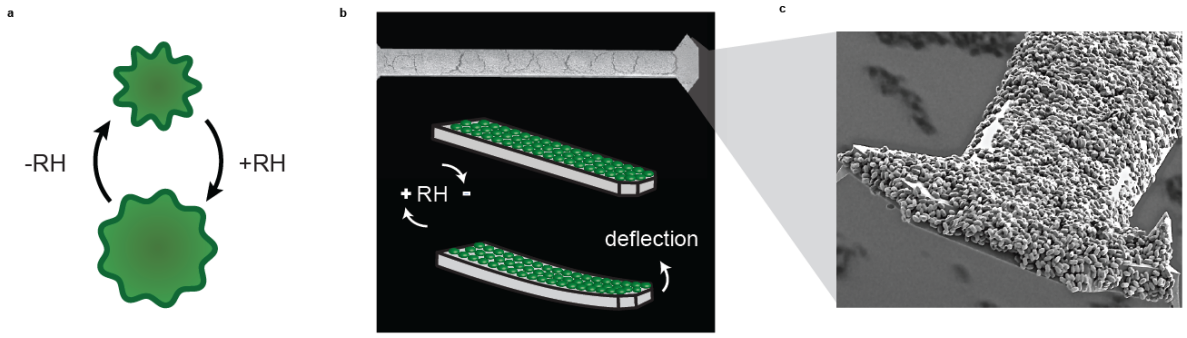


**Figure 3.1| Microcantilever design for studying spore water transport.** **a**, spores change shape rapidly when equilibrating in the presence of humidity gradients. **b**, Traditional AFM cantilevers are unilaminally coated in spores and their physical size change at the nanoscale results in deflection at the microscale (cantilever is ~200 μm in length). **c**, Cantilever tip is shown coated with spores through electron microscopy (SEM).

Cantilevers are coated with spores on only one side with a traditional airbrush spray-gun to produce the desired bi-layer actuation. The spores naturally adhere to cantilevers. The spore suspension is centrifuged to pellet the cells, whereby they are mixed 1:1 in water/ethanol before deposition. A bottled nitrogen air source is used to maintain a clean mixture devoid of contaminants and the cantilevers are stored in clean boxes. In order to secure the absence of spores on the backside of cantilevers, a donor cantilever chip was used as a mask, although several other masks were attempted in arriving at this protocol (see Fig 3.2).

In order to adjust the hydration parameters in contact with the spores atop the cantilevers, the entire AFM is housed inside of an environment control unit (ECU). A stream of air is directed into the ECU opposite the AFM to vary the RH. Humidity is controlled by mixing dry air (~ 5% RH) provided by a laboratory air source with humid air (>90% RH) generated by passing the laboratory air through a bubbler (An air-stone from JW Pet Company is used to bubble air into water in an Erlenmeyer flask). A variable power computer fan is positioned approximately 10cm from the

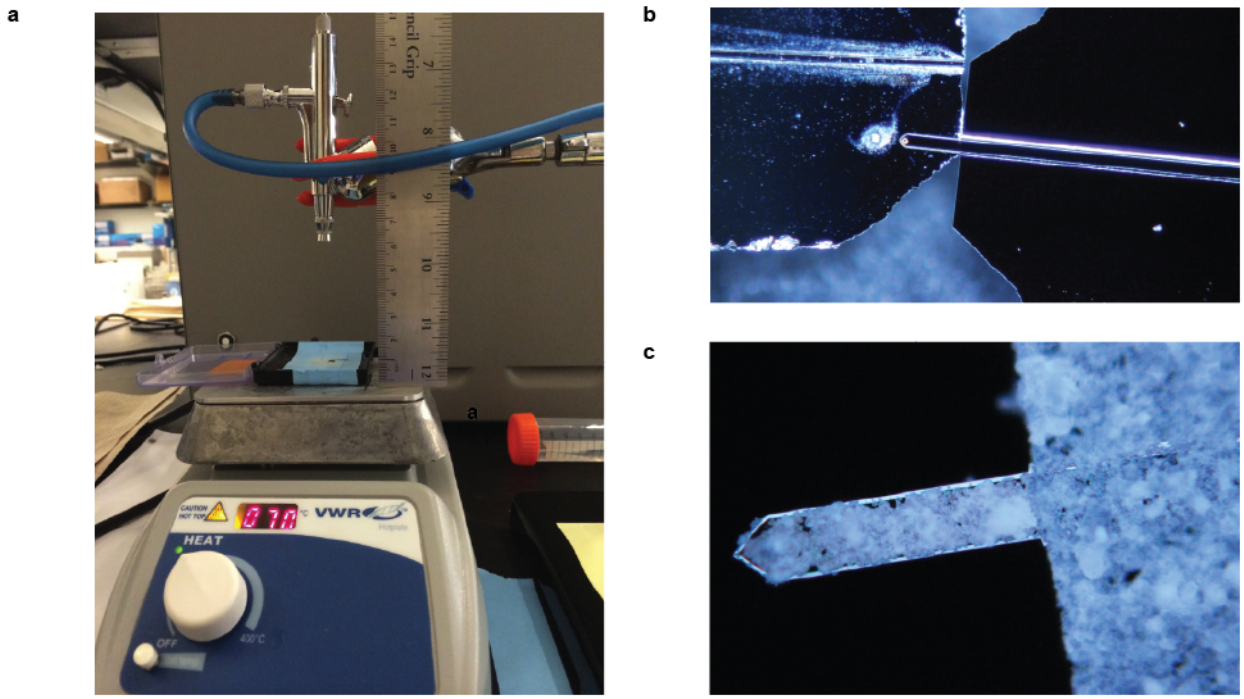


**Figure 3.2| Spray coating of cantilevers.** a, The air-brush spray-gun is positioned above the cantilever to be coated, which is masked with a donor chip as in **b**, to produce a unilaminal coating as shown in **c**. Note the cantilevers shown in these panels are not of the dimensions used for the majority of the data collection and are specific to the preliminary set-up and AFM system used within that setup.

cantilever to facilitate evaporation and air mixture near the spores. A mild fan setting producing an air speed of 0.2 m/s is used, as further increases in fan power does not alone affect the time constants observed (see Chapter 4 for a more detailed schematic of the ECU). The fact that the fan did not affect time constants alone, further reinforces the importance of pore size in scaling the transport speed.

In order to evacuate the internal spore water so that kinetics could be observed, a variable power fiber-coupled 1000mA LED of wavelength 455nm (Thorlabs, Newton, NJ) is used to rapidly evaporate water from the spores and control cantilevers (see Figure 3.3). The LED provides ~ 1ºC change at the cantilever surface, and because temperature affects vapor saturation exponentially, this slight heating provides a dramatic change in the internal water content of the spore. The LED is

manipulated with a photography focusing-rail slider coupled to a stereotactic manipulator scavenged from a microscope stage such that the heat source may approach the cantilever within <1 mm. The LED is positioned so as to allow maximal evaporative deflection. Finer manipulation and alignment of the LED to the cantilever is accomplished with endoscopes embedded within the ECU and positioned at the side and above the Multimode head. LED power is scaled manually such that the weaker deflection during dry conditions is comparable in amplitude to that of the more wetted conditions.

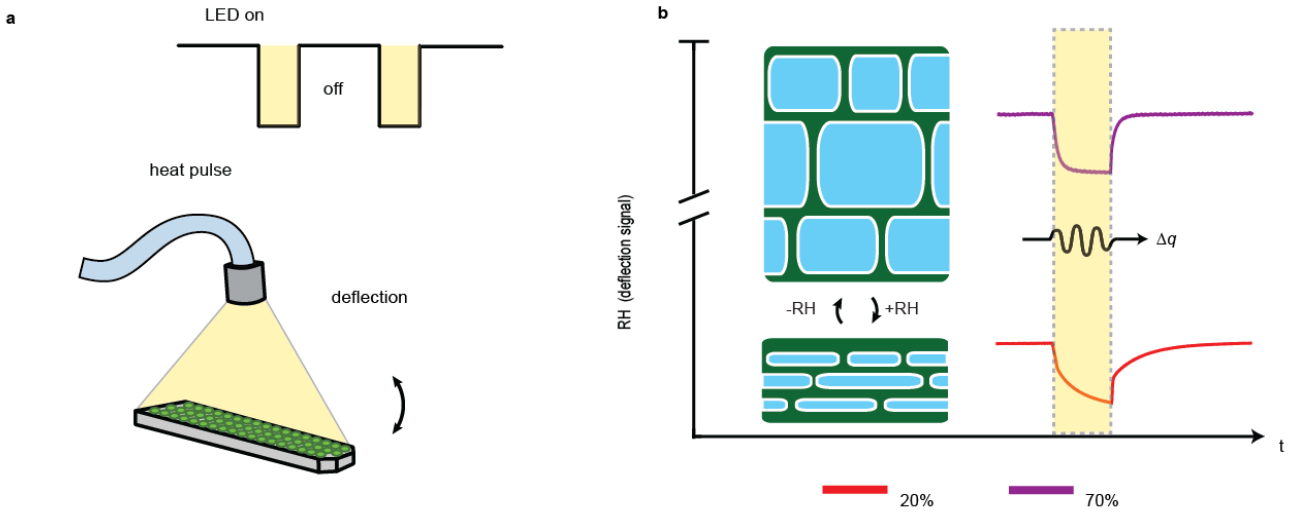


**Figure 3.3| Basic micro-sensor system for studying water sorption during hydration re-equilibration of spores.** **a,** LED is pulsed to rapidly evaporate water from the spore's outer coat and cortex. The inner core is inaccessible to external water. **b,** the spore dimensions change at different relative humidity set-points, and this results in different transport kinetics.

A Labview routine times the triggering of the heat-pulse LED, as well as collects cantilever deflection, humidity, and temperature data. Phase shift signal, an indicator of mass exchange, is calculated in Labview in real-time. Data acquisition is timed via an external function generator and sampled with 5ms resolution once temperature and humidity are stabilized within +/- 0.5%/ °C. A

three-second loop-time is utilized to allow ample re-equilibration of the cantilever under the slowest conditions. Five signal loops, consisting of a 600ms LED pulse, followed by a 2400ms recovery period are integrated.

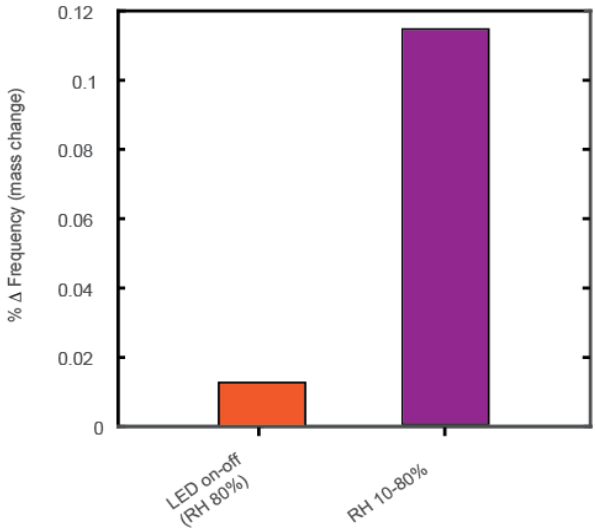


**Figure 3.4| Thermal pulse mass displacement response versus wide humidity range.** The fundamental frequency of a cantilever coated with spores is shown in two water exchange cases: (left) water mass displacement as a result of thermal pulse and (right) in response to full range humidity indicating that the evaporative perturbation deviation from set-point is low relative to overall chemical potential available to the study.

The relative magnitude of the photothermal effects on the chemical equilibrium state between the environment and porous spore material is shown in Figure 3.4 as characteristic cantilever frequency shift (spore water mass displacement) versus the total water uptake available throughout the experiment. As is clearly depicted, the evaporative perturbation from the heat source, even in the most hydrated environment, produces a minimal mass displacement and allows maintenance of the set-point humidity for data collection at each step throughout the course of the study.

As evident in Figure 3.3b, the speed of sorption in wet conditions is much faster than that of dry conditions. This is, in fact, quite different from what would be expected were the spore simply a bag of water-vapor responding diffusively to the outside moisture. In such a case, the relationship between the time of sorption and the chemical potential available (external relative humidity), would be linear, and opposite in polarity such that restoration of chemical equilibrium in dry conditions would be faster (less water to transport). In fact, we observe the opposite with the spore sorption. In the spore, dimensional changes of the pore

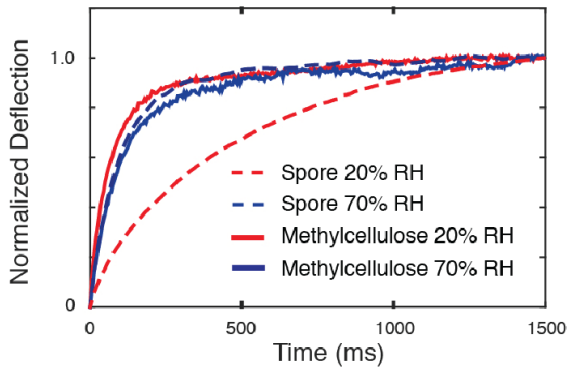


**Figure 3.5| Spore transport versus alternative biopolymer transport.** Methylcellulose also produces an actuating effect as shown above, however, it's internal dimensions do not expand appreciably with humidity, unlike the spore, thus the speed is not attenuated as noticeably in the dehydrated state when compared to the spore. Actuation is very fast for methylcellulose, indicating good exposure to atmosphere.

appear to result in faster transport as the pores are opened, and because this effect is non-linear there appears to be some contribution from the fluid to hydraulic resistance as well.

Several control organic polymeric substances were examined via the water-transport cantilever sensor apparatus, including dextrose and methylcellulose (Figure 3.5). Because response speed seemed releatively fast in both hydrated and dehydrated conditions, it was inferred that the spore was behaving uniquely to limit water exchange. In order to understand if the spore peptidoglycan alone could recapitulate this effect, this material as isolated from several species was examined, courtesy of Dr. Simon Foster (University of Sheffield, UK). Interestingly, the isolated peptidoglycan was also able to produce an actuating effect, but failed to induce the wide ranging differences between transport in wet and dry conditions. Again, this confirms that the dimensional changes during hydration are affecting the speed of transport but differently than within the intact spore (see Fig 3.6).

In the spore, quite differently from purified materials, the humidity indeed appears to speed up

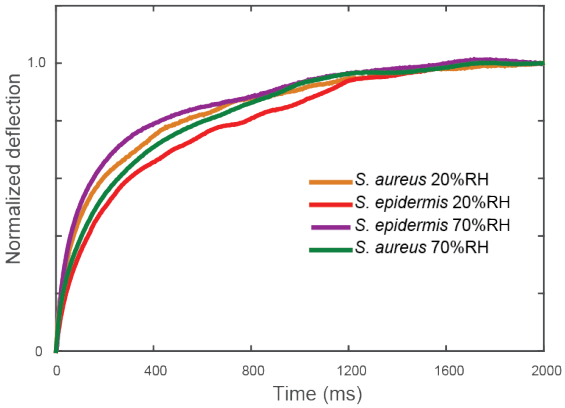


**Figure 3.6| Transport kinetics of isolated peptidoglycan from several species.** The purified cell wall materials also respond to evaporation to produce an actuation and transport of water can be measured, however no appreciable differences could be seen between dry and wet conditions. Generally, the response time was very slow for these materials, indicating that they provided poor atmosphereic exchange.

water transport non-linearly (see Fig 3.7). The sorption curves actually follow an exponential decay function, similar to the charging of a capacitor, and so we can think of the non-linear shape analogously, where the hydromechanical re-charging (sorption) is limited by the capacity of the spore to hold water (humidity-state dependent as in Fig 3.7b) and some physical resistance of the water's flow (either hydraulic or electrostatic). For a capacitor charging event this 'swelling' time could be described as $t \sim RC$. Because the spore's water transport does not depend directly on its ability to hold water (capacity), there must be some resistive contribution of the water to its swelling time. Fortunately, for a porous material, such a theory has been developed, which can illuminate these viscous contributions to swelling.

Poroelastic theory was developed by Belgian-American engineer, Maurice Anthony Biot, to aid petroleum engineers in their efforts to maximize fluid flow from porous rocks. The general theory is essentially a derivative of Darcy's law. In this form, it can be summarized as the change in fluid pressure with respect to time being dependent on the pore size, d, and the pressure propagation per displacement depth as follows:

$$\frac{\partial \mathrm{P}}{\partial \mathrm{t}} = -\frac{\mathrm{B}\mathrm{d}^2}{\mu}\frac{\partial^2 \mathrm{P}}{\partial \mathrm{x}^2} \tag{1}$$

where $\mu$ is the viscosity of the fluid, and B is bulk modulus of the resistive medium[85]. Note that ($\geq$2-6 Gpa), we treat this as the spore's modulus which we derive experimentally later in the Chapter.

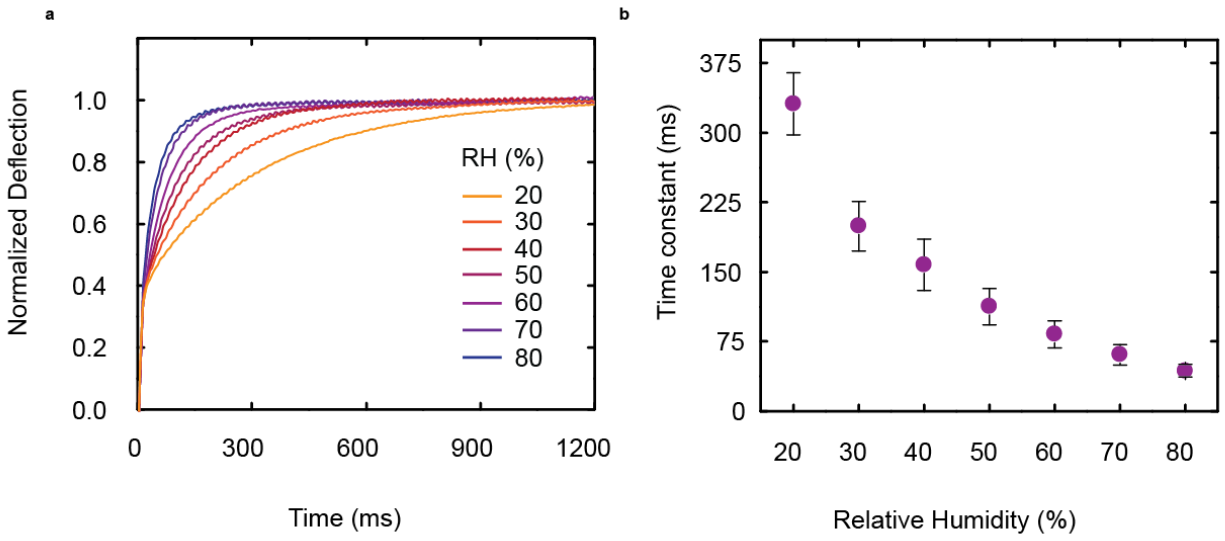


**Figure 3.7| Humidity-dependency of sorption time is non-linear. a,** Humidity is fixed to some setpoint value and then after photo-thermal perturbation, response kinetics of water transport are shown, such that swelling is faster in wetter conditions. **b,** Transport time constant for each humidity state shows that this relationship is non-linear, and so the water transport speed appears to be affected by pore dimension changes as well as the effective viscosity of the water. n=7 cantilevers, error bars are standard error of the mean.

This theory allows us to treat internal spore water vapor-pressure in a diffusive manner, such that it propagates into the spore over time as the spore re-equilibrates to the ambient external environment.

The poroelastic time can then be simplified as

$$\tau \sim \frac{\alpha L^2}{D_p} \tag{2}$$

which depends on poroelastic diffusivity, $D_p$, the thickness of the region over which pressure spreads, $L$, and $\alpha$, which is a prefactor that depends on the geometry of the system.

In this work, experimental time constant is determined by fitting normalized deflection signals with an exponential decay function. We examined phase signal versus deflection signal and at this timescale (<1s), the transport kinetics produce identical time constants. As such, we assume that the

deflection signals are proportional to the amount of water released from the spores, and we can determine an approximate relationship between the response time, diffusivity, and the thickness of coat and cortex layers. This is accomplished by solving the appropriate diffusion equation with the following mixed boundary conditions: (1) concentration (pressure) is constant at the outer surface of the spore and (2) no diffusion (spread of pressure) takes place across the core/cortex interface, i.e. an insulated boundary. Although the spore has an approximately circular cross section, we approximate the coat and cortex layers to be flat because the thickness of these layers is about three times smaller than the spore radius. By solving the one-dimensional diffusion equation (with pressure propagation instead of mass transfer) with these boundary conditions, one can show that the relative pressure in the spore is given by the following expression:

$$\Delta P(t) = 1 - \sum_{n=0}^{\infty} \frac{8}{\pi^2(2n+1)^2} e^{\left(\frac{-D_P(2n+1)^2\pi^2 t}{4L^2}\right)} \tag{3}$$

Here $\Delta P$ is the relative mass of water ($P_t/P_\infty$), $t$ is the time after a photo-thermal pulse, $n$ is an integer, $D_P$ is the poroelastic diffusivity, and $L$ is the total thickness of the coat and cortex layers. Numerically evaluating this expression and determining the time point when pressure reduces to 1/e gives the approximate relationship for time constant $\tau$ where $\alpha$ is 0.32. This allows proper scaling of $D_p$. This is important for where $D_p$ is also related to the properties of the porous material and the pore fluid such that

$$D_p \sim \frac{Ed^2}{\eta} \tag{4}$$

where $E$ is the longitudinal elastic modulus of the poroelastic material, $d$ is the effective pore diameter, and $\eta$ is the viscosity of the fluid. The longitudinal elastic modulus $E_L$ is related to the shear modulus $G$ and Poisson's ratio $\nu$ as follows:

$$E_L = \frac{2G(1-v)}{1-2v} \tag{5}$$

Poisson's ratio scales the shear modulus between radially and longitudinally expansive materials such as a rubber (0.5) to cork (0). To estimate the value of $E_L$ as a function of relative humidity, we take advantage of another parameter, $H$, that can be directly determined from the relative humidity dependent spore height measurements. $H$ relates changes in pore fluid pressure to the relative change in volume. $H$ is given by:

$$H = \frac{VdP}{dV} \tag{6}$$

Here $V$ is the volume of the poroelastic material and $P$ is the pore fluid pressure. $H$ can be expressed as:

$$H = \frac{2G(1+v)}{3(1-2v)} \tag{7}$$

Hence,

$$H = \frac{(1+v)}{3(1-v)} E_L \tag{8}$$

Note that for typical values of $v$, $E_L \sim H$. Therefore, we determined $H$ from the changes in spore volume with the changing effective pressure of spore water. The relative change in spore volume can be estimated from the AFM-based height measurements in Figure 3.8, which show an approximately linear relationship between spore diameter and relative humidity:

$$R(\rho) \approx R_0 + \beta \tag{8}$$

Here, $R$ is the radius of the spore as a function of relative humidity, $\rho$. $R_0$ is the radius corresponding to 0% relative humidity and $\beta$ is the linear scaling ratio. Based on measurements shown in in Fig. 3.8, $R_0$ is 300 nm and $\beta$is 50 nm.

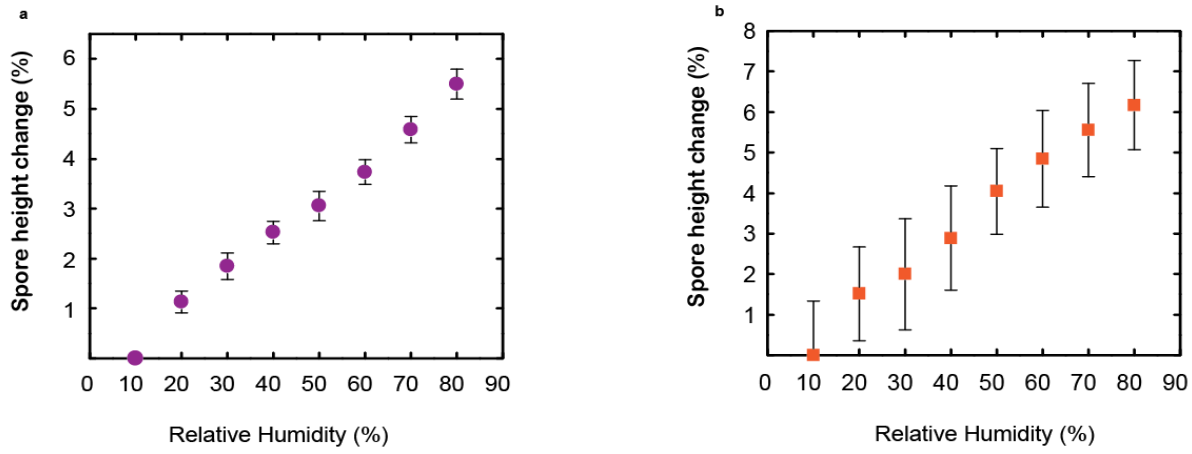


**Figure 3.8| Humidity-dependency height change is approximately linear.** **a**, WT spores of *B. subtilis* are shown as measured by height change in tapping-mode AFM. **b**, mutant spores (*Cot E ger E)* lacking most of their coat structure are shown to expand slightly more overall. n=15, error bars represent standard error.

The effective pore water pressure can be determined from the chemical equilibrium of water inside and outside the spores, which leads to the following relationship:

$$P_{eff}(\rho) \approx \frac{RT}{V_M} \ln \rho \tag{9}$$

Here $P_{eff}$ is the effective pressure of water in spore nanopores, $R$ is the gas constant, $T$ is temperature, $V_M$ is the molar volume of water in spore nanopores, and $\rho$ is the relative humidity. Although molar volume can vary slightly with effective pressure, we approximate it as constant for simplicity and use $V_M = 18$ cm$^3$.

This relationship can be derived from the standard Gibbs relationship for chemical potential

$$\mu_w \sim RT\ln[A] \tag{10}$$

where $\mu_w$ is the chemical potential of the water, and water activity [A] is defined by relative humidity $\rho$,

$$\mu_A \sim P_{eff}(\rho) \cdot \tag{11}$$

Hence the effective pressure inside the pores is also in proportion to the relative humidity outside once equilibrium is achieved.

By differentiating $P_{eff}$ and $V$ we find the following approximate relationship between elastic modulus and relative humidity:

$$H \approx H_0\left(1 + \frac{R_0}{\beta\rho}\right) \tag{12}$$

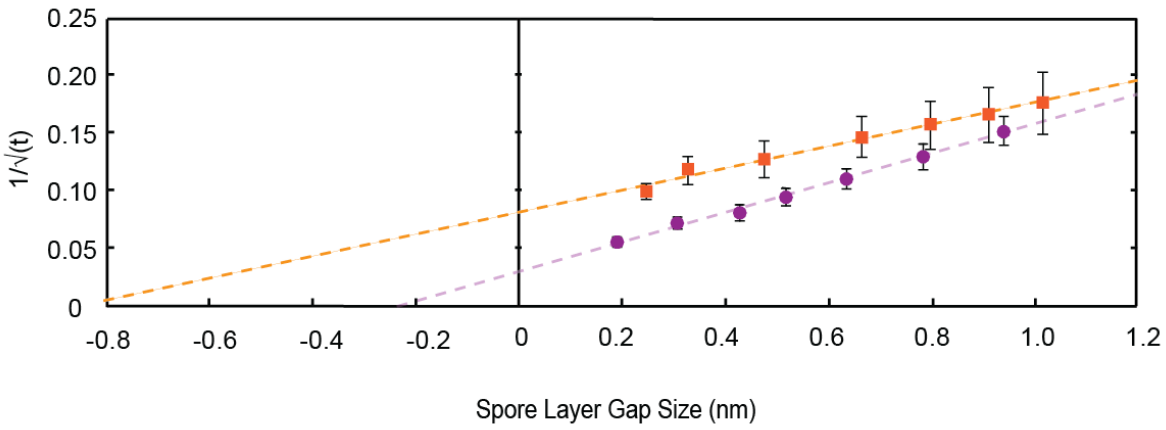


**Figure 3.9| Inverse-square poroelastic relationship in the spore.** WT spores (purple circle) are shown versus coatless mutants (orange square). Pore size tunes transport speed non-linearly. Data and standard error are derived as described in Fig 3.8, 3.11.

Here, $H_0 = 0.5RT/V_M$. Note that the above relationship diverges as relative humidity approaches 0, and it is only used for $\rho$ values between 0.2 and 0.8.

To illustrate that poroelastic theory is indeed appropriate for modeling the spore, we expect the inverse time constant to be proportional to the square of the pore diameter as it undergoes humidity-dependent swelling[86](Figure 3.9).

The effective diffusion length of water into the spore, L, is modeled as a composite of the water-responsive/accessible materials of the coat and cortex. We estimate the spore layer thicknesses from two modes of measurement using the calibrated scale bars and the ImageJ software package (NIH). First, we performed FIB-SEM on vacuum-dried WT spores and measured the depth of the cortex to be 68.82 +/- 3.35 nm. 90nm microtomed sections of the spores were produced and cortex thickness measured by standard tapping-mode AFM to be 72.72 +/-3.51 nm. Published TEM images of WT spores indicate the coat and cortex to be of approximately equivalent lengths[38,87,88]. Together,

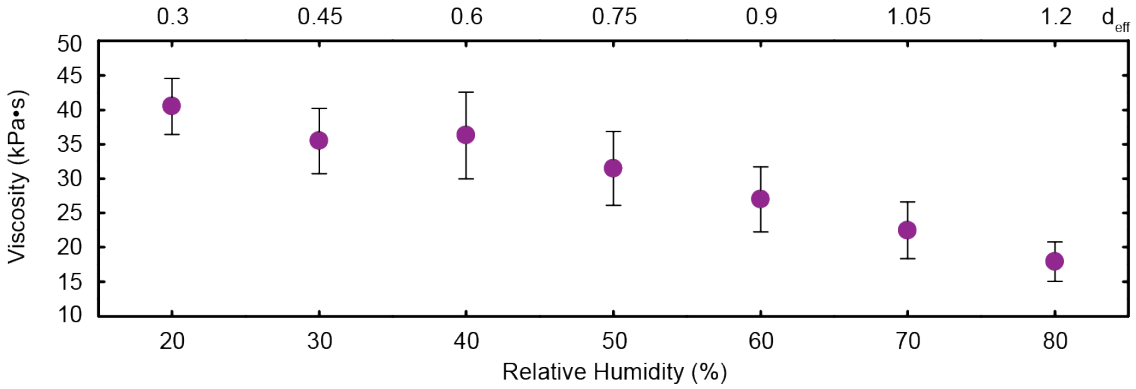


**Figure 3.10| Effective viscosity depends upon the confinement length in each set-point humidity state.** The effective viscosity at each set-point is scaled by the elasticity of the porous spore coat/cortex material. Note that the confinement length ($d_{eff}$) varies from about 1.5nm (100%RH) down to zero at 0% RH. $d_{eff}$ is estimated based on density of wet and dry spores versus total protein density as well as size exclusion of molecules through sieving effects. See the end of Chapter 2 for more detailed calculations pertaining to estimations of *d*. n=15 spores as in Fig 3.8 and error is standard error of the mean for the 7 cantilevers (data in Fig 3.7).

these measurements agree with TEM studies of detached WT spore coats indicate the coat to be approximately 66nm[89].

These analyses suggest an effective viscosity of greater than 7 orders of magnitude that of liquid bulk phase water. This of course implies that there is tremendously slow water inside of the spore, which can have vast implications on the spore biology. In essence, slow water could reflect slow general biochemistry in the outer spore layers or it could indicate localized immobilization such as lipid domains, hydrostatic cross-links, or other small-scale structures. Recent reports indicate that the viscosity of the inner signaling membrane in the spore is much greater than the vegetative form and that this fluidity is regained upon germination[40]. We also see that viscosity depends on the elastic modulus as so the effective water viscosity is different at each set-point humidity as is shown in Figure 3.10.

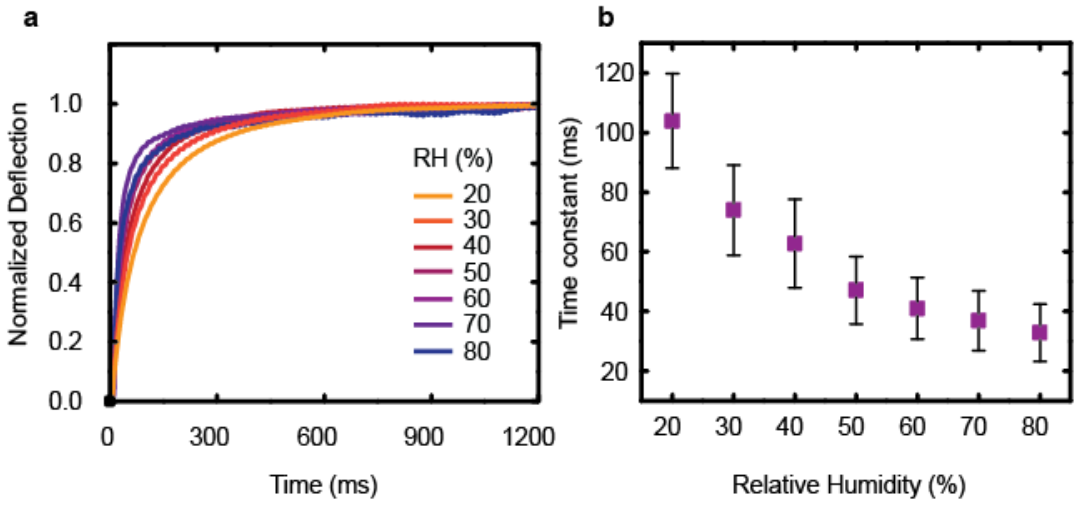


**Figure 3.11| The effect of spore coat upon water transport in the outer layers. a,** cantilever deflection traces are shown plotted for each set-point humidity for mutant spores lacking the outer coat (*Cot E ger E*) **b,** time constants are plotted for each humidity. n=15, error bars represent standard error.

Thus far we have treated the outer layers of the spore as a single homogenous object, and so it would be useful to test this assumption. The mutant spores with deletions in *cot E* and *ger E* both

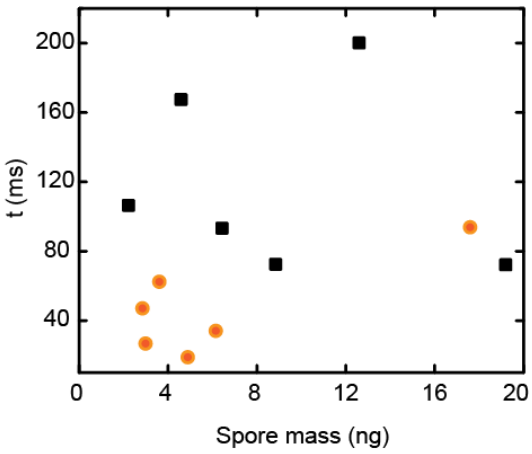


**Figure 3.12| Stochastic effect of additional spores upon response time of the system.** The lack of clear association between the cantilever response and the quantity of spores indicates that deflection is measuring behavior of individual spore hydration rather than bulk transport properties. Mean t (RH 50%) for WT [square] is ~118 ms and ~47.1 ms for cotE gerE [circle] (n=6 cantilevers, Two tailed T, p=.015).

display coat deficiencies and the co-expression of both mutations yields a bacterium with spores devoid of all but a few nanometer layers of the coat. The *cot E ger E* mutants display greater strain, and faster time of swelling that WT (See Figure 3.11). Because the coat approximately doubles the radial dimensions of the spore, *d*, and due to the poroelastic relationship where the time constant is proportional to $1/d^2$, we can assume the coat material behaves similarly to the cortex. Although the actual architecture may differ significantly between coat and cortex matrices, poroelastic swelling of both materials appears to converge. It is noted that where the *cot E ger E* mutants do retain a small skin of coat layer we might observe this as the slight attenuation in time constant from the theoretical prediction (~5% slower).

Figure 3.12 shows the stochastic effect of spore mass/cantilever on the sorption time constant. WT (square) and *cotE gerE* (circle) spores per cantilever estimates based upon Carrera *et al* 2008 spore mass of 1.96E-13 g and harmonic mass estimate: $2\pi f=\sqrt{(4k/m_{eff})}$. Spore layer calculation is based upon estimating that spores occupy a cross-sectional area of 0.5 $\mu m^2$ (one cantilever yields 18,000 spores per layer). Spore-layer estimates closely approximate observed quantities from SEM.

The force transducing interface between the spore and ambient water, responsible for its shape change, occurs at the coat/cortex surfaces. We have examined the cortex directly using AFM (see

Figure 3.13). This was accomplished by microtoming very thin 90nm sections of cortex and embedding these onto a TEM mesh. Interestingly it was possible to observe some evidence of humidity responsiveness in the fine peptidoglycan structure, as has also been observed by others in vegetative cells[90]. Note the scale of imaged spores is not indicative of *in vivo* pore dimensions because the material naturally exists under great compression. This compression is relieved as the material can expand unrestrained out of the sectionl field of view (spore material is filleted by a TEM). The strands we observe are likely stitched together, electrostatically and/or through the water structure itself, at points which approach distances on the order of a nanometer.

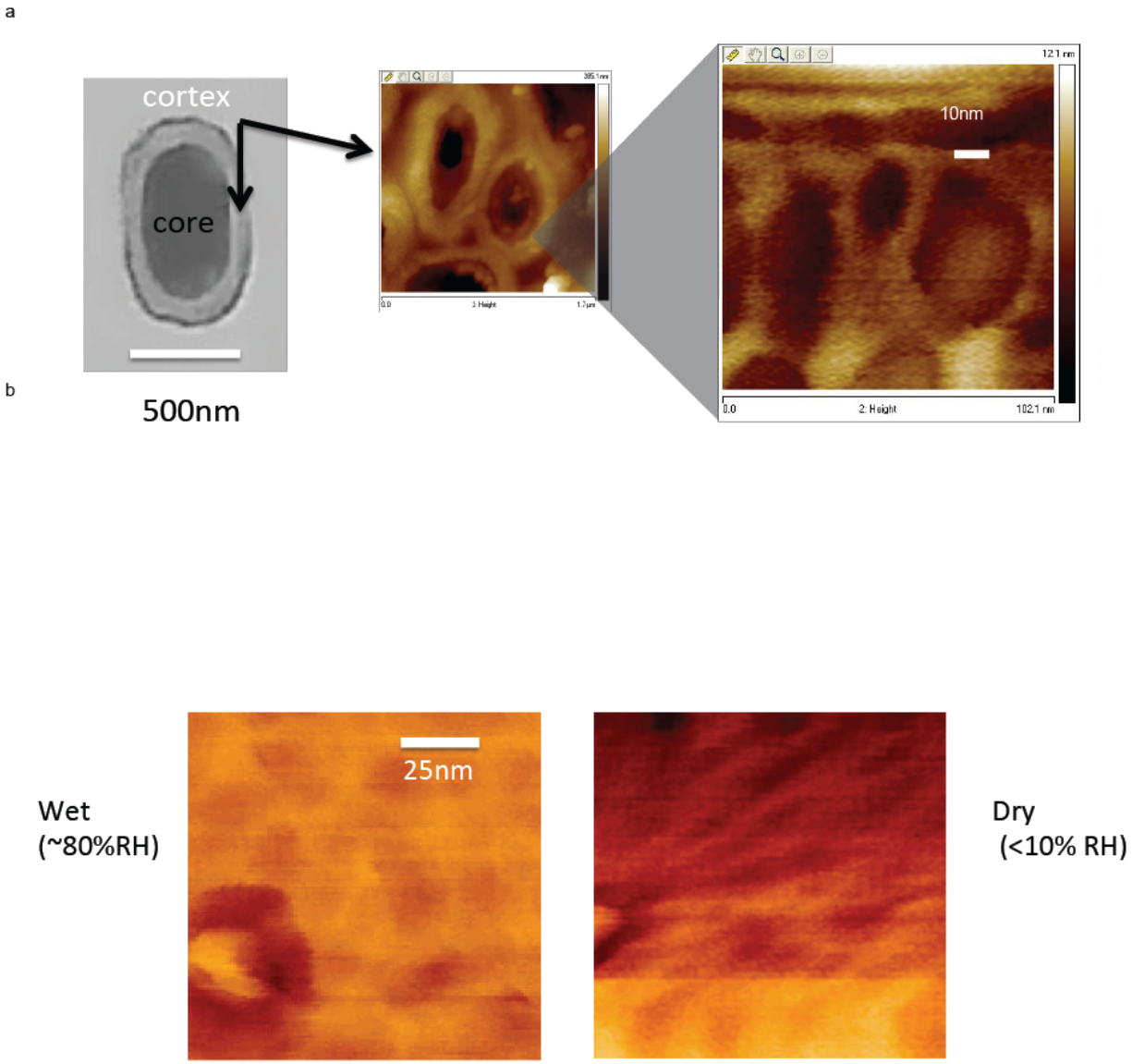


**Figure 3.13| Spore cortex depth measurements. a,** spores are imaged via FIB-SEM and through microtomed sections on AFM. These measurements allow determination of the cortex size within the spore's water-responsive outer layers. **b,** the microtomed section retains some humidity responsive behavior, although nanopore size is not easily resolved, we see some microstructures and change in relation to *in vivo* is exaggerated due to the nature of the method, where z-expansion is unrestrained.

The transport of spore water has been examined in the past, however these studies, rely traditionally on NMR where immobilized water is not available to study[58,91]. The studies are able to discuss the rotational relaxation times but admit that these rates cannot reveal water transport accurately. This is because the core is essentially inaccessible to water and yet rotational relaxation can be provided nonetheless. These rates indicate that the core is locked into a rotationally aligned state. This could result physically from an attempt by the molecules to maximize compressive surface dissipation (density gain) during dehydration of development. Deuterium studies also can only reveal water which is indeed exchanged, and interestingly, studies were unable to show that water was exchanged at all in air after equilibration with the external atmosphere even after weeks[57]. Generally, it is agreed between the NMR scientists that water exchange occurs on the order of less than a second. Recently, single-spore studies have been performed with chambered micro-cantilevers[83]. The micro-sensors are able to resolve transport as low as 200 ms (*Cot E Ger E).* They also quantify the amount of water exchanged to be approximately ~100fg, which agrees with our estimates from the bilayer micro-sensor (harmonic mass estimate as in Fig. 3.12).

In summary, the spore's structure is continually rearranged due to ambient hydration conditions. An AFM-based cantilever system was developed here in order to probe these kinetics in relation to water transport. The method may prove of use to water scientists interested in directly adjusting confinement lengths with nanometer resolution. The observed structural rearrangements within the spore can confine the water to a single molecule paradigm during dry moments and at most 2-3 water molecules when approaching full hydration, and these extreme physically restrictive milieus result in water transport behavior that is slower than bulk flow in effective viscosity by more than 7 orders of magnitude. This slowed water scenario improves the temporal resolution of existing spore-water transport methods and has wide-ranging implications for the slowing of biochemistry both in

general and particularly within the spore at surfaces open to exchange with non-core water in the external environment.

# Chapter 4: Thermodynamic Studies of Spore Water Bonding

We have so far observed highly viscous water transport within the spore, yielding an average effective viscosity of water greater than 7 orders of magnitude that of liquid water in bulk. It is known that viscosity depends upon hydrogen bonding[92]. We can learn a lot about the macro-structure of spore water from the bond-coordination. Can the inflated effective viscosity be accounted for in terms of intermolecular water-bond strength inside of the spore?

Stimuli responsive materials like the spore cortex remain in high demand for myriad applications within the fields of biomedicine, adaptive-architecture, robotics, and alternative energy [93-96]. Previously, it has been demonstrated that the spore's cortex possesses extraordinary ability to perform work in the presence of humidity gradients (see Figure 4.1)[52]. The spore-water system is extremely energy dense, outperforming existing synthetic shape-change materials. Cycling the spore through alternating wet and dry periods produces efficient, engine-like qualities analogous to the Carnot system[52]. The cantilever is pre-loaded under constant humidity from I to II, and then force is held constant while it is hydrated so that the system can undergo isobaric principles of constant force and experience volume change exclusively due to heat dissipation as chemical equilibrium shifts (humidity change). In this case, one can think of the spore-water as a piston and the water's potential to equilibrate as the fuel. In the case of this experiment, a cantilever preloads the system to maintain zero-force, isopsychric regimes, and work is performed by driving alternating humidity polarity. At

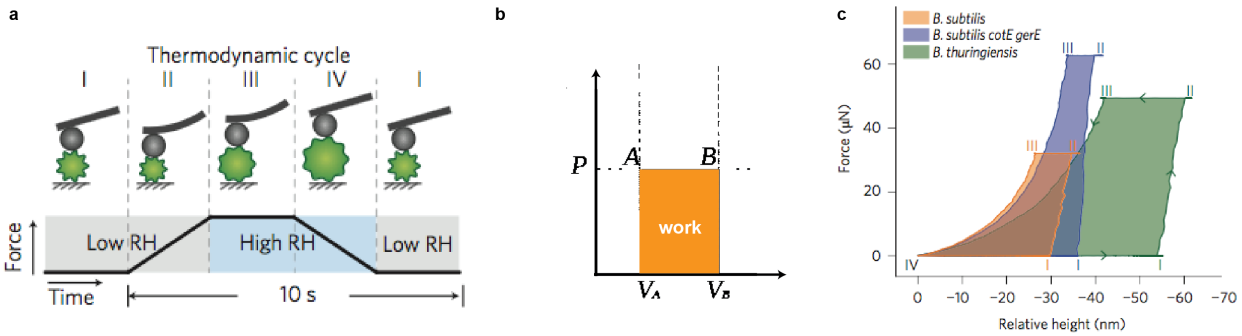


**Figure 4.1| Spore water transport provides a high energy-density work cycle. a**, From Chen et al 2013 spores provide isobaric engine-like behavior in the presence of humidity gradients and expand along isobaric lines. The idealized plot, adapted from *Wikipedia* in **b**, is squared due to perfectly isochoric process due heat to input, $Q$, to the gaseous system and surroundings while actual work due to water exchange for spores is shown in **c**.

the same time the water is being stretched, it is coupling the spore to the ambient environment and allowing work to be performed by the water due to heat-driven relative humidity flux. This also implies that the water is expanding as well, which perhaps suggests some phase transition. Importantly, the spore is harvesting power from the environment.

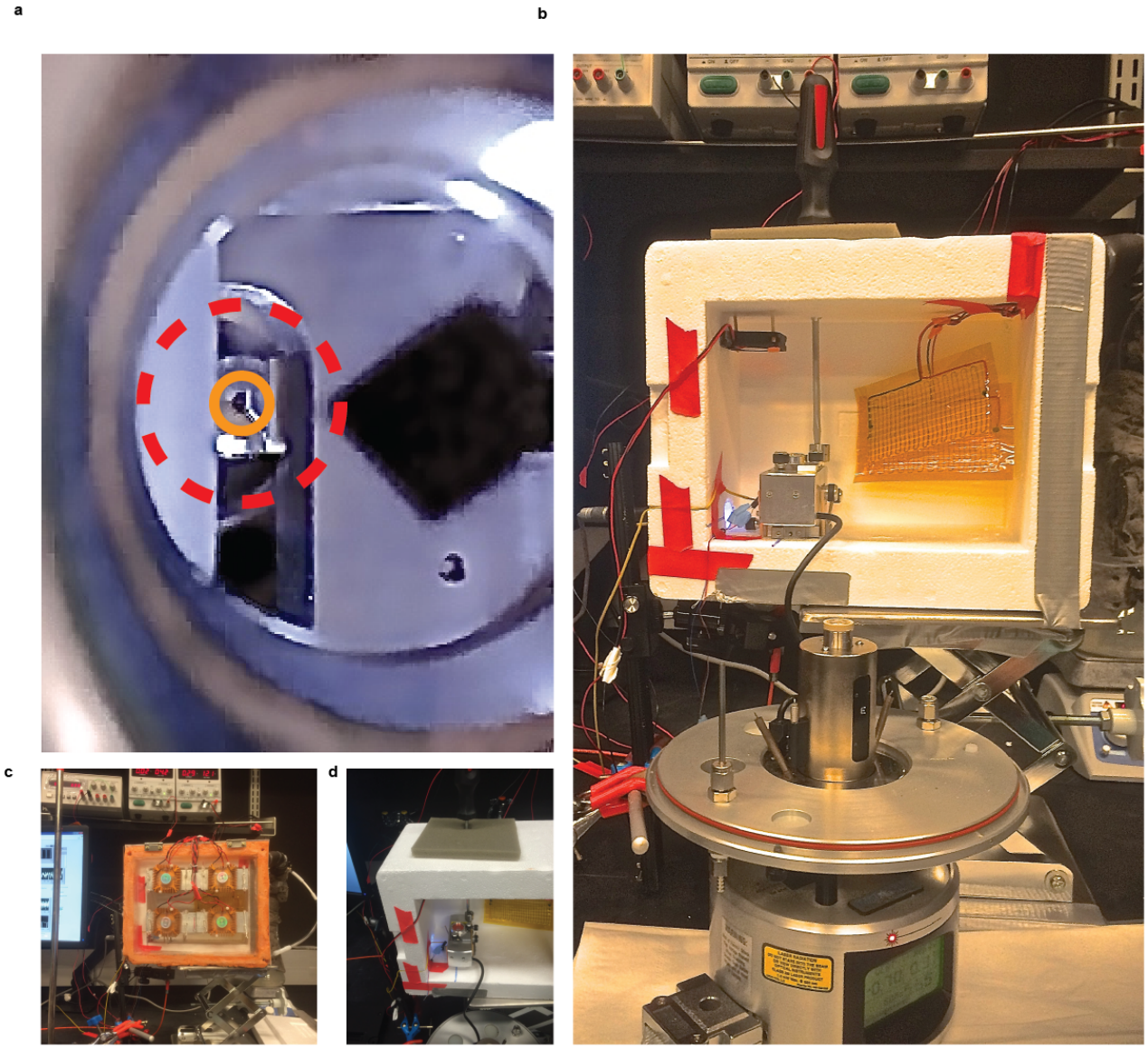


**Figure 4.2| Spore water thermodynamics apparatus. a**, Top-down view of the spore-coated cantilever inside the ECU. Note the fiber-optic barrel is outlined in red dotted line while the cantilever is shown circled in solid yellow. It is viewed and aligned through the endoscope at this vantage as well as from the side **b**, Chamber view shows the AFM head housed inside of the thermally isolated box. Resistance-based heaters are in yellow. **c,** shows the thermoelectric cooler arrangement with radiators and sensors are viewed from above in **d** (endoscopic camera for **a** was added after this photo was taken).

For the water to perform these pulling actions upon the spore, we understand that the water must act as an intermolecular chain[97]. As this chain navigates nanoconfinement within the elastic

pores, one possible explanation for spore water's particular strength and effective viscosity could be increased intermolecular bonding. We can understand bond-coordination through intermolecular activation energy, which can be quantified through temperature dependence. A greater degree of bonding means more bonds to break and a higher activation energy, with greater temperature dependence.

To examine the bond coordination at each humidity/structure-state of the spore, a series of thermodynamic experiments were designed and performed in which humidity was held constant (isopsychric). To detail molecular behavior, the spore-water set-up was adjusted to allow examination of water's temperature dependence during transport. An environmental control unit (ECU) was constructed, as is shown in Figure 4.2, of insulating polystyrene to house the spore-coated cantilevers (mounted in the head of a Bruker Multimode AFM), sensors, temperature control elements, and heat pulse LED (see Figure 4.2a). Humidity inside the enclosure is measured using a Honeywell HIH-4021 and temperature with a thermocouple (Agilent U1180A) along with a data acquisition card (National Instruments BNC-2110) coupled to the master Labview acquisition program. Humidity can be adjusted through a bifurcating valve system where some portion of the airstream is bubbled through a liquid flask. A heating supply was necessary below the flask in order to maintain the higher humidity measurements. Temperature and humidity sensors were aligned within 1cm of the cantilever tip.

Endoscopic cameras were used to align the cantilever to the LED pulse. To achieve fine temperature control within the ECU, a series of thermoelectric coolers (Eathtek, LLC, San Jose, CA) is arrayed in parallel and connected to a variable power supply. Where sufficient cooling was not achieved via the TECs, -20°C, commercial ice-pack were used. For the hotter end of the spectrum, an array of resistance-based heaters (WireKinetics Co. LTD, Taipei, Taiwan) was controlled via a separate power supply (see Figure 4.2d).

Using this setup, an isopsychric temperature dependence was observed. The trend is expected, with liquids becoming less viscous as heat is added. Water transport speed increased accordingly in warmer conditions (see Figure 4.3a). The degree of this temperature dependence can tell us about the coordination of the molecular water. This can be understood in that the temperature dependence simply implies that for a highly bound molecular ensemble, one would expect that raising overall temperature by a constant amount should produce massive viscous changes. Consider that raising a block of ice by 1 degree would require considerably more energy than the equivalent volume of liquid. Therefore, by producing greater viscous changes across a fixed temperature difference, we are

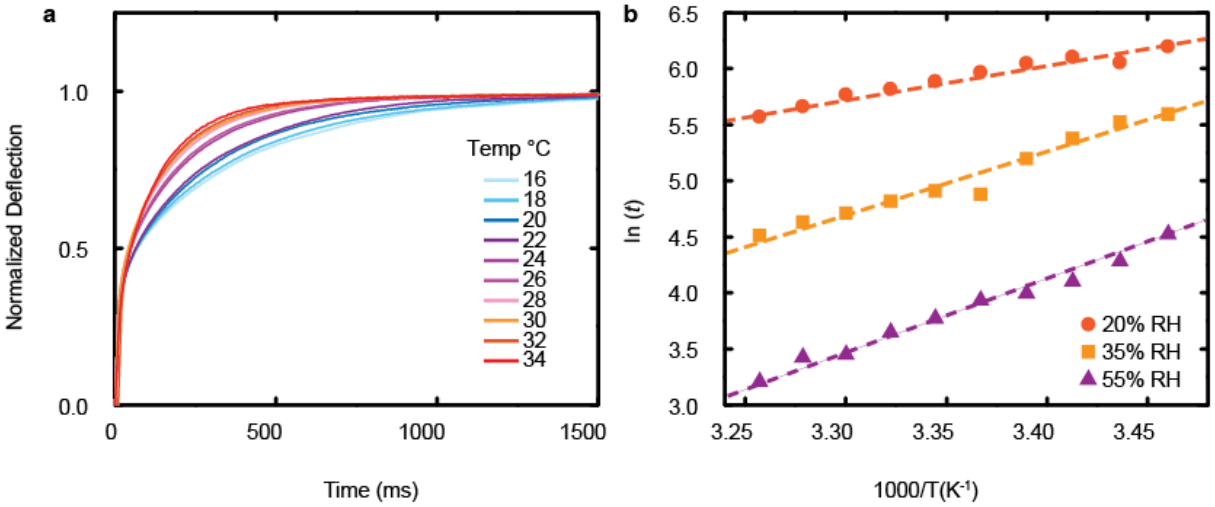


**Figure 4.3| Spore water temperature dependence is relative humidity dependent. a**, **a** typical cantilever spectrum displaying temperature dependence with a fixed set-point humidity. Warmer conditions produce a faster sorption trace of water transport **b,** this set-point humidity provides a variable temperature dependence, where plotted as ln(t) vs. $T^{-1}$, the slope reveals the activation energy of making and breaking intermolecular H-bonds.

measuring higher bond energy, $Q$. Again consider that more bonding in ice results in a higher $Q$ than the less-bonded liquid form[92]. This can be quantified through the Arrhenius relationship,

$$\eta \sim e^{\frac{Q}{RT}} \tag{13}$$

where $Q$ is the activation energy of making and breaking intermolecular bonds, $R$ is the molar gas constant, and $T$ is temperature.

A range of these processes is shown plotted logarhythmically in 4.3b. where we observe the slope as a quantitative readout of the bond character, and activation energy of intermolecular mobility. We note that these values for spore water approach that of solid phase ice. Recently, activation

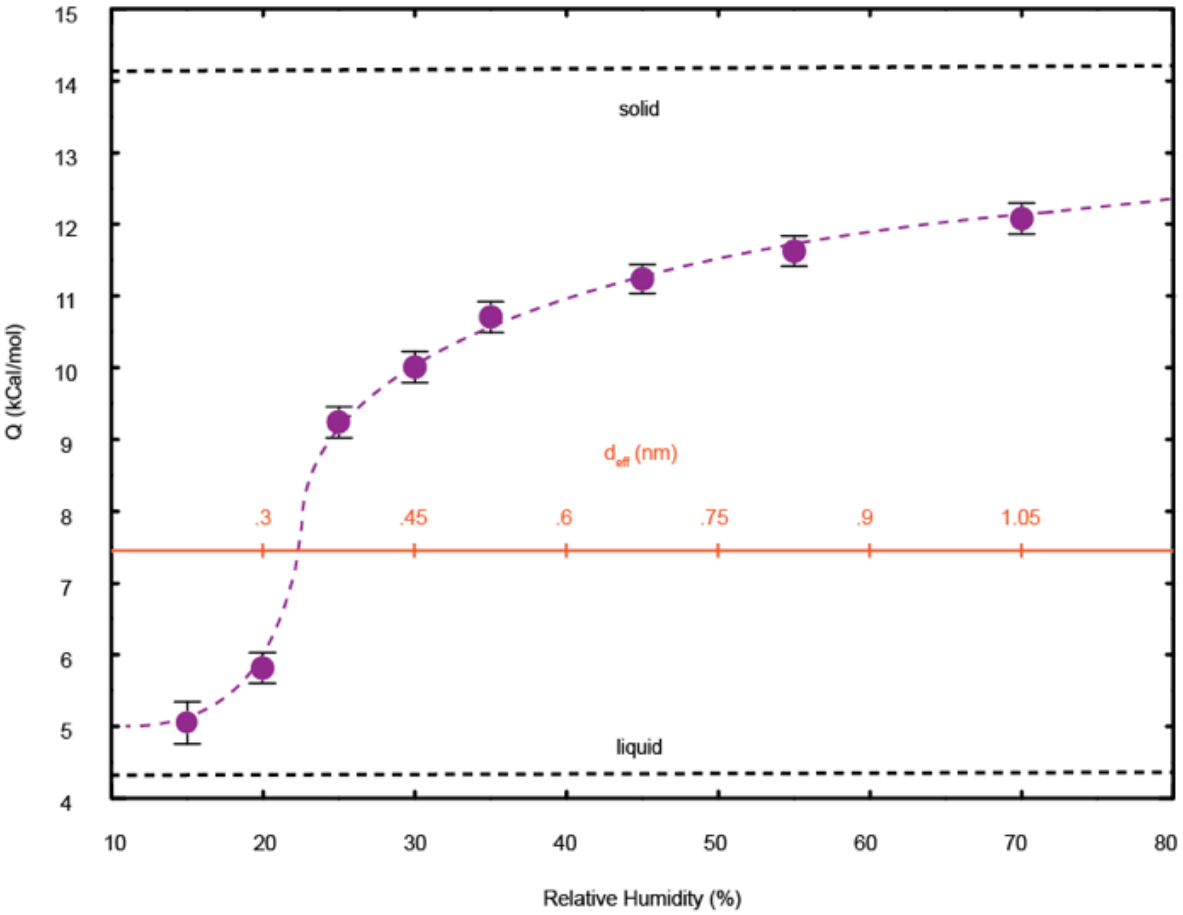


**Figure 4.4| High-*Q* transition process in the spore water.** Below 25% relative humidity, a very low bond-coordination is observed, close to that of liquid water with activation energy, $Q$, at 5-6 kCal/mol. With increased relative humidity, the spore water takes on a bond configuration approaching that of solid phase water (~4 H-bonds per molecule). n=3 cantilevers for each humidity, which corresponds to a complete temperature course as shown in Fig 4.3. $Q$ is derived from regression of temperature course with $r^2 > 0.95$. Error bars are standard error of the mean.

energies echoing these measurements at comparable confinement lengths have been reported for water transport in carbon nanotubes[98]. It can be seen that the slope and bond character increase with increased relative humidity. We looked at some other natural polymers such as methylcellulose and dextrose. In particular, it was noted that the increase of $Q$ with relative humidity persisted, however, the process appeared monotonic, whereas the spore produced a distinct S-shaped response (see Figure 4.4). Here, there appears a step in $Q$ between low and high humidity indicating that there are two separate processes being observed. The nature of this transition is open to interpretation.

With typical biopolymers, such as DNA[99,100], we should indeed expect multiple small hydration events, as shells are layered onto the molecule. This is the sort of smoothed constant response observed for methylcellulose. For the spore, on the other hand, this two-step process (Fig 4.4) is more likely indicative of a change in the confinement paradigm. Under this hypothesis, the water would be highly confined down to as low as 1 water per pore layer (low RH). After 25%RH, a second water can fit into the space (>3Å) within the spore material. At this point, the water present is now interacting with other waters and a sharp increase in bond-character is observed. This also presents the possible onset of a meso-scale water structure (Fig 4.5b), and interestingly also directly corresponds to the physiological humidity range where vegetative bacteria are found[45,101]. It is thus plausible that this first water ordering event indicates triggering of a humidity sensing behavior for the organism, by awakening a highly tensioned, highly bound water structure in the presence of physiologically relevant hydration environments.

This ordered water structure, available to the spore after 25%RH, is perhaps increasingly fragile, subject to perturbation, as the water is less dense than in bulk. Where the water structure participates in H-bond cross-links within the spore material, it could subject the spore structure to failure if it were to disintegrate suddenly to fast liquid form.

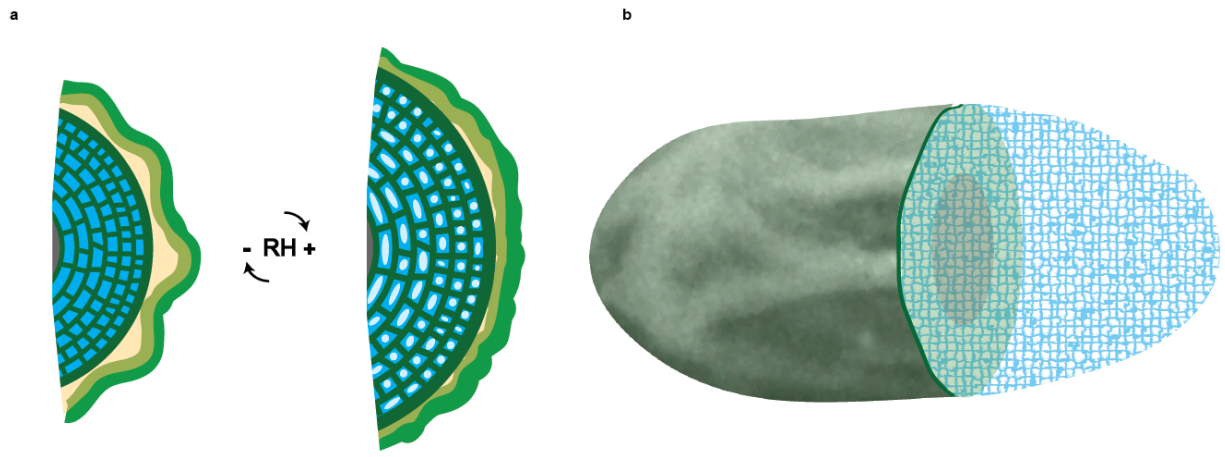


**Figure 4.5| Spore water structure.** **a**, Shape-change ability of the spore water structure during humidity states **b,** Illustration of hypothesized spore water structure, highly bound (>3 H-bonds), under great tension, and theoretically subject to perturbations by adulterants, pressures, and surfactants. SEM adapted for cartoon in **b** from Chen *et al,* 2013.

The spore increases in volume as it senses more and more humidity ambiently (Fig 4.5a). Because surface area increases only with a square of the radius, and volume increases cubically, the surface effects would be expected to eventually yield to hydraulic flow as the pores open and conditions approach 100%RH. However, this is not possible, for water transport is not slowed in direct proportion, in accordance with the confinement paradigm detailed poroelastically in Chapter 3. Note that these water conduits within the spore are estimated at a range of only ~1-5 molecules diameter. This means that surface effects extend from all sides radially, likely focusing and amplifying environmentally defined geometry to ~2.5 waters.

In the alternative, the high energy water observed above 25%RH (Fig 4.4) could also be explained by a sort of molecular hopping event. There is indication that the aspect ratio of pores is largely responsible for whether flow will be hydraulic or involve a liquid-vapor-liquid transition[102]. This multiple phase transition would also cost a lot of energy in the breaking and forming of new bonds during the transport process. Under this hypothesis, the surface water would exist as a sort of film, whereby the water molecules would hop between hydrophilic domains of the spore material. Surfactants, including alanine,[103] can also serve to organize water and join into the forming of regularly ordered structures. Consider the simple soap bubble. This process forms structures because the surfactant, soap, adsorbs water, which maximizes hydrogen bonding with its neighbors, thereby minimizing surface area. The films coordinate at tetrahedral angels (Plateau borders) to one another, again maximizing bonding. This simplest water structure is but a single surface, with area minimized, which is therefore spherical, and we call a bubble. Any number of organic adulterants, including salt, are likely to destroy, but at the very least, rearrange a bubbled hydrated structure like this.

In summary, the spore has evolved as an evaporation-harvesting machine, capable of leveraging forces greater than known synthetic shape-change materials, it is only natural to assume that the organism will put this effort to use. The spore is strong (stiff) and can change shape dramatically and quickly due to ambient humidity. This expanded spore form stretches and tensions water. We know this must be the case from our understanding of poroelastic equilibration kinetics. Also, there are serious density/mass discrepancies in water absorption quantities. In order to understand how tensioned spore water is coordinated, particularly in the fully expanded spore structure, intermolecular bond-energy was examined through Arrhenius temperature dependence of viscosity. This revealed absolute confinement likely for the dehydrated spore and a distinct highly bound structure close to the activation energy of ice at ~25% relative humidity. These characterizations enlighten our understanding of the viscous spore water from Chapter 3, such that a

picture of a spore water structure emerges, which is first established when the spore encounters a favorable hydration environment in the physiological survival zone. Once the tensioned spore water structure is erected and tensioned at the cost of naturally occurring evaporative flux, it remains remarkably stable and yet is theoretically subject to all known physical destabilizers of structured water including pressure, electro-static adulterants (salts, small molecules, etc..), and surfactants. Stimuli known to germinate spores through unknown mechanisms satisfy these qualities.

# Chapter 5: Spore Slowed Water in Liquid Media & Germination

Because slowed spore biochemistry could result from the observed slowed water transport, it is hypothesized this water structure may stabilize dormancy, either directly or through stabilization of the highly tensioned spore architecture. Spore germination is typically observed in liquid cultures, and so in order to understand how the water structures detailed in the previous Chapters, could impact germination we must understand whether this transport character persists in the fully hydrated spore. It is important to bear in mind that spore germination in nature does not occur in liquid necessarily, for the model spore is a soil bacterium, and so a range of hydration steady-states are expected. For this line of inquiry, a new biophysical apparatus was developed. This setup allows examination of water transport as it is variably affected by addition of germinants, heat activation, and transport frequency (efficiency).

The basic method to biophysically examine the spore biology begins by immobilizing the spore so that it can withstand significant compression forces in liquid. This was accomplished through the

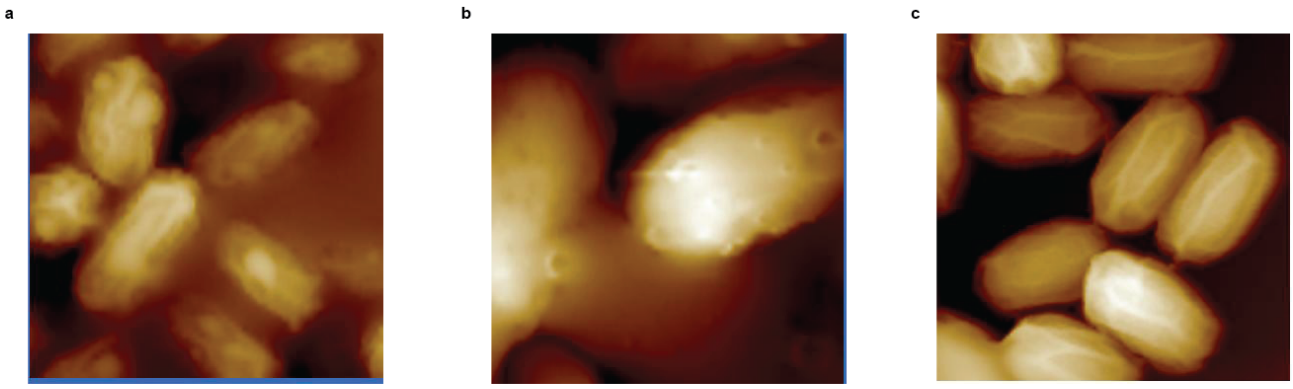


**Figure 5.1| Tapping mode AFM images of fully hydrated spores embedded in epoxy** **a**, cured in epoxy NOA-89 did not retain enough surface above the of the epoxy layer. Similarly, in **b**, NOA-81, although able to avoid this issue required precise timing of the curing cycle in order to obtain adhered but optimally exposed spores as shown in **c**.

use of UV-curing epoxies (See Fig 5.1). Several adhesives were attempted, however, NOA-81 was eventually selected (Norland Optical, Cranbury, NJ). Immobilization was produced through radiative pre-curing the epoxy on an AFM disc substrate. The optimization of this regime was accomplished empirically. It was found that 3.5 minutes of pre-cured epoxy on steel substrate followed by the addition of a small 10µl spore suspension, followed by evaporation in air (or nitrogen stream), followed by additional curing of 5 minutes, produced the most effective sample preparation. Several gentle washes in DI water removed spores that would otherwise float onto the tip or into the path of the scanning probe and laser signal to AFM.

It was then necessary to germinate spores. Several common methods were investigated including L-alanine but because we were interested in how the nutrient sensation might relate to water transport, a nutrient broth known as AGFK (50 mM potassium phosphate buffer (pH 7) containing 10 mM L-Ala (Ala-induced germination) or 50 mM potassium phosphate buffer (pH 7) containing 10

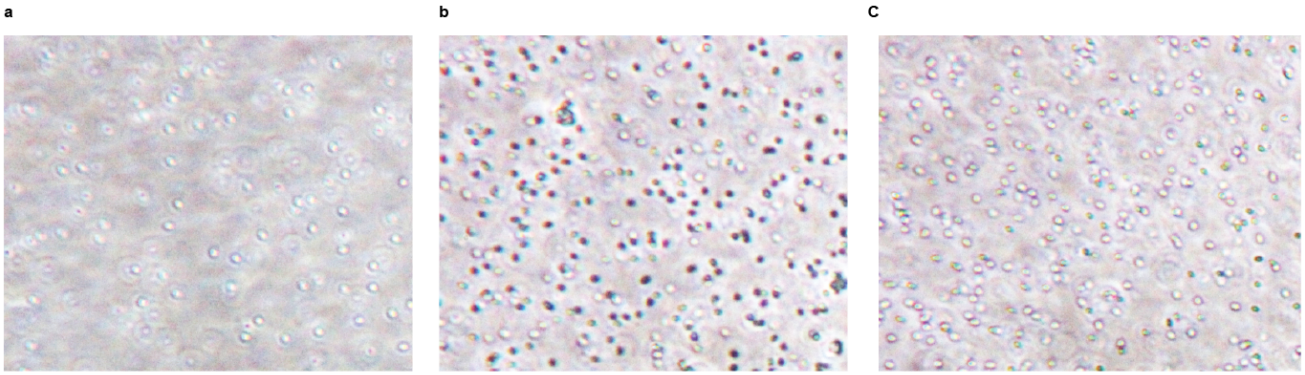


**Figure 5.2| Verification of germination by phase contrast microscopy.** Spores are observed after 3 hours exposure in **a**, control (only heat) and **b**, AGFK+heat and **c**, L-Alanine+heat.

mM L-Asn, 10 mM D-Glu, and 10 mM D-Fru)[42]. was eventually used as it is a standard nutrient mixture in *B. subtilis* experiments[104]. The spores are always pre-treated with heat at 70ºC for 30 minutes

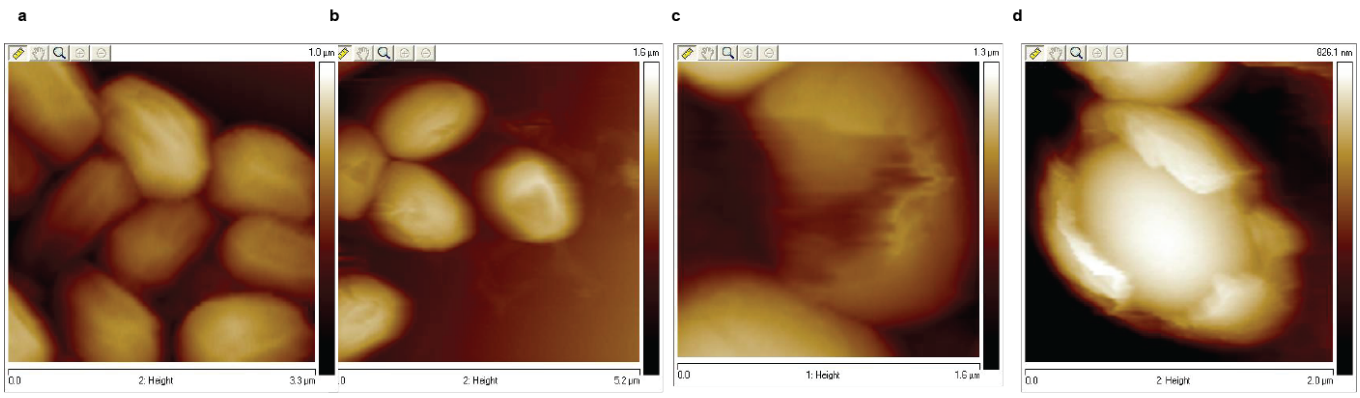


**Figure 5.3| Visualization of Germination by tapping-mode AFM. a**, spores are shown prior to addition of AGFK nutrient stimuli **b,** 3 hours post-AGFK addition structural changes are evident in the spores (cracks form, wrinkles gone) **c,** 24 hours post-AGFK shows significant deterioration of the coat and cortex.

prior to addition of germinants. Figure 5.2 shows the characteristic darkened appearance of spores having been exposed to germinants when viewed through a phase-contrast microscope after 3 hours. Adhered spores could then we examined via AFM, while considering batch-matched replicates under phase contrast simultaneously for the appearance of germination. AFM visualization of germination is shown in Figure 5.3.

After the spores were adhered with sufficient surface available to AFM examination in water, it was necessary to design a routine to collect water transport information. Transport was assayed via force volume AFM as shown in Figure 5.4. Force-volume AFM has a deep history of application in characterizing living cell systems in addition to serving traditional rheological material science applications[86,105]. The principle underpinning this method is simple, where experimenters are generally interested in a material property known as elastic modulus or simply, stiffness. Elastic modulus is a relation of stress applied to strain experienced by the material. While similar to the Hookean spring constant, elastic modulus does not depend upon the material's shape. Most materials respond elastically through the force volume cycle to some limit, whereby a yield-strength is reached, and


**Figure 5.4| Spores water transport kinetics are examined via force volume AFM. a**, schematic of the force volume method in liquid where the adhered spores are pressed repeatedly at some frequency by which the timescale of direct contact is described by the forced transport frequency, $\omega_T$. Adapted from Chen *et al* 2013. **b**, Force experienced by the cantilever (deflection signal) is shown plotted against displacement as the spore/substrate system approaches the tip. **c**, fluid-imaging cell inside of the Multi-mode AFM head chamber necessary for germinant addition.

permanent plastic deformation is achieved. Most biological materials display some aspects of this elasticity and some aspects of fluid viscously where the applied force is partially dissipated through transport flow and heat losses.

Note that the hysteresis present in Figure 5.4b, where the trace and retrace do not match paths precisely, is indicative of viscous losses in the material being assayed. This can also be indicative of adhesion between the tip and sample during retraction and so care must be taken when examining data. A perfectly elastic material would follow the identical approach and retract path. The spore is expected to behave extremely elastically as it is very stiff and resists permanent deformations[51,52]. Adhered spores are pressed repeatedly at some nominal frequency, where the specific % duty of this cycle in direct contact with the spore has a characteristic timescale, whereby the inverse of this time is can be referred to as the forced transport frequency or simply, $\omega_T$. Initially, the transport frequency was estimated from spore water transport in air (Chapters 3 & 4), with maximally hydrated WT spores displaying a time constant approaching <50ms, or $\omega_T \sim$ 20Hz.

The hysteresis of the force distance curve can tell us about the water transport inside of the spore and where the water structure is absorbing the most energy. For the purposes of standardizing analysis this hysteresis was normalized to the approach curve and hysteresis heat maps were generated as in Figure 5.5c,d. We define the hysteresis viscoelastically as the energy losses to heat through the relation,

$$U = Q + W \tag{14}$$

Where the *U* is the total internal energy of the spore before and after the cycle and

$$W = \oint \sigma d\varepsilon \tag{15}$$

and where $\varepsilon$ is the strain in response to the stress $\sigma$ applied through the cantilever tip. By performing the same work on the system with the AFM in each cycle, we essentially measure differences in U (hysteresis), which are exclusively accounted for by *Q*. This assumes we are approximating the compression in one dimension. A purely elastic system would not display such losses dissipated as heat to its surroundings[106]. In a typical polymer, these viscous losses are thought of as the molecular creep of long polymer chains as they return to equilibrium in the material. For the spore, this viscous component cannot so readily be attributed in their entirety to the material, because these losses appear at least partially transport dependent, as we shall see later (and have seen in Chapters 3 and 4 for air-water exchange in the spores). In fact, the spore appears to work across a wide range of character from viscous to elastic depending on the biological stimuli available, as was first observed for the liquid system during the described germination protocol.

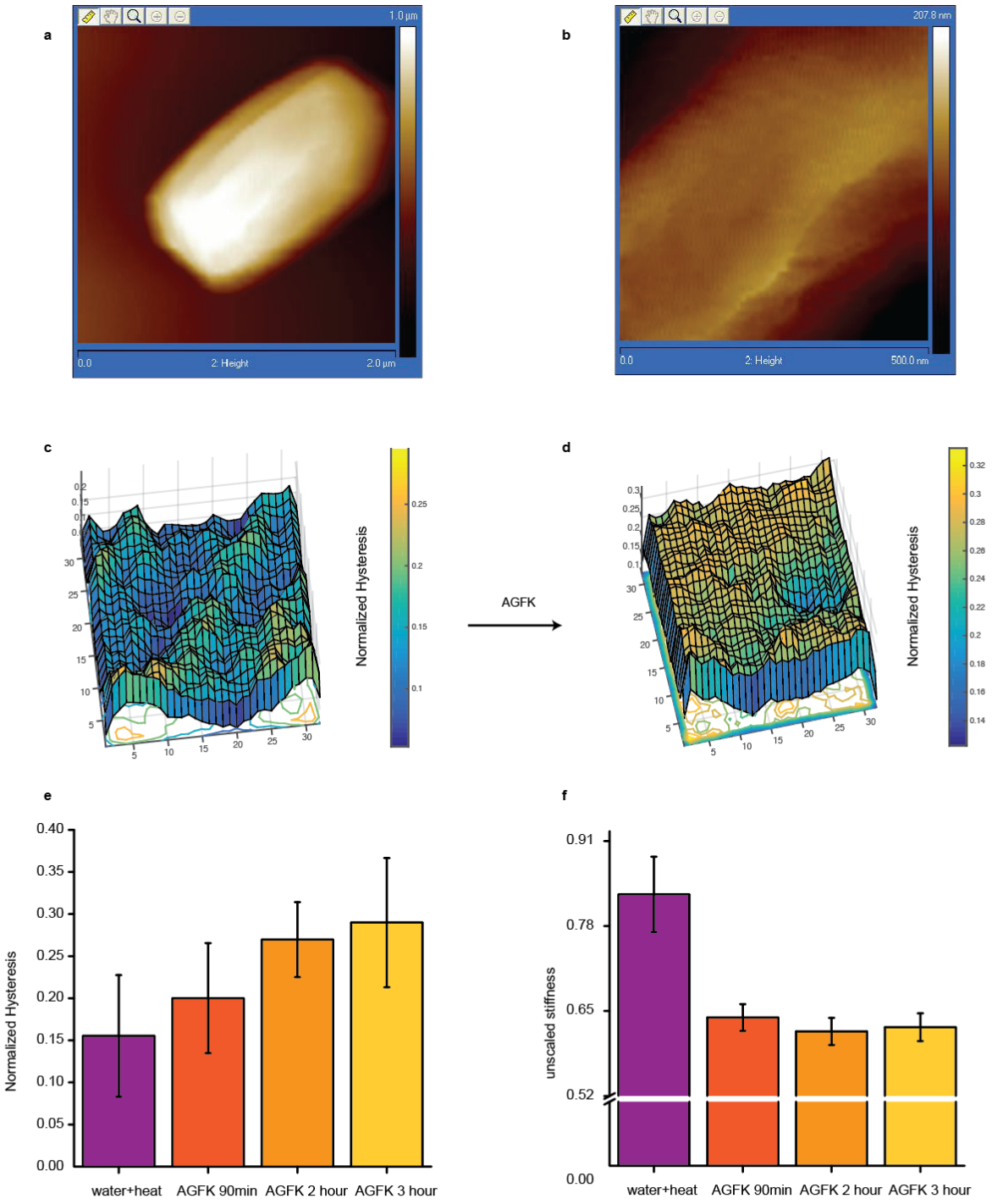


**Figure 5.5| Germinants produce mechanical perturbations to the viscoelasticity of the spore.** **a**, A single spore cell is imaged through tapping-mode AFM **b,** The spore is focused to a 500nm patch, which is then assayed through force-volume mode for viscous loss modulation before and after AGFK treatment as is depicted in **c,** and **d,** The mean hysteresis and standard deviations of 1024 force-volume cycles is shown plotted in **e,** as well as the resultant stiffness, which is shown in **f,** where the result is indicative of at least 3 separate experiments.

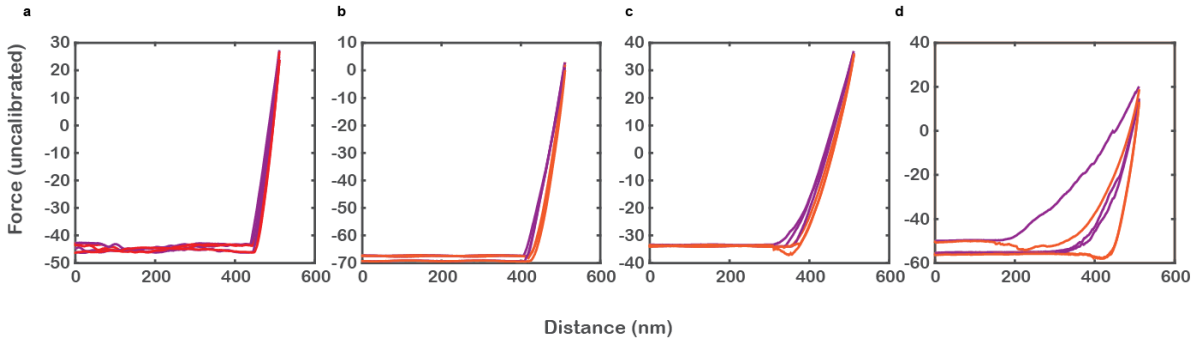


**Figure 5.6| Loss of stiffness during germination.** **a**, spores (here a single cell) are measured in DI water at and after addition of AGFK at **b,** 30 minutes **c,** 60 min **d,** 90 min. 3 measurement loops are shown for consecutive nanoscale patches on the ridge of a germinating spore. Approach is shown in purple and retract in red. Stiffness is approximately proportional to the slope of these curves. Data is representative of at least 3 separate experiments.

Loss hysteresis is directly related to germination (see Fig 5.5e,f). Although the timing of the events differs from spore to spore, it is always seen that germination in accompanied by increased energy losses. Though such losses could be due to slowed sorption of liquid, it is more likely that this reflects the loss of structural integrity as we note the stiffness is also decreasing (see Fig 5.5f, 5.6). This trend is observed regardless of whether stiffness is considered via the approach or retract curves. The loss of stiffness within minutes of germinant addition is interesting because it occurs before any visible signs are apparent (i.e. coat cracking, wrinkle loss, etc..). Along the viscoelastic continuum, the spore drifts toward viscous as it germinates.

Many cells displayed some heightened degree of hysteresis in response to heat treatment alone, which could be quantified as is shown in Figure 5.7. This trend did not track with stiffness, which appeared unaffected by heat. It should also be noted that ~25% of the WT cells also exhibit this activation without any heat treatment (experiment 1, Fig 5.7a). A similar proportion of cells did not respond at all (as exemplified by experiment 3, Fig 5.7a). To that end, it was also noted that the

recovery from heat activation varied significantly from minutes to hours to days (see Fig 5.9). There is some evidence to support the notion this reflects general variability of the natural distribution of

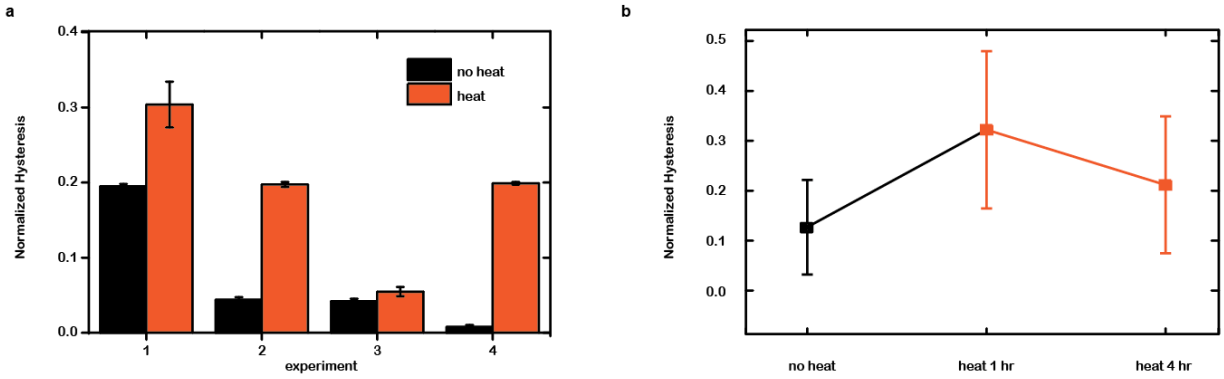


**Figure 5.7| Heat activation alone induces transient mechanical effects on some spores.** Spores are heated at 70°C for 30 minutes and **a**, single cells are shown where1024 FV curves are averaged. Error bars or standard error of the mean **b,** transient nature of the effect is shown after 4 hours. Spores hysteresis approached baseline by d4 and later time points, although significant germination at the sample obscured evaluation of the effects magnitude (n=8 no heat, n=12 heat).

the spore germination processess[107]. It seems that some spores in a given population will require a higher heat activation temperature so this may result in the variable material properties we observe.

To the question of whether the spore water transport is the cause of this heat-activation related hysteresis, the answer appears to tend toward the negative. Because this effect was long lived, on the order of hours or even days, the heat, more likely, served to unwind certain polymeric structures, thus inducing creep. This can be deduced for two reasons. First, the spores can be cooled on ice after the heat activation process, and are no doubt in thermal equilibrium with the bath in which the transport experiment in performed. In other words, it is not expected that heat-induced molecular effects upon water's effective viscosity would persist upon cooling. Second, there is much evidence available in the literature that heat activation-like effects can be simulated chemically[108]. This results in reduction of disulfide bridges or other denaturing events to the tertiary protein structures within the spore[108].

Furthermore, it is possible that some heated spore material was ejected during imaging and contributed through increased tip-surface adhesion, which could also produce the transient hysteresis. It is further noted that spores often germinate from heat treatment alone, and their shells can be seen during imaging.

Viscous losses can be indicative of the water transport and heat dissipation, where tip adhesions, and mechanical disruption can be ruled out. Below a certain timescale, water cannot re-enter the porous material as quickly as it is forcibly evacuated and a loss hysteresis is observed. A material may behave very elastically and stiff if it is forced too quickly, such that the liquid cannot escape at all. When the material is forced and relaxed very slowly, a second hysteresis may appear as a result of a more plastic deformation wherein the properties of anhydrous material is observed. In order to understand where the spore water is transport limited in liquid, a frequency sweep of indentation/relaxation was performed as shown in Figure 5.8. For these experiments, spores were adhered as described previously and imaged in water, but no heat activation or chemical treatment was performed. Hysteresis was therefore observed only as a function of frequency of indentation.

The most interesting feature of the frequency sweep, is that the hysteresis is minimized after the indentation time of 100ms and seems to be maximized at about 50ms (Fig 5.8a, b). In either case, the elasticity of the material seems to stabilized until about 800ms, where poroelastic theory suggests that we are thoroughly dehydrating the material and thus measuring a more permanent material deformation. A 50ms transport time is very close to that which we measure in humid air as the relative humidity approaches 100% ($\omega_T \sim 20$Hz), and so it is very likely that in the case of this frequency sweep experiment, we are in fact measuring transport related losses. In other words, within the spores studied, indentation hysteresis maxima correspond to predicted transport limited timescale. It was furthermore noted that clean, rounded AFM tips produced the most pronounced dip in frequency

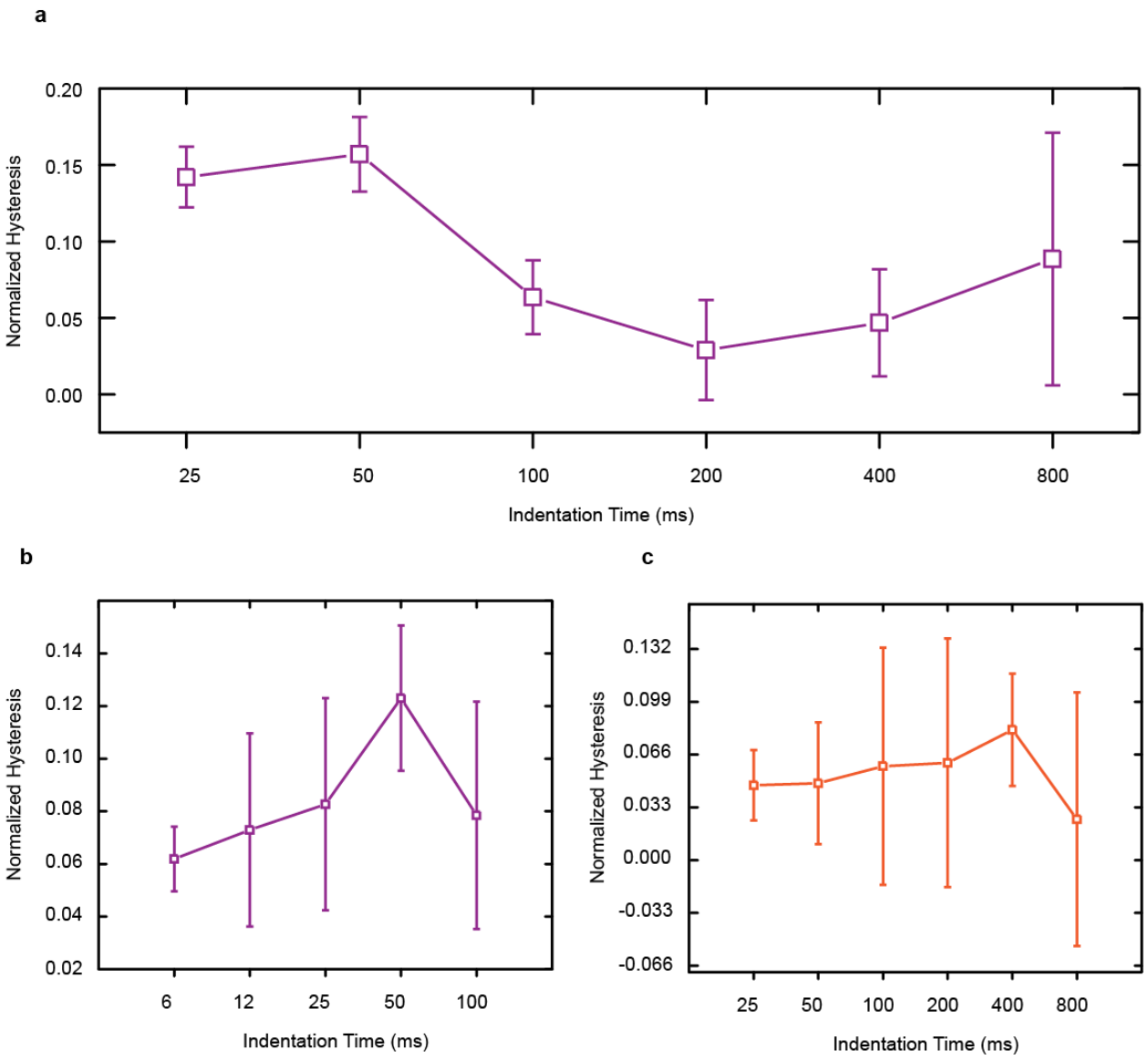


**Figure 5.8| Frequency dependency of loss hysteresis.** **a**, wide spectrum of indentation frequency results in different viscous loss character. The fast end of the spectrum follows the predicted poroelastic transport limitation from air measurements in Chapters 3 & 4. n=7 spores in separate experiments. Error bars represent the standard error of the mean, each experiment is comprised of 1024 force volume cycles **b,** shows reduced bandwidth frequency sweep (single spore; error bars represent standard deviation for 1024 plots) **c,** substrate (error as in **b**).

sweep results. To this end, the cantilever tip radius was widened with application of silicon nitride for later experiments, and so the scale of the effect may have been diminished due to adhesions. Generally, the observation of increased losses due to transport viscosity below the predicted poroelastic frequency supports the notion that the spore poroelastically structures water in a high

energy micro-scale object. That the structure retains its elasticity for a frequency roughly approximating the predicted transport from Chapter 3, supports the observation that the high energy water structure present within the spore. It is recognized that this structure must rapidly deteriorate upon germination as evidenced increased transport hysteresis accompanied by stiffness losses.

A catalyst, or enzyme, is a substance that modifies the transition state to lower the activation energy. In the spore-water to spore system, the spore material is analogous to an anti-enzyme, whereby it acts to enhance the activation energy of internal water-water transition states. Similarly, the spore water structures themselves could act to raise the activation energy of the transition from dormant bacterium (spore) into the vegetative form, thus qualifying the spore-water as an anti-enzyme to the spore biochemistry. It has been repeatedly suggested that the signal-sensitive inner membrane is immobilized through some unknown mechanism[16,109], compressed through some unknown mechanism[110,111], and so we advance the possibility that this is at least in part mediated by the high energy internal water structures, and that these water structures are susceptible to physical-chemical perturbation, in particular surfactants (universal germinants), thus lending credence to the idea that the structures function as a signal-sensitive extension of the native spore biology. Even in the event of direct ligand-binding in cell-wall-triggered alternative germination[112], it may first be necessary for certain amino acids in those fragments to relieve the spore's physical tension via water and participating electrostatics. More generally, immobilized biochemistry cannot function in signaling until it is unrestrained.

In summary, the spore's structure is quickly rearranged during germination. In these liquid-AFM studies, this rearrangement is indicated by loss of elasticity through the force-volume method. Heat-activation, a necessary precursor to nutrient germination for many laboratory spores, including those studied here, produces mechanical effects on its own, though not through loss of elasticity, and

so is likely explained by transient polymer uncoiling within the spore material. In liquid, the loss of elasticity can also tell us about the water transport, as the magnitude of hysteresis appears frequency dependent. Importantly, the onset of this transition in the frequency domain for the spore in liquid corresponds to the predicted poroelastic time constant from chapter 3, where spore pores reach a maximum expansion. In other words, the spore's water structure dissipates heat most where transport is limited and water appears to remain slow. The fact that evaporation cannot provide this immobilization will be addressed in the following chapter. These findings overall support the idea that the spore contains a high energy water structure that persists in liquid, which may theoretically serve a biological signaling function within the bacterium.

# Chapter 6: Water State Sensation Hypothesis and Future Directions

Taken as a whole, in this work I have developed an experimental apparatus to measure nanoscale water transport behavior in the bacterial spore, and observed unusually slow water with bond energy approaching that of ice, at room temperature. These observations raise the possibility that spore cortex/coat-water system evolved in part to mechanically survey ambient conditions suitable to kick-start its lifecycle. The energy to accomplish this re-awakening in the absence of metabolism may be stored in part through water's nanoscale interactions with itself and its environment (manuscript in submission), which physically manipulate the mechanical integrity of the

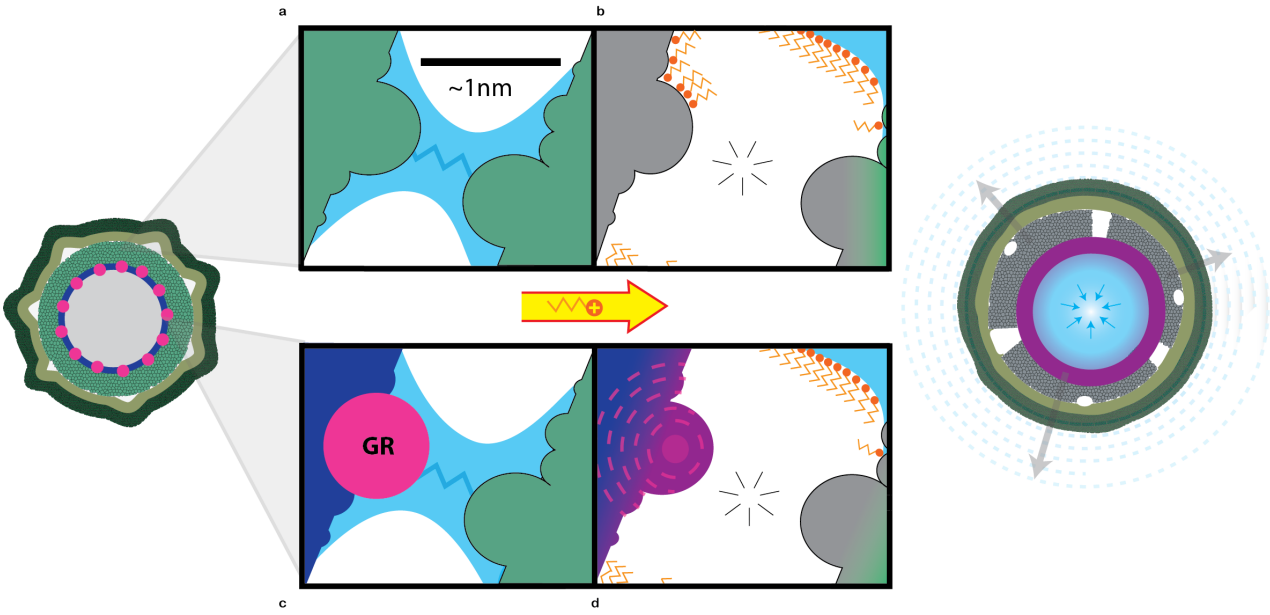


**Figure 6.1| Spore water sensation hypothesis for physiological germination. a,** Cross-section of highly tensioned dormant spore at left, with cortical water participating in structural integrity **b,** nutrient germinants help to disrupt water surface tension* releasing cortical tension **c,** signal sensitive inner membrane is shown with GR clusters, also stabilized through tensioned water and, released as shown in **d** either through cortical relaxation or directly through disruption of surface tension* by physiological germinants**.** Release of tensioned inner membrane assists in diffusion of GR proteins as the lipid membrane regains its fluidity, initiating poration, core hydration, and downstream outgrowth program. Un-tensioned, committed-to-germination spore is shown at right, where internal volume increase produces a pumping effect drawing water inward.

spore, either stabilizing dormancy structurally or are otherwise via physical contact with emergence-from-dormancy biochemistry. This expands an initial idea proposed in *Science,* 1960 by J.C. Lewis, N.S. Snell and H.K. Burr that the low water content of the spore core is accomplished through compressive contraction during development[2]. The hypothesized water structures are developed as the core is dehydrated in sporulation and contributes, along with the spore material, to a tremendous tension within the dormant organism. This dehydration is accomplished through layered assembly of the highly hygroscopic cortex material and places the spore material under tensions in the range of hundreds of MPa. When this tension is relieved the spore "pops", much like a soap bubble. This tension release within the hygroscopic materials allows lipid signaling structures at the sensitive inner membrane (IM) to diffuse and homogenize due to increased membrane fluidity. This diffusion leads to IM poration and water influx from the cortex to the core. The water-permeated core produces and amplifies a complex downstream cascade of events terminating in outgrowth of a vegetative cell.

In general, the data indicate a physically slow spore-water paradigm, which cannot be ordered in the traditional sense, due to the heterogeneous nature of spore surfaces. This has myriad implications for biology. It has recently been proposed that spore water chemistry may explain how radiation-induced free-radicals are stabilized and sequestered from the core[81]. The reliance of the water on high energy bonding raises the possibility that water, like the spore structure itself, is subject to physical environmental perturbations (temperature, pressure, volume, and electrostatics/chemistry). The universal germinant across species, dodecylamine, is a chemical whose action consists of surface tension disruption[16]. Under the hydrosensation hypothesis, disruption of the spore-water's surface tension (surfactant replacement) would hydrostatically uncouple cross-linked hydrophilic spore structures and in some part un-tension the spore, such that the inner membrane regains fluidity, and through de-rafting and diffusion of GR clusters, results in the appearance of functional IM-channels serving DPA, water, and other biochemistry. It is widely shown that protein

surfaces adsorb water similar to surfactants and can be outcompeted by stronger, sterically appropriate, chemical surfactants. At the very least, water is widely denoted as the universal biological solvent, and hydrodynamic immobilization of biochemistry is necessarily reinforced by the magnitude of water immobilization within the biomaterials observed through these experiments. It is after all, a net hydrodynamic resistance term which by some nominal molecular motion threshold comes actually to define dormancy biologically as metabolic pause; metabolism of course requiring liquid solution chemistry.

Collapse of adsorbed water patterns under tension can be seen in 'popping' of a bubble. The spore water's release of the tensioned spore structure participates in a first line of germination transmission, which sets off a chain reaction, eventually resulting in the reanimation of the organism. Thus, the spore architecture may act physical-chemically upon the water, raising the internal solution's water-on-water activation. Furthermore, it appears that this immobility is influenced by both nanoscale short-range solution/surface chemistry (germinants) as well as microscale sensory events (spore-swelling during hydration, stiffness change during germinant sensation).

In another instance of hydrosensation, in a physiologically relevant humidity range the spore pores expand to allow entrance of small, soluble germinants. In the absence of any water, the spore does not physically accept molecules or other small particulates into its cortex/coat layers[19]. The swelling behavior propagates down to the commensurate length scale of the heterogeneous transport lattice, where high energy water is tensioned across the expanded pores. In this way, macroscopic hydration and nutrient chemistry alike can direct the variable immobility of this tensioned spore-water, which is of course responsible for directly solubilizing/stabilizing, and therefore transmitting kinetic impulse to the biological machinery governing the lifecycle of the bacterium. The slow spore water may serve as part of a primal signaling apparatus comprised of simple water molecules.

Indeed, because the internal water is under extreme physical paradigms (i.e. tremendous negative pressure <150MPa, nanoconfinement <1.5nm), it is forcibly coordinated into highly activated configurations. This behavior is totally unlike anything known to produce such anomalous water during confinement, as these surface ordering is produced by a commensurately scaled lattice. In the spore, the peptidoglycan polymer is heterogeneous at the surface level and so we must explain the slow water differently. We see this spore water transport slow nonlinearly with macro-dimensional excursions (as is expected during poroelastic confinement); however, this may not alone address how the spore remains slow when hydrated (fully expanded geometry). Here we offer that immobilization during variable hydration may result directly from a transition from total confinement (molecular isolation) to an activated, patterned water-water phase, where water is clustered and slowed at regular but isolated hydrophilic spore moieties. We observe this process energetically as a transition between two hydrogen bonding regimes near ~25%RH.

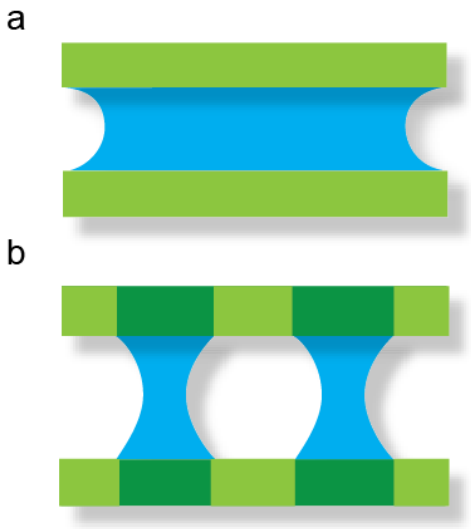


**Figure 6.2| Proposed mechanisms for slowed water.** **a,** Water is confined and its viscosity is a result of absolute immobilization **b,** Water is organized by adsorbing to the hydrophilic regions of the spore material producing a tensioned structure where transport must involve molecular hopping and individual molecules transition from liquid to vapor band back to liquid.

The high-bond- arrangement may be explained in two ways, both of which we observe as the quantity of intramolecular bonds per molecule abruptly shifts, and both of which appear to assist in maintenance of a dormant biochemical environment. Indeed, it has been suggested that pore diameter alone might directly specify the bifurcation between these two transport processes (Fig 6.2); absolute

hydraulic resistance and a liquid-vapor-liquid 'hopping' type water behavior[102]. For this event, as the spore confinement paradigm is relaxed due to porous expansion, a high energy molecular 'hopping' transition is required. In this case, the spore would switch between confinement at low humidity followed by a sublimation/deposition dominated state where the water is slowed locally at spore material moieties that can participate in hydrogen bonding. Such a vapor-liquid-vapor transition is one energetically costly event that could account for the high temperature dependent water transport observed. At present, we are working to simulate conditions similar to the spore's confinement paradigm using molecular dynamics, which might help us to refine our understanding of the exact nature of the real observed slow water. In either case, regular patterning of water, between hydrophobic and hydrophilic islands within the spore might allow coordination of soluble biochemistry into very stable configurations by raising the energy barrier of water transport locally.

The slow water we observe cannot be explained by traditional means, which rely upon crystal patterning at commensurately scaled molecular surfaces, which the spore does not contain. It is at least possible that highly hydrogen-bonded, tensioned water may be produced within the organism to participate in sensing its environment while dormant and thus participate in the regulation of its lifecycle. In the past few decades it has become increasingly clear that biology makes use of mechanics for signaling and sensation[113]. Mechanosensing includes but is not limited to sensing the presence of other cells. For the spore, the mechanosensing of favorable environments through changes to water-state hypothesis satisfies the need for a primitive sensing mechanism in the absence of metabolism, particularly in light of the understanding that spore-forming organisms are among the most ancient life-forms in Earth's biological record.

Spore water signaling hypothesis extends a mechanical role for spore water physics in air alone, however we note that water transport appears to be similar speeds in liquid. To that end, there are

possible mechanisms, which we will investigate at length in future studies, to explain how the organism could retain a physically tensioned architecture, subject to physical destabilization by pressures, surfactants, and nutrient germinants in liquid. Despite the lack of tension due to evaporation, the spore has indeed expanded maximally when dropped into liquid (it is presumably limited by the coat and/or extension of peptidoglycan polymers). Beyond some critical threshold, the porous spore material has exposed all H-bonding and other electrostatically possibilities for maintaining tension within its architecture[60]. The cell wall peptidoglycan is essentially a polyelectrolyte gel. It is indeed possible that these electrostatic interactions dominate in liquid, but remain susceptible to hydrostatics (pressures, surfactants, electric field pulses). Note that spores are ubiquitously germinated with pulsed electric fields[17]. This observation implies that electrostatic integrity of the organism is essential for dormancy. Also, the pulsing of a field will produce ponderomotive forces within the water, which will displace the dielectric molecules toward the region of greatest field density, potentially undoing tensile forces[114 115]. With this in mind, it is worth re-emphasizing that ~50% of backbone peptides found in spore peptidoglycan are cleaved to single residues of hydrophilic lactam while 25% are cleaved to hydrophobic alanines, and the remainder exist as hydrophobic branches, such that only about 10% of the equivalent branches form covalently[116]. This gives the cortex its flexibility, but the integrity and stiffness might be expected to arise from non-covalent interactions - hydrostatic or electrostatic.

In the future, we will use our force volume AFM platform to examine effects of surfactant-perturbation to mechanical properties of the cell. We hope to resolve the timing of these events so as to know whether water tension release precedes germination and, if so, by how much. This can be accomplished by placing a spherical indenting cantilever tip on the crest of a spore and repeatedly pressing on that location while adjusting the solution chemistry. Structural mutants can be utilized in combination with this method to understand the physical contributions to germination behavior. For

example, it is conceivable that mutants with larger pore diameter (less cortical cross-linking) may reveal divergent chemical germination thresholds.

In summary, the spore's lifecycle is harmonized with the formation and destruction of different water states. In the future, studies will focus on the timing of the germination triggering and extension of this hypothesis to liquid germination. Together, this work has provided observations of slow spore water and provided plausible mechanisms to explain this behavior. These observations support the hypothesis that the spore may utilize physical water states to navigate dormancy.

# References


1 Popham, D. L. Specialized peptidoglycan of the bacterial endospore: the inner wall of the lockbox. *Cellular and molecular life sciences : CMLS* **59**, 426-433 (2002).

2 Lewis, J. C., Snell, N. S. & Burr, H. K. Water Permeability of Bacterial Spores and the Concept of a Contractile Cortex. *Science* **132**, 544-545, doi:10.1126/science.132.3426.544 (1960).

3 de Hoon, M. J., Eichenberger, P. & Vitkup, D. Hierarchical evolution of the bacterial sporulation network. *Current biology : CB* **20**, R735-745, doi:10.1016/j.cub.2010.06.031 (2010).

4 Driks, A. & Eichenberger, P. *The bacterial spore : from molecules to systems*. (ASM Press, 2016).

5 Vreeland, R. H., Rosenzweig, W. D. & Powers, D. W. Isolation of a 250 million-year-old halotolerant bacterium from a primary salt crystal. *Nature* **407**, 897-900, doi:10.1038/35038060 (2000).

6 McKenney, P. T., Driks, A. & Eichenberger, P. The Bacillus subtilis endospore: assembly and functions of the multilayered coat. *Nature reviews. Microbiology* **11**, 33-44, doi:10.1038/nrmicro2921 (2013).

7 Kennedy, M. J., Reader, S. L. & Swierczynski, L. M. Preservation records of micro-organisms: evidence of the tenacity of life. *Microbiology* **140 ( Pt 10)**, 2513-2529, doi:10.1099/00221287-140-10-2513 (1994).

8 Angert, E. R. Alternatives to binary fission in bacteria. *Nature reviews. Microbiology* **3**, 214-224, doi:10.1038/nrmicro1096 (2005).

9 Fujita, M. & Losick, R. Evidence that entry into sporulation in Bacillus subtilis is governed by a gradual increase in the level and activity of the master regulator Spo0A. *Genes Dev* **19**, 2236-2244, doi:10.1101/gad.1335705 (2005).

10 Driks, A. Bacillus subtilis spore coat. *Microbiology and molecular biology reviews : MMBR* **63**, 1-20 (1999).

11 Daniel, R. A., Drake, S., Buchanan, C. E., Scholle, R. & Errington, J. The Bacillus subtilis spoVD gene encodes a mother-cell-specific penicillin-binding protein required for spore morphogenesis. *Journal of molecular biology* **235**, 209-220 (1994).

12 Bukowska-Faniband, E. & Hederstedt, L. Cortex synthesis during Bacillus subtilis sporulation depends on the transpeptidase activity of SpoVD. *FEMS microbiology letters* **346**, 65-72, doi:10.1111/1574-6968.12202 (2013).

13 McKenney, P. T. & Eichenberger, P. Dynamics of spore coat morphogenesis in Bacillus subtilis. *Molecular microbiology* **83**, 245-260, doi:10.1111/j.1365-2958.2011.07936.x (2012).

14 Black, E. P. *et al.* Factors influencing germination of Bacillus subtilis spores via activation of nutrient receptors by high pressure. *Appl Environ Microb* **71**, 5879-5887, doi:Doi 10.1128/Aem.71.10.5879-5887.2005 (2005).

15 Vepachedu, V. R. & Setlow, P. Role of SpoVA proteins in release of dipicolinic acid during germination of Bacillus subtilis spores triggered by dodecylamine or lysozyme. *Journal of bacteriology* **189**, 1565-1572, doi:10.1128/JB.01613-06 (2007).

16 Setlow, P., Wang, S. & Li, Y. Q. Germination of Spores of the Orders Bacillales and Clostridiales. *Annual review of microbiology*, doi:10.1146/annurev-micro-090816-093558 (2017).

17 Shin, J. K. *et al.* GERMINATION AND SUBSEQUENT INACTIVATION OF BACILLUS SUBTILIS SPORES BY PULSED ELECTRIC FIELD TREATMENT. *Journal of Food Processing and Preservation* **34**, 43-54, doi:10.1111/j.1745-4549.2008.00321.x (2010).

18 Shah, I. M., Laaberki, M. H., Popham, D. L. & Dworkin, J. A eukaryotic-like Ser/Thr kinase signals bacteria to exit dormancy in response to peptidoglycan fragments. *Cell* **135**, 486-496, doi:10.1016/j.cell.2008.08.039 (2008).

19 Scherrer, R., Beaman, T. C. & Gerhardt, P. Macromolecular Sieving by Dormant Spore of Bacillus-Cereus. *Journal of bacteriology* **108**, 868-& (1971).

20 Christie, G., Gotzke, H. & Lowe, C. R. Identification of a receptor subunit and putative ligand-binding residues involved in the Bacillus megaterium QM B1551 spore germination response to glucose. *Journal of bacteriology* **192**, 4317-4326, doi:10.1128/JB.00335-10 (2010).

21 Paredes-Sabja, D., Shen, A. & Sorg, J. A. Clostridium difficile spore biology: sporulation, germination, and spore structural proteins. *Trends in microbiology* **22**, 406-416, doi:10.1016/j.tim.2014.04.003 (2014).

22 Griffiths, K. K., Zhang, J., Cowan, A. E., Yu, J. & Setlow, P. Germination proteins in the inner membrane of dormant Bacillus subtilis spores colocalize in a discrete cluster. *Molecular microbiology* **81**, 1061-1077, doi:10.1111/j.1365-2958.2011.07753.x (2011).

23 Korza, G. & Setlow, P. Topology and accessibility of germination proteins in the Bacillus subtilis spore inner membrane. *Journal of bacteriology* **195**, 1484-1491, doi:10.1128/JB.02262-12 (2013).

24 Troiano, A. J., Jr., Zhang, J., Cowan, A. E., Yu, J. & Setlow, P. Analysis of the dynamics of a Bacillus subtilis spore germination protein complex during spore germination and outgrowth. *Journal of bacteriology* **197**, 252-261, doi:10.1128/JB.02274-14 (2015).

25 Ghosh, S., Zhang, P., Li, Y. Q. & Setlow, P. Superdormant spores of Bacillus species have elevated wet-heat resistance and temperature requirements for heat activation. *Journal of bacteriology* **191**, 5584-5591, doi:10.1128/JB.00736-09 (2009).

26 Creighton, T. E. Prediction of Protein Structure and the Principles of Protein Conformation. Gerald D. Fasman, Ed. Plenum, New York, 1989. xiv, 798 pp., illus. $95. *Science* **247**, 1351-1352, doi:10.1126/science.247.4948.1351-a (1990).

27 Popham, D. L., Helin, J., Costello, C. E. & Setlow, P. Analysis of the peptidoglycan structure of Bacillus subtilis endospores. *Journal of bacteriology* **178**, 6451-6458 (1996).

28 Warth, A. D. & Strominger, J. L. Structure of the peptidoglycan from spores of Bacillus subtilis. *Biochemistry* **11**, 1389-1396 (1972).

29 Atrih, A., Zollner, P., Allmaier, G. & Foster, S. J. Structural analysis of Bacillus subtilis 168 endospore peptidoglycan and its role during differentiation. *Journal of bacteriology* **178**, 6173-6183 (1996).

30 Cooper, G. R. & Moir, A. Amino acid residues in the GerAB protein important in the function and assembly of the alanine spore germination receptor of Bacillus subtilis 168. *Journal of bacteriology* **193**, 2261-2267, doi:10.1128/JB.01397-10 (2011).

31 Dodatko, T. *et al.* Bacillus cereus spores release alanine that synergizes with inosine to promote germination. *PloS one* **4**, e6398, doi:10.1371/journal.pone.0006398 (2009).

32 Shrestha, R., Lockless, S. W. & Sorg, J. A. A Clostridium difficile alanine racemase affects spore germination and accommodates serine as a substrate. *The Journal of biological chemistry* **292**, 10735-10742, doi:10.1074/jbc.M117.791749 (2017).

33 Pauwels, E., De Cooman, H., Waroquier, M., Hole, E. O. & Sagstuen, E. Solved? The reductive radiation chemistry of alanine. *Physical chemistry chemical physics : PCCP* **16**, 2475-2482, doi:10.1039/c3cp54441a (2014).

34 Billiot, E., Agbaria, R. A., Thibodeaux, S., Shamsi, S. & Warner, I. M. Amino acid order in polymeric dipeptide surfactants: effect on physical properties and enantioselectivity. *Analytical chemistry* **71**, 1252-1256 (1999).

35 Setlow, B., Cowan, A. E. & Setlow, P. Germination of spores of Bacillus subtilis with dodecylamine. *Journal of applied microbiology* **95**, 637-648 (2003).

36 Wang, G., Yi, X., Li, Y. Q. & Setlow, P. Germination of individual Bacillus subtilis spores with alterations in the GerD and SpoVA proteins, which are important in spore germination. *Journal of bacteriology* **193**, 2301-2311, doi:10.1128/JB.00122-11 (2011).

37 Velasquez, J., Schuurman-Wolters, G., Birkner, J. P., Abee, T. & Poolman, B. Bacillus subtilis spore protein SpoVAC functions as a mechanosensitive channel. *Molecular microbiology* **92**, 813-823, doi:10.1111/mmi.12591 (2014).

38 Sahin, O., Yong, E. H., Driks, A. & Mahadevan, L. Physical basis for the adaptive flexibility of Bacillus spore coats. *J R Soc Interface* **9**, 3156-3160, doi:10.1098/rsif.2012.0470 (2012).

39 Atrih, A. & Foster, S. J. The role of peptidoglycan structure and structural dynamics during endospore dormancy and germination. *Antonie van Leeuwenhoek* **75**, 299-307 (1999).

40 Loison, P. *et al.* Direct investigation of viscosity of an atypical inner membrane of Bacillus spores: a molecular rotor/FLIM study. *Biochimica et biophysica acta* **1828**, 2436-2443, doi:10.1016/j.bbamem.2013.06.028 (2013).

41 Nickels, J. D. *et al.* The in vivo structure of biological membranes and evidence for lipid domains. *PLoS biology* **15**, e2002214, doi:10.1371/journal.pbio.2002214 (2017).

42 Wuytack, E. Y., Soons, J., Poschet, F. & Michiels, C. W. Comparative study of pressure- and nutrient-induced germination of Bacillus subtilis spores. *Appl Environ Microbiol* **66**, 257-261 (2000).

43 Setlow, P. Germination of spores of Bacillus species: what we know and do not know. *Journal of bacteriology* **196**, 1297-1305, doi:10.1128/JB.01455-13 (2014).

44 Lindsay, J. A., Lindsay, J. A. & Murrell, W. G. Changes in density of DNA after interaction with dipicolinic acid and its possible role in spore heat resistance. *Current microbiology* **12**, 329-333, doi:10.1007/BF01567892 (1985).

45 Zvyagintsev, D. G. *et al.* Dynamics of spore germination and mycelial growth of streptomycetes under low humidity conditions. *Microbiology* **78**, 440-444, doi:Doi 10.1134/S0026261709040079 (2009).

46 Ling, G. N., Niu, Z. & Ochsenfeld, M. Predictions of polarized multilayer theory of solute distribution confirmed from a study of the equilibrium distribution in frog muscle of twenty-one nonelectrolytes including five cryoprotectants. *Physiological chemistry and physics and medical NMR* **25**, 177-208 (1993).

47 Westphal, A. J., Price, P. B., Leighton, T. J. & Wheeler, K. E. Kinetics of size changes of individual Bacillus thuringiensis spores in response to changes in relative humidity. *Proc Natl Acad Sci U S A* **100**, 3461-3466, doi:10.1073/pnas.232710999 (2003).

48 Zhang, P., Thomas, S., Li, Y. Q. & Setlow, P. Effects of cortex peptidoglycan structure and cortex hydrolysis on the kinetics of Ca(2+)-dipicolinic acid release during Bacillus subtilis spore germination. *Journal of bacteriology* **194**, 646-652, doi:10.1128/JB.06452-11 (2012).

49 Gallo, P. *et al.* Water: A Tale of Two Liquids. *Chem Rev* **116**, 7463-7500, doi:10.1021/acs.chemrev.5b00750 (2016).

50 Ciccarelli, F. D. *et al.* Toward automatic reconstruction of a highly resolved tree of life. *Science* **311**, 1283-1287, doi:10.1126/science.1123061 (2006).

51 Chen, X. *et al.* Scaling up nanoscale water-driven energy conversion into evaporation-driven engines and generators. *Nat Commun* **6**, 7346, doi:10.1038/ncomms8346 (2015).

52 Chen, X., Mahadevan, L., Driks, A. & Sahin, O. Bacillus spores as building blocks for stimuli-responsive materials and nanogenerators. *Nat Nanotechnol* **9**, 137-141, doi:Doi 10.1038/Nnano.2013.290 (2014).

53 Harrington, M. J. *et al.* Origami-like unfolding of hydro-actuated ice plant seed capsules. *Nat Commun* **2**, 337, doi:10.1038/ncomms1336 (2011).

54 Dawson, J., Vincent, J. F. V. & Rocca, A. M. How pine cones open. *Nature* **390**, 668-668 (1997).

55 Pickard, W. F. The Ascent of Sap in Plants. *Prog Biophys Mol Bio* **37**, 181-229 (1981).

56 Finn, J. K. & Norman, M. D. The argonaut shell: gas-mediated buoyancy control in a pelagic octopus. *Proceedings. Biological sciences / The Royal Society* **277**, 2967-2971, doi:10.1098/rspb.2010.0155 (2010).

57 Friedline, A. W. *et al.* Water Behavior in Bacterial Spores by Deuterium NMR Spectroscopy. *Journal of Physical Chemistry B* **118**, 8945-8955, doi:10.1021/jp5025119 (2014).

58 Kaieda, S., Setlow, B., Setlow, P. & Halle, B. Mobility of core water in Bacillus subtilis spores by 2H NMR. *Biophysical journal* **105**, 2016-2023, doi:10.1016/j.bpj.2013.09.022 (2013).

59 Costa, T., Isidro, A. L., Moran, C. P., Jr. & Henriques, A. O. Interaction between coat morphogenetic proteins SafA and SpoVID. *Journal of bacteriology* **188**, 7731-7741, doi:10.1128/JB.00761-06 (2006).

60 Ou, L. T. & Marquis, R. E. Electromechanical interactions in cell walls of gram-positive cocci. *Journal of bacteriology* **101**, 92-101 (1970).

61 Vollmer, W. & Holtje, J. V. The architecture of the murein (peptidoglycan) in gram-negative bacteria: vertical scaffold or horizontal layer(s)? *Journal of bacteriology* **186**, 5978-5987, doi:10.1128/JB.186.18.5978-5987.2004 (2004).

62 Dmitriev, B., Toukach, F. & Ehlers, S. Towards a comprehensive view of the bacterial cell wall. *Trends in microbiology* **13**, 569-574, doi:10.1016/j.tim.2005.10.001 (2005).

63 Plomp, M., Leighton, T. J., Wheeler, K. E., Hill, H. D. & Malkin, A. J. In vitro high-resolution structural dynamics of single germinating bacterial spores. *P Natl Acad Sci USA* **104**, 9644-9649, doi:Doi 10.1073/Pnas.0610626104 (2007).

64 Meroueh, S. O. *et al.* Three-dimensional structure of the bacterial cell wall peptidoglycan. *Proc Natl Acad Sci U S A* **103**, 4404-4409, doi:10.1073/pnas.0510182103 (2006).

65 Elbaum, R., Zaltzman, L., Burgert, I. & Fratzl, P. The role of wheat awns in the seed dispersal unit. *Science* **316**, 884-886, doi:Doi 10.1126/Science.1140097 (2007).

66 Masic, A. *et al.* Osmotic pressure induced tensile forces in tendon collagen. *Nat Commun* **6**, 5942, doi:10.1038/ncomms6942 (2015).

67 Wheeler, T. D. & Stroock, A. D. The transpiration of water at negative pressures in a synthetic tree. *Nature* **455**, 208-212, doi:Doi 10.1038/Nature07226 (2008).

68 Chiavazzo, E., Fasano, M., Asinari, P. & Decuzzi, P. Scaling behaviour for the water transport in nanoconfined geometries. *Nat Commun* **5**, doi:Artn 3565
Doi 10.1038/Ncomms4565 (2014).

69 Maheshwari, P. *et al.* Phase Transition of Nanoconfined Water in Clay: Positron Annihilation, Nuclear Magnetic Resonance, and Dielectric Relaxation Studies. *J Phys Chem C* **117**, 14313-14324, doi:Doi 10.1021/Jp403212c (2013).

70 Hu, M., Goicochea, J. V., Michel, B. & Poulikakos, D. Water Nanoconfinement Induced Thermal Enhancement at Hydrophilic Quartz Interfaces. *Nano Lett* **10**, 279-285, doi:Doi 10.1021/Nl9034658 (2010).

71 Algara-Siller, G. *et al.* Square ice in graphene nanocapillaries. *Nature* **519**, 443-445, doi:10.1038/nature14295 (2015).

72 Ceriotti, M., Cuny, J., Parrinello, M. & Manolopoulos, D. E. Nuclear quantum effects and hydrogen bond fluctuations in water. *Proc Natl Acad Sci U S A* **110**, 15591-15596, doi:10.1073/pnas.1308560110 (2013).

73 Chaplin, M. Opinion - Do we underestimate the importance of water in cell biology? *Nat Rev Mol Cell Bio* **7**, 861-866, doi:10.1038/nrm2021 (2006).

74 Chaplin, M. Do we underestimate the importance of water in cell biology? *Nat Rev Mol Cell Biol* **7**, 861-866, doi:10.1038/nrm2021 (2006).

75 Hill, A. E., Shachar-Hill, B. & Shachar-Hill, Y. What are aquaporins for? *J Membrane Biol* **197**, 1-32, doi:10.1007/s00232-003-0639-6 (2004).

76 Parisi, M., Dorr, R. A., Ozu, M. & Toriano, R. From Membrane Pores to Aquaporins: 50 Years Measuring Water Fluxes. *J Biol Phys* **33**, 331-343, doi:10.1007/s10867-008-9064-5 (2007).

77 Volker, J. & Breslauer, K. J. Communication between noncontacting macromolecules. *Annu Rev Biophys Biomol Struct* **34**, 21-42, doi:10.1146/annurev.biophys.33.110502.133332 (2005).

78 Lin, J., Balabin, I. A. & Beratan, D. N. The nature of aqueous tunneling pathways between electron-transfer proteins. *Science* **310**, 1311-1313, doi:10.1126/science.1118316 (2005).

79 Fuxreiter, M., Mezei, M., Simon, I. & Osman, R. Interfacial water as a "hydration fingerprint" in the noncognate complex of BamHI. *Biophysical journal* **89**, 903-911, doi:10.1529/biophysj.105.063263 (2005).

80 Cameron, I. L., Kanal, K. M. & Fullerton, G. D. Role of protein conformation and aggregation in pumping water in and out of a cell. *Cell Biol Int* **30**, 78-85, doi:10.1016/j.cellbi.2005.09.010 (2006).

81 Friedline, A. W. *et al.* Sterilization Resistance of Bacterial Spores Explained with Water Chemistry. *The journal of physical chemistry. B* **119**, 14033-14044, doi:10.1021/acs.jpcb.5b07437 (2015).

82 Longo, G. *et al.* Rapid detection of bacterial resistance to antibiotics using AFM cantilevers as nanomechanical sensors. *Nat Nanotechnol* **8**, 522-526, doi:10.1038/NNANO.2013.120 (2013).

83 Knudsen, S. M. *et al.* Water and Small Molecule Permeation of Dormant Bacillus subtilis Spores. *Journal of bacteriology*, doi:10.1128/JB.00435-15 (2015).

84 Shen, S., Narayanaswamy, A., Goh, S. & Chen, G. Thermal Conductance of Bi-Material Afm Cantilevers. *Proceedings of the Asme International Mechanical Engineering Congress and Exposition, Vol 13, Pts a and B*, 799-802 (2009).

85 Biot, M. A. General Theory of Three-Dimensional Consolidation. *J Appl Phys* **12**, 155-164, doi:10.1063/1.1712886 (1941).

86 Hu, Y. H., Zhao, X. H., Vlassak, J. J. & Suo, Z. G. Using indentation to characterize the poroelasticity of gels. *Appl Phys Lett* **96**, doi:Artn 121904

10.1063/1.3370354 (2010).

87 Nagler, K., Setlow, P., Reineke, K., Driks, A. & Moeller, R. Involvement of Coat Proteins in Bacillus subtilis Spore Germination in High-Salinity Environments. *Appl Environ Microb* **81**, 6725-6735, doi:10.1128/Aem.01817-15 (2015).

88 Wells-Bennik, M. H. J. *et al.* Bacterial Spores in Food: Survival, Emergence, and Outgrowth. *Annu Rev Food Sci T* **7**, 457-482, doi:10.1146/annurev-food-041715-033144 (2016).

89 Ghosh, S. *et al.* Characterization of spores of Bacillus subtilis that lack most coat layers. *Journal of bacteriology* **190**, 6741-6748, doi:10.1128/Jb.00896-08 (2008).

90 Dover, R. S., Bitler, A., Shimoni, E., Trieu-Cuot, P. & Shai, Y. Multiparametric AFM reveals turgor-responsive net-like peptidoglycan architecture in live streptococci. *Nat Commun* **6**, 7193, doi:10.1038/ncomms8193 (2015).

91 Sunde, E. P., Setlow, P., Hederstedt, L. & Halle, B. The physical state of water in bacterial spores. *Proc Natl Acad Sci U S A* **106**, 19334-19339, doi:10.1073/pnas.0908712106 (2009).

92 Cho, C. H., Urquidi, J. & Robinson, G. W. Molecular-level description of temperature and pressure effects on the viscosity of water. *The Journal of chemical physics* **111**, 10171-10176, doi:10.1063/1.480367 (1999).

93 He, X. M. *et al.* Synthetic homeostatic materials with chemo-mechano-chemical self-regulation. *Nature* **487**, 214-218, doi:Doi 10.1038/Nature11223 (2012).

94 Sidorenko, A., Krupenkin, T., Taylor, A., Fratzl, P. & Aizenberg, J. Reversible switching of hydrogel-actuated nanostructures into complex micropatterns. *Science* **315**, 487-490, doi:Doi 10.1126/Science.1135516 (2007).

95 Stuart, M. A. C. *et al.* Emerging applications of stimuli-responsive polymer materials. *Nature materials* **9**, 101-113, doi:Doi 10.1038/Nmat2614 (2010).

96 Yashin, V. V. & Balazs, A. C. Pattern formation and shape changes in self-oscillating polymer gels. *Science* **314**, 798-801, doi:Doi 10.1126/Science.1132412 (2006).

97 Tyree, M. T. The ascent of water. *Nature* **423**, 923-923, doi:10.1038/423923a (2003).

98 Tunuguntla, R. H. *et al.* Enhanced water permeability and tunable ion selectivity in subnanometer carbon nanotube porins. *Science* **357**, 792-796, doi:10.1126/science.aan2438 (2017).

99 Tao, N. J., Lindsay, S. M. & Rupprecht, A. The dynamics of the DNA hydration shell at gigahertz frequencies. *Biopolymers* **26**, 171-188, doi:10.1002/bip.360260202 (1987).

100 Pissis, P. & Kyritsis, A. Hydration studies in polymer hydrogels. *J Polym Sci Pol Phys* **51**, 159-175, doi:10.1002/polb.23220 (2013).

101 Cameron, R. E. & Conrow, H. P. Soil Moisture Relative Humidity and Microbial Abundance in Dry Valleys of Southern Victoria Land. *Antarct J Us* **4**, 23-& (1969).

102 Lee, J., Laoui, T. & Karnik, R. Nanofluidic transport governed by the liquid/vapour interface. *Nat Nanotechnol* **9**, 317-323, doi:10.1038/NNANO.2014.28 (2014).

103 Young, G. T. *Amino Acids, Peptides and Proteins*. (Royal Society of Chemistry, 2007).

104 Harwood, C. R. & Cutting, S. M. *Molecular biological methods for Bacillus*. (Wiley, 1990).

105 Moeendarbary, E. *et al.* The cytoplasm of living cells behaves as a poroelastic material. *Nature materials* **12**, 253-261, doi:Doi 10.1038/Nmat3517 (2013).

106 Christensen, R. M. *Theory of viscoelasticity*. 2nd edn, (Dover Publications, 2003).

107 Zhang, P., Setlow, P. & Li, Y. Characterization of single heat-activated Bacillus spores using laser tweezers Raman spectroscopy. *Optics express* **17**, 16480-16491, doi:10.1364/OE.17.016480 (2009).

108 Keynan, A., Evanchik, Z., Halvorson, H. O. & Hastings, J. W. Activation of Bacterial Endospores. *Journal of bacteriology* **88**, 313-318 (1964).

109 Moir, A. & Cooper, G. Spore Germination. *Microbiol Spectr* **3**, doi:10.1128/microbiolspec.TBS-0014-2012 (2015).

110 Nicholson, W. L., Munakata, N., Horneck, G., Melosh, H. J. & Setlow, P. Resistance of Bacillus endospores to extreme terrestrial and extraterrestrial environments. *Microbiol Mol Biol R* **64**, 548-+, doi:Doi 10.1128/Mmbr.64.3.548-572.2000 (2000).

111 Stewart, G. S., Eaton, M. W., Johnstone, K., Barrett, M. D. & Ellar, D. J. An investigation of membrane fluidity changes during sporulation and germination of Bacillus megaterium K.M. measured by electron spin and nuclear magnetic resonance spectroscopy. *Biochimica et biophysica acta* **600**, 270-290 (1980).

112 Dworkin, J. & Shah, I. M. Exit from dormancy in microbial organisms. *Nature reviews. Microbiology* **8**, 890-896, doi:10.1038/nrmicro2453 (2010).

113 Vogel, V. & Sheetz, M. Local force and geometry sensing regulate cell functions. *Nat Rev Mol Cell Biol* **7**, 265-275, doi:10.1038/nrm1890 (2006).

114 Shneider, M. N., Pekker, M. & Fridman, A. Theoretical Study of the Initial Stage of Sub-nanosecond Pulsed Breakdown in Liquid Dielectrics. *Ieee T Dielect El In* **19**, 1579-1582 (2012).

115 Caupin, F. *et al.* Exploring water and other liquids at negative pressure. *J Phys-Condens Mat* **24**, doi:Artn 284110
10.1088/0953-8984/24/28/284110 (2012).
116 Meador-Parton, J. & Popham, D. L. Structural analysis of Bacillus subtilis spore peptidoglycan during sporulation. *Journal of bacteriology* **182**, 4491-4499 (2000).